1993

Resonant Vibrations of the Irish Folk Harp

Patrick Healy
Technological University Dublin, paddy.healy25@gmail.com

Resonant Vibrations of the Irish Folk Harp

Submitted for the award of

M.Sc.

to

The Department of Pure and Applied Physics

University of Dublin

October 1993

by

Patrick M.A. Healy B.Sc. H.Dip.Ed.

Dept. of Physics

Dublin Institute of Technology

Kevin St.

Dublin 8

Table of Contents

Table of Figures

Acknowledgements

I wish to thank my Dublin Institute of Technology supervisor, Dr. Matthew Hussey, both for proposing this project and for his advice and guidance during its execution. I wish to thank Dr. Eric Finch, my Trinity College supervisor, for his helpful visits and advice.

Dr. Bernard Richardson gave me invaluable advice on my visit to University of Wales, Cardiff and later on telephone.

I wish to thank Dr. Alexander Bell, Stevenson College, Edinburgh, for kindly lending me a copy of his Ph.D. thesis on the concert harp and for his helpful advice on the telephone.

I am deeply grateful to the technician staff at DIT (Kevin Street) for the huge amount of voluntary support work they undertook. In particular, I wish to acknowledge the unstinting efforts of Alexander Campbell and James Callis. My thanks also to James Robinson for taking and developing the photographs in this work.

I wish to thank the DIT Research Committee and Eolas (the Irish Science and Technology Agency) for the grants I received for this work.

I am deeply appreciative of the loan of vital equipment over an extended period by the Department of Control Systems and Electrical Engineering at DIT Kevin Street and in particular for the advice and help of Dr. Bill Grimson in the area of signal and data processing.

Declaration

I declare that except where otherwise stated, this thesis is entirely my own work and has not been submitted to this or any other University as an exercise for any other Degree award.

This research was carried out by me in the Department of Physics, Dublin Institute of Technology, Kevin Street, under the supervision of Dr. Matthew Hussey and Dr. Eric Finch.

I hereby give permission to the library to lend or copy this thesis.

_____

Patrick M.A. Healy.

Summary

An analysis of the resonant vibrations of an O'Meachair cedar and mahogany Irish folk harp is reported. A report is also made of a small number of measurements carried out on an O'Meachair spruce and maple Irish folk harp. The structure and operation of the harp is described.

The theory of small vibrations of plates and wooden boards is set out.

The system devised to measure input admittance at driving points on the harp body over a frequency range 0 - 2 kHz is described. Tests of its linearity and of its frequency flatness are reported.

Resonant vibrations of an isolated held and barred soundboard are identified over the frequency range 0 - 1 kHz by input admittance and phase measurement. Using the Chladni powder pattern method, modal shapes on the soundboard are identified and resonant modes of vibration are classified in accordance with Richardson's notation. Plots of input admittance versus position along the length of the soundboard are presented for each resonant frequency. Input admittance measurements across the soundboard, as part of the determination of modal classification, are also reported.

Input admittance measurements on the sound board of the O'Meachair cedar and mahogany Irish folk harp are reported. A plot of admittance versus frequency at string point G3 over the frequency range 0 - 2 kHz is presented as a suitable representation of the characteristic admittance profile of the instrument. Resonant vibrations of the harp are identified over the frequency range 0 - 2 kHz. At each resonant frequency from 0 - 1 kHz, plots of input admittance along the length of the soundboard are presented. Modal classifications are suggested with the assistance of input admittance measurements at positions off the central bars. Two resonant modes, which are not soundboard modes, are investigated and tentatively identified. Effective modal masses and string tensions are determined.

Based on a small number of measurements, the low frequency resonant modes of an O'Meachair spruce and maple Irish folk harp are tentatively identified by comparison with the admittance profile of the cedar and mahogany harp.

Suggestions are made for further work, with a view to applying scientific methods to the construction of Irish folk harps.

Dedication

This thesis is respectfully dedicated to my parents, James Healy and Johannah Meaney of Clonmel, Co. Tipperary, without whose sacrifices I would have been unable to attend university.

Introduction

This thesis is a report on an acoustical investigation of the modern Irish Folk Harp. The principal work was carried out on an instrument crafted by Colm Ó Meachair, Harp-maker, Dublin which had a soundboard of quarter-sawn cedar and a body of mahogany. Some additional work was carried out on an Ó Meachair harp with spruce soundboard and maple body for comparison purposes. The latter instrument was kindly lent for a brief time for this work by Áine Ní Dhúill, harpist on concert and Irish folk harp.

The Irish folk harp is commonly used both for solo instrumental performances and in accompaniment. The harpist and the singer are often the same person.

The sound quality of the instrument is readily identified as having a marked similarity to that of the concert harp, but also as having significant differences[1].

The modern Irish folk harp is closely related to the Scottish Clarsach. In the book "The Harp's a Wonder"[2], Maher says, "a Cláirseach [ancient] is the one most resembling the Irish harp of today. The Scots, to their credit, use the words `Clarsach' to describe their instrument of similar size to the Irish harp."

Initial acoustical research on the harp was carried out by Firth at the University of St. Andrew's, Scotland. He examined a Clarsach which he had crafted himself. His report [3] was confined to the response of the instrument over the frequency range 0 - 1000 Hz.

In later work [4], Firth investigated and reported on many aspects of harps, including ancient Irish wire-strung harps.

A major work [5] on the acoustics of the concert harp was presented by Bell to the University of St. Andrews in 1987.

Earlier, Bell and Firth had jointly reported [6] investigations on vibrations of the concert harp soundboard and soundbox.

In his work on the Clarsach, Firth reported[3] a whole-body mode at frequency 210 Hz, and the first soundboard modes in the completed instrument at frequencies 308 Hz, 428 Hz, 620 Hz and 830 Hz. He did not detect a Helmholtz resonance at the soundbox cavity. In his conclusions he states, "The first four resonances in a completed soundbox are due to waves moving lengthwise in the soundboard."

One of the objectives of the work reported here was to investigate whether Firth's results and conclusions are valid for the cedar and mahogany harp and for Irish folk harps in general.

It was intended to establish the characteristic admittance plot over the frequency range 0-1000 Hz for the instrument and to investigate the resonant vibrational modes in this frequency region.

REFERENCES

[1]Communications with Áine Ní Dhúill, harpist, and with Colm Ó Meachair, harp-maker, Marley Craft Centre, Dublin. (1993).

[2]Maher, T., The Harp's a Wonder. Uisneach Press, Lynn Industrial Estate, Mullingar, Ireland (1991).

[3]Firth, I.M., On the Acoustics of the Harp. Acus, 37, pp148-154 (1977).

[4]Firth, I.M., On the Acoustics of the Harp. Proceedings of the Institute of Acoustics, Spring Conference, Swansea, pp 55 - 64 (1984).

[5]Bell, A.J., An Acoustical Investigation of the Concert Harp. PhD thesis presented to the University of St. Andrews, Scotland, January (1987).

[6]Firth, I.M. and Bell, A.J., Vibrations of the Concert Harp Soundboard and Soundbox. Proceedings of the Institute of Acoustics, Spring Conference, Swansea, pp 65 - 73 (1984).

Chapter 1

MUSICAL INSTRUMENT ACOUSTICS

1.1 Instrument as a sound source

The tonal quality of a musical instrument is so special and unique that one can distinguish between the same note played on different instruments. Indeed, one can distinguish between the same note played on versions of the same instrument produced by different luthiers. The search for the secrets of the Stradivarius violin has preoccupied researchers and musicians for centuries[1].

The secrets lie in the vibrations of the instrument and the response of the human auditory system to the sound energy produced by these vibrations. The body of the instrument is designed to act as a combined resonator and sound source. In a stringed instrument, the vibrating string is the source of the vibration. Without resonant amplification, the sound emitted by the vibration of a string is almost inaudible as will be found by plucking the string of an electric guitar which has not been plugged in to the electricity supply. But in an acoustic instrument, such as the harp, the vibrating string sets the entire body of the instrument into vibration. The sound heard is produced by these vibrations. "Amplification" is thus achieved through mechanical resonances of the body structure and, in particular, of the large light-weight plate(s) which form the soundboard. Such plates are efficient sound radiators, unlike a stretched string with its small surface area.

The body of a stringed instrument has however an uneven response to excitation at different frequencies, as can be seen from figure 1.1. This figure shows plots of response (input admittance) versus frequency for a violin, cello and double bass. Each instrument has an overall characteristic frequency response profile, and in each instrument there are large and sharp variations in response as frequency changes.

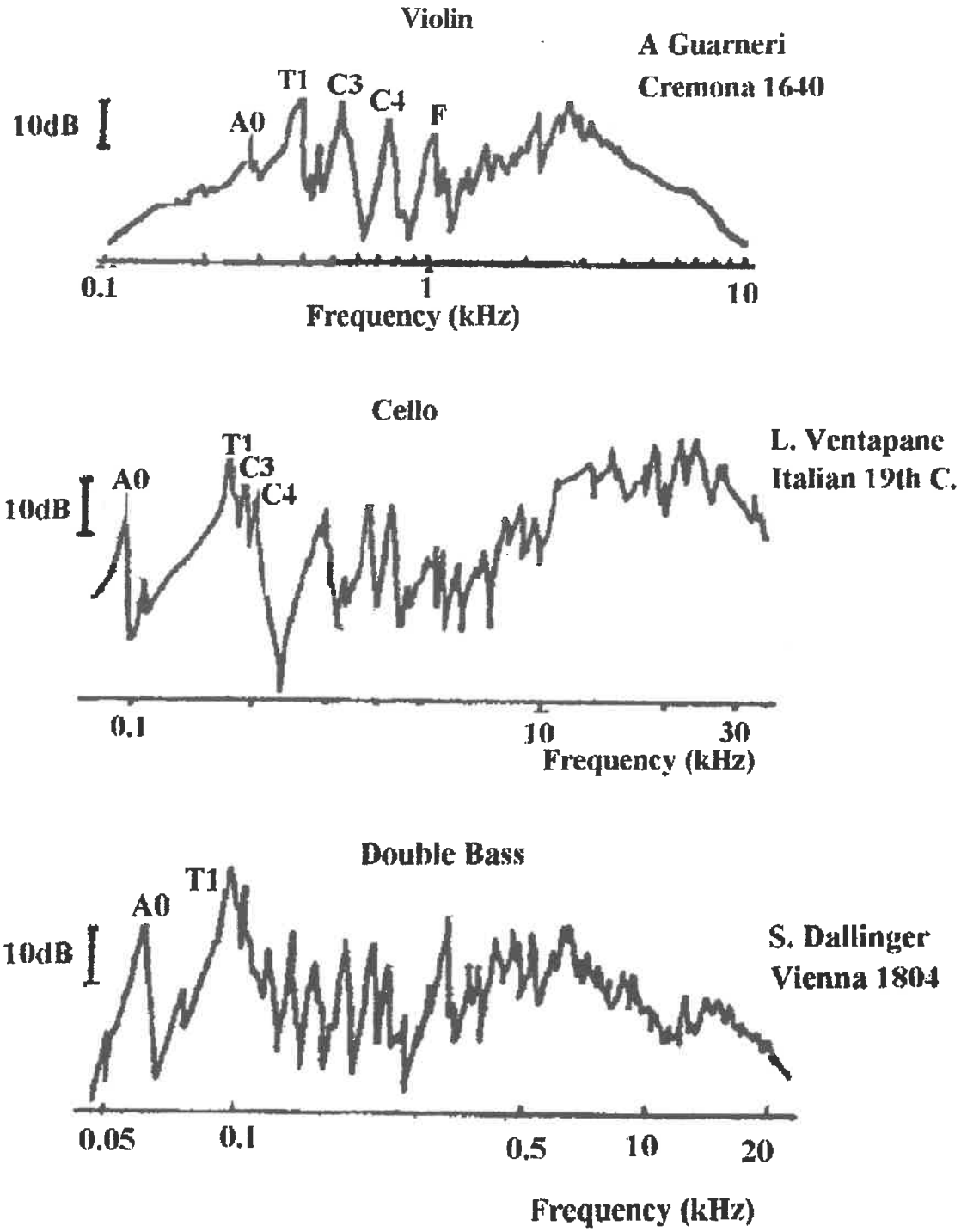

Figure 1.1 Input Admittance of Some Stringed Instruments [after Askensfelt[2]]

A plucked string in its steady state of vibration contains overtones which, in simple textbook terms, are harmonics or integral multiples of the fundamental vibrating frequency. In practice, the frequency of overtones can differ significantly from these values due to factors[3] such as the significant stiffness of real strings, the clamping effect of the string hole on string ends and the fact that the string anchor point on the soundboard is itself vibrating. Amplitude of vibration varies from one overtone to another. While there is a general tendency for amplitudes to decline with increasing harmonic number[4], this tendency may be counteracted by factors such as plucking position[5] along the length of the string and the variation with frequency of coupling conditions between string and soundboard at the string point.

The uneven frequency response of the instrument body produces different amplifications at each frequency. This uneven frequency response of the body operating on the input spectrum of the string helps to give a unique tone to each instrument.

In addition to the steady state frequencies of the vibrating string, there are other frequencies input to the body. The initial pluck is an impulsive excitation containing essentially a continuous spectrum. It therefore can set in motion a wide range of the vibrational resonances (modes) of the body. Although these die out over a short time, leaving only the steady state string spectrum resonantly amplified in a characteristic way, they make a vital contribution to the unique temporal quality of the musical note from a particular instrument.

The manner in which the note dies away also affects its perceived tonal quality. In the case of the harp, according to Richardson[6], the variation in the tension of the string, while vibrating, inputs a driving force perpendicular to the board which can regenerate decayed harmonics and overall, give rise to non-linear decays.

1.2 Admittance

The driving point or input admittance is the velocity of the point on the body or soundboard driven per unit driving force, under conditions of steady state alternating driving force. For a given instrument the admittance varies with the frequency as shown in figure 1.1 and with the position of the driving point.

The amplitude of the a.c. force input to the body from a plucked string varies with frequency, while the admittance is a measure of the response of the driven point when the same force amplitude is input at all frequencies. The admittance enables one to assess the relative resonant amplification at all frequencies in the testing range. The plot of driving point admittance versus frequency, the so-called "admittance plot" is therefore the fingerprint[7] of the instrument. As shown in figures 1.1 it has a different shape for each instrument. The shape or profile is characteristic of that instrument and is linked to the tonal quality or timbre of the notes from that instrument. Differences between the admittance plots of versions of the same basic instrument can indicate considerable differences in tonal quality between these instruments. It will be seen from the results of this work, that although different versions of the harp have similar admittance plots, they do display important differences.

1.3 Construction of Musical Instruments

The frequencies at which resonances occur, the strength of the response at each resonant frequency and the sharpness or Q factor of each resonance are related to the mechanical parameters of the instrument body. These parameters include the elasticities of its component materials, their densities and the geometric shape of the body. In addition, where there is an air cavity, its volume, dimensions, hole areas and lip thicknesses also play a role. Another important factor is the coupling between different resonant modes and this will be discussed in chapter 5.

In principle, therefore, it should be possible to construct a musical instrument of good tonal quality by first determining and optimising the physical parameters of

the body and of the strings. This has been done with a degree of success for instruments of the violin family by Carleen Hutchins, the pioneer of musical instrument acoustics who is also a luthier[8]. A Stradivarius has not been replicated but it is claimed that instruments of very good tonal quality have been produced.

However, in general, it can be said that variations in the physical properties of wood (the most common instrument body material), even in adjacent pieces from the same tree, together with the intricacies of mode coupling, make the task of reproducibly constructing a wooden musical instrument based on quantitative physical parameters a very complex one.

A further problem is exemplified by the very weak response of the body of the harp to excitation over a frequency range which includes the fundamental frequencies of its bass strings. This can be seen from the admittance plots contained in chapter 5 of this work. Nevertheless, on plucking a bass string the pitch corresponding to its fundamental frequency of vibration is clearly heard by the ear. The explanation lies in the fact that the ear hears the pitch which corresponds to the repeat time of the sound wave incident on it. Several overtones of the bass string lie in a frequency range in which there is a strong response from the body of the instrument. Superposition of the sound waves corresponding to these overtones gives rise to a wave whose repeat time is that of the fundamental frequency of the string. For example, a tone made up of frequency components 500 Hz, 600 Hz and 700 Hz repeats at a time interval of 0.01 s which corresponds to a frequency of 100 Hz. Consequently the pitch perceived is that corresponding to 100 Hz. It is therefore clear that a knowledge of the manner in which the ear perceives pitch is also necessary for the scientific construction of musical instruments

According to Richardson[9], the best instruments are constructed by individual makers or by small groups of skilled craftsmen, who work to traditional designs and employ mainly hand-tool techniques. "The most elusive aspect of the maker's art is his ability to produce instruments with consistent or predetermined tone qualities.... At present, all but the very best of makers

perform this task with a very high degree of uncertainty. Makers are not secretive about their methods but find that their knowledge is difficult to share because their skills are intuitive and acquired over long periods while apprenticed to a master luthier." These observations by Richardson are supported by Áine Ní Dhúill[10], harpist, and by Colm Ó Meachair, harp-maker, Dublin[11].

Nevertheless, a Japanese company is mass-producing Irish folk harps and marketing them on a world scale, including in Ireland. According to Gráinne Yeats, eminent Irish Folk Harpist and recording artiste, the mass-produced harps are adequate for students learning to perform[12].

It is becoming clear that if the Irish harp-maker is to survive economically, traditional skills must be complemented by the methods of science and technology.

It is hoped that this work will form a small contribution to the process of making scientific methods available to Irish harp-makers.

References

---

[1]Hutchins, C.M., The Physics of Violins; Scientific American, Nov, pp 78 - 93 (1962)

[2]Askenfelt, A., Eigenmodes and Tone Quality of the Double Bass. CASNL, 38, pp 34 - 36 (Nov 1982).

[3]Benade Arthur, H., Fundamentals of Musical Acoustics, Chapter 16, p 313, Dover Publications Inc., New York, 1990.

[4]Taylor, C.A., The Physics of Musical Sound; pp 41 - 43, English University Press, London (1966).

[5]Benade Arthur, H., Fundamentals of Musical Acoustics, Chapter 7, p 102, Dover Publications Inc., New York, 1990.

[6]Richardson, B.E., Vibrations of Stringed Musical Instruments, University of Wales, Review, Vol. 4 pp 13 - 20 (1988).

[7]Richardson, B.E., Good Vibrations; Physics Education, Vol. 25, No. 1, p 36 (Jan 1990).

[8]Hutchins, C.M., 1981 Scientific American 245,170. (1981)

[9]Richardson, B.E., Vibrations of Stringed Musical Instruments, University of Wales, Review, (1988).

[10]Communications with Áine Ní Dhúill, harpist. (1993)

[11]Communications with Colm Ó Meachair, harp-maker. (1993)

[12]Communications with Gráinne Yeats, harpist. (1993)

Chapter 2

STRUCTURE AND OPERATION OF HARPS

2.1 The Ó Meachair Cedar and Mahogany Harp

This Ó Meachair cedar and mahogany harp has 34 strings, two short of five octaves. The shorter strings at the upper (treble) end produce the higher pitch notes. The lowest pitch string is a C and the highest is an A. Each octave contains 7 notes. It is usual in the harp to count octaves from the treble end downwards, each octave beginning with an E string and ending with the F string below. Calthorpe[1] classifies the topmost three strings (F, G, A) as being above the first octave, while Firth[2] classifies the same strings as first octave. As the harp in the experiments reported in this thesis was tuned with an electronic tuner working to an even-tempered scale with the A above middle C set at 440 Hz, and in order to avoid confusion, the strings in these experiments were classified as in table 2.1.

The treble strings are of nylon and the bass strings are of wire wound on silk. The transition from one string material to the other takes place between E4 and F4. The strings make an angle of 40° to the soundboard at F1 and of 37° to the soundboard at F5. A very gradual variation in the angle takes place between these string points. Firth[2] quotes a string angle of 32° for the Clarsach examined by him.

Cross-blades on the curve or string-arm, when turned upwards, increase the pitch of each string by one semitone.

The soundboard is of quarter-sawn cedar, believed to be of the Western Red variety. The pieces are edge-jointed so that the grain runs across the board perpendicular to the string plane. The thickness of the soundboard tapers from 4.5 mm at the base end to 1.5 mm at the treble end. The spruce soundboard on the Clarsach examined by Firth[2] tapered in thickness from 8 mm to 2 mm.

String Name	Frequency as Tuned (Hz)
A 1	1760.0
G 1	1568.0
F 1	1396.0
E 1	1318.4
D 1	1174.8
C 1	1046.6
B 2	987.8
A 2	880.0
G 2	784.0
F 2	698.4
E 2	659.2
D 2	587.4
C 2	523.3
B 3	493.9
A 3	440.0
G 3	392.0
F 3	349.2
E 3	329.6
D 3	293.7
C 3	261.6
B 4	247.0
A 4	220.0
G 4	196.0
F 4	174.6
E 4	164.8
D 4	146.9
C 4	130.8
B 5	123.5
A 5	110.0
G 5	98.0
F 5	87.3
E 5	82.4
D 5	73.5
C 5	65.4

Table 2.1 Stringing on Irish Folk Harp

Its extreme width at the base end was 6.0 cm less than that of the Ó Meachair Cedar and Mahogany Harp.

All other wooden parts are of mahogany, including strain bar, cover bar, soundbox, column and string arm. The salient dimensions are set out in figures 2.1(a), (b), (c) and (d).

2.2 The Ó Meachair Spruce and Maple Harp

In the Ó Meachair Spruce and Maple Harp the stringing is identical to that of the Ó Meachair Cedar and Mahogany Harp. The only change in soundboard measurement is that the spruce soundboard tapers from 4 mm in thickness at the bass end to 1 mm in thickness at the treble end. The maximum height of the spruce and maple harp is slightly greater at 130.5 cm than that of the former one.

While the overall shapes of the soundbox and air-holes are the same in the two harps, the dimensions show small but significant differences. The relevant dimensions of the spruce and maple harp are set out in figures 2.2(a), (b) and (c).

References

[1]Calthorpe, N., Begin the Harp. Waltons Mnf. Ltd., Dublin, Ireland (1986).

[2]Firth, I., Acoustics of the Harp. Acus, 37, pp 148 - 154 (1977).

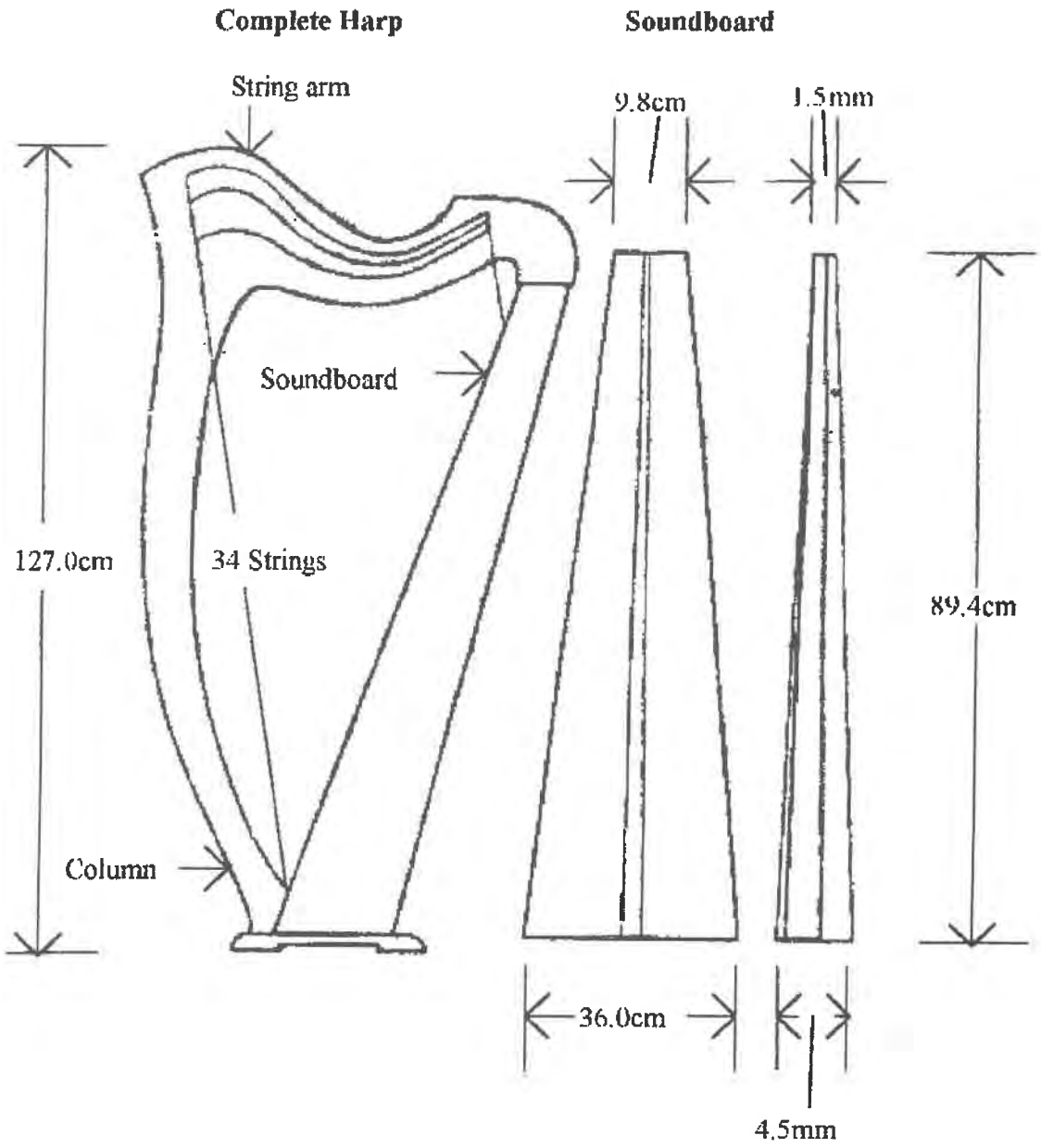

Figure 2.1(a) Dimensions of Ó Meachair Cedar and Mahogany Harp.

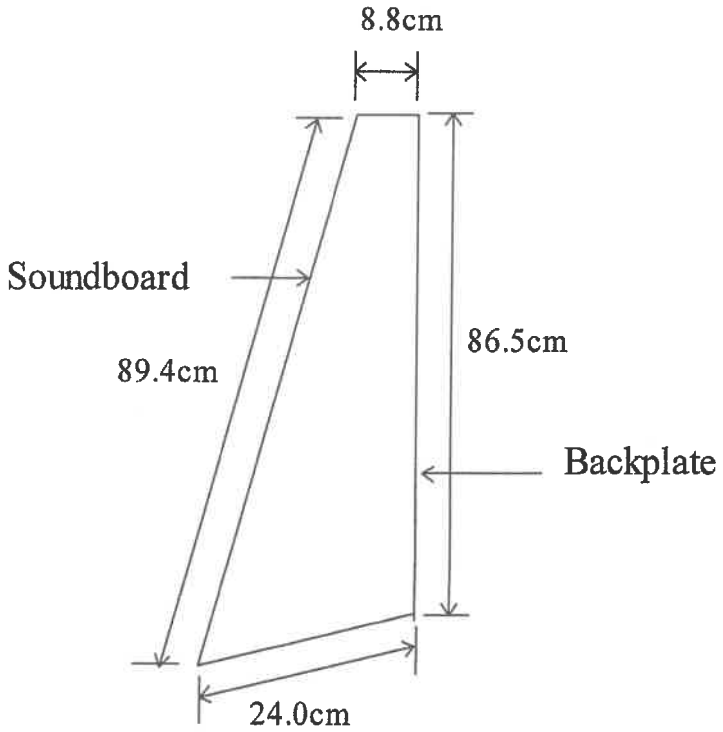

Sideview of Soundbox

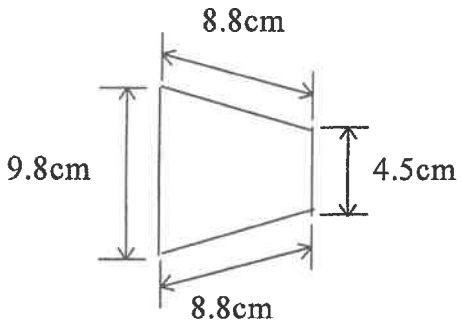

Top view of soundbox

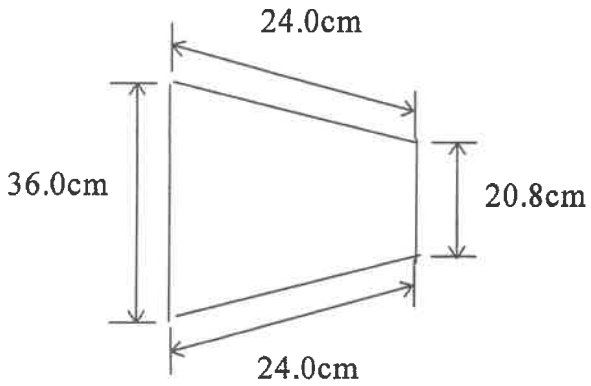

Bottom view of soundbox

Figure 2.1(b) Dimensions of Ó Meachair Cedar and Mahogany Harp.

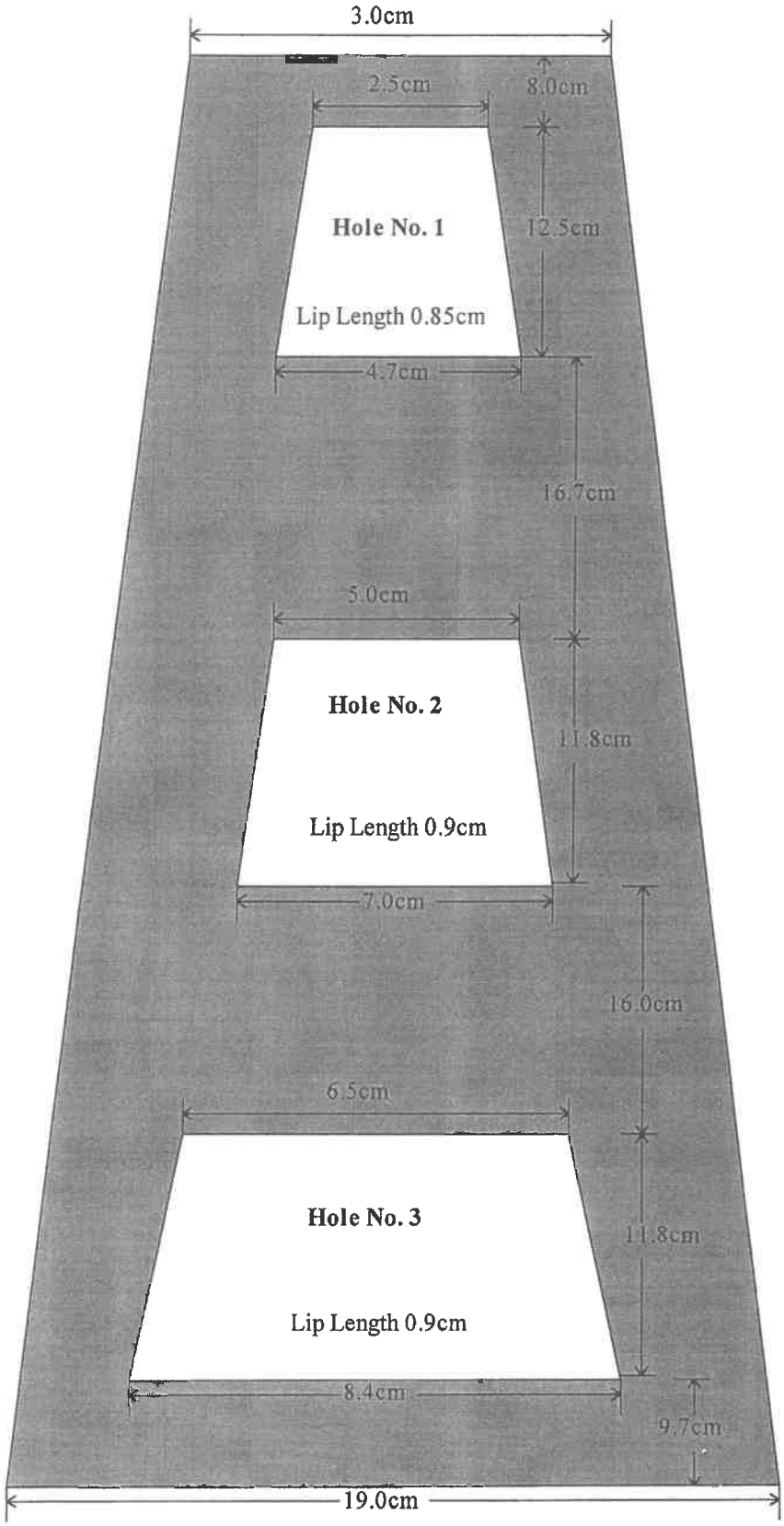

Figure 2.1(c) Dimensions of Ó Meachair Cedar and Mahogany Harp.

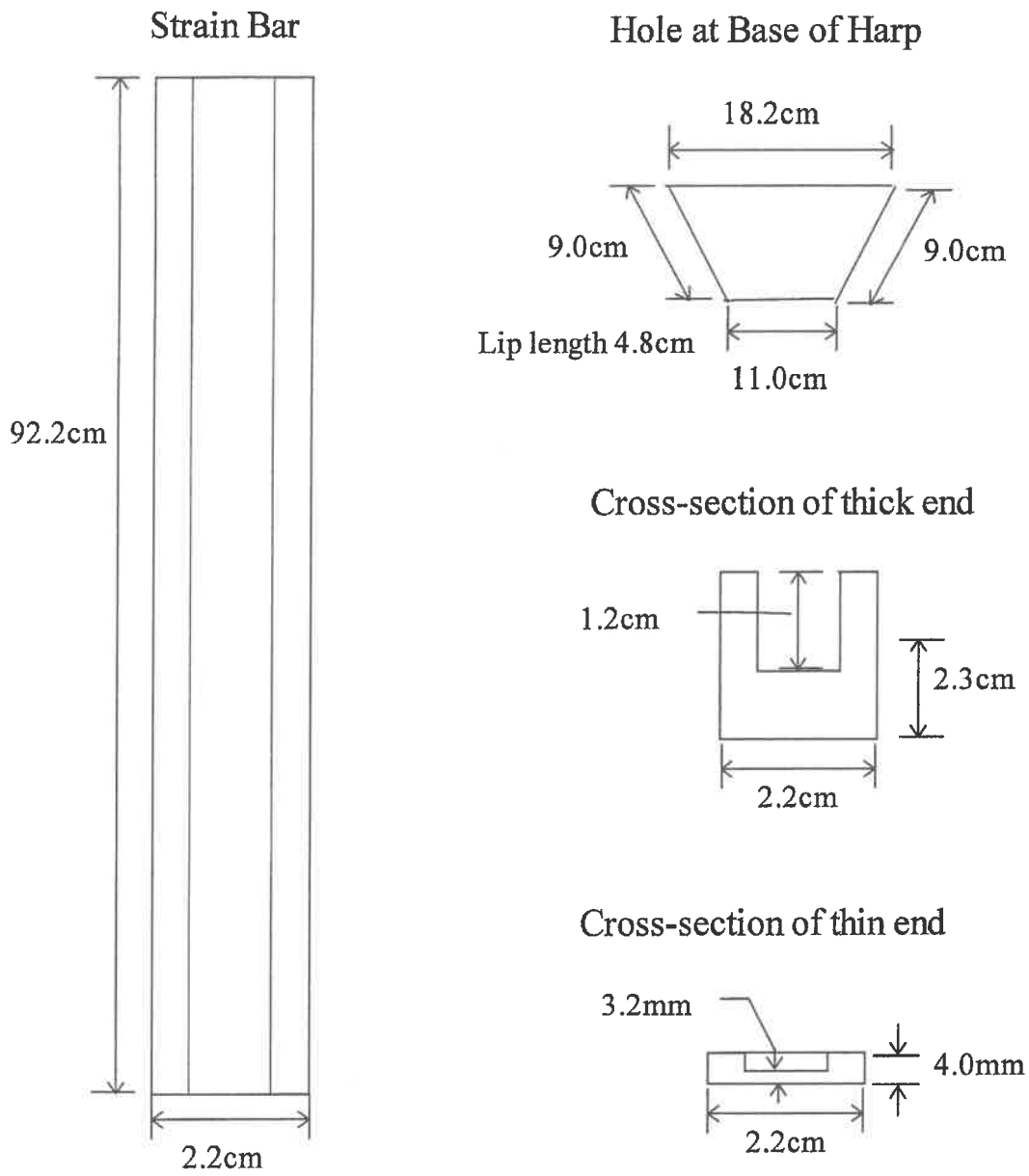

Figure 2.1(d) Dimensions of Ó Meachair Cedar and Mahogany Harp.

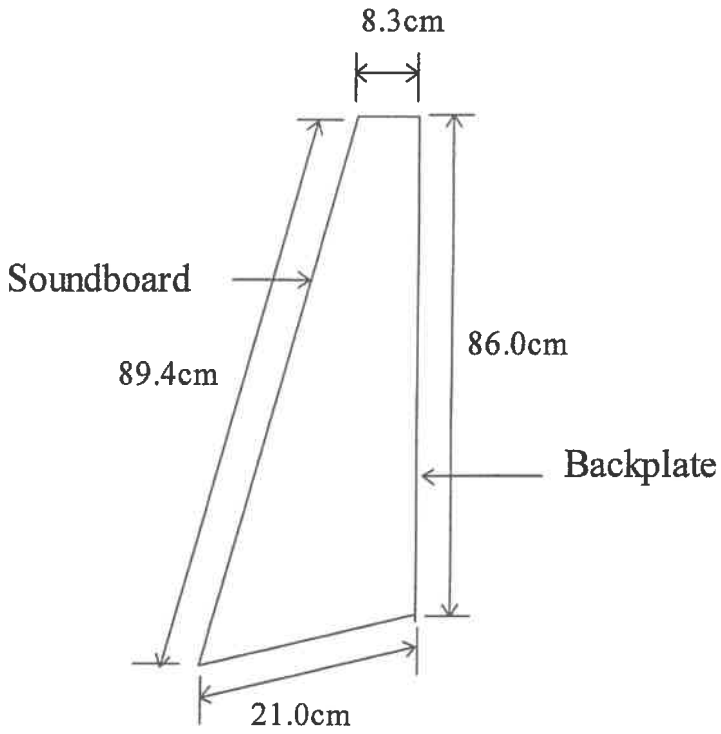

Sideview of Soundbox

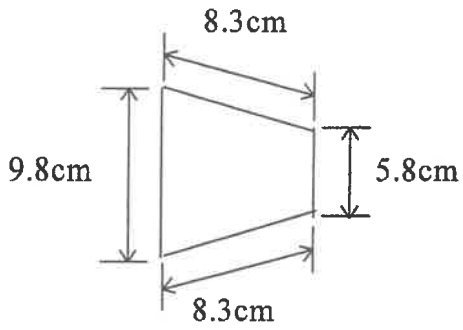

Top view of soundbox

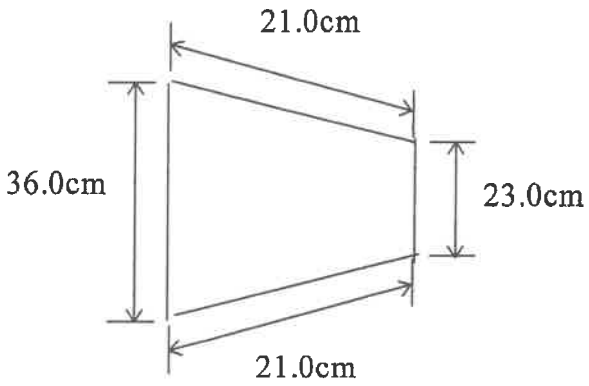

Bottom view of soundbox

Figure 2.2(a) Dimensions of Ó Meachair Spruce and Maple Harp.

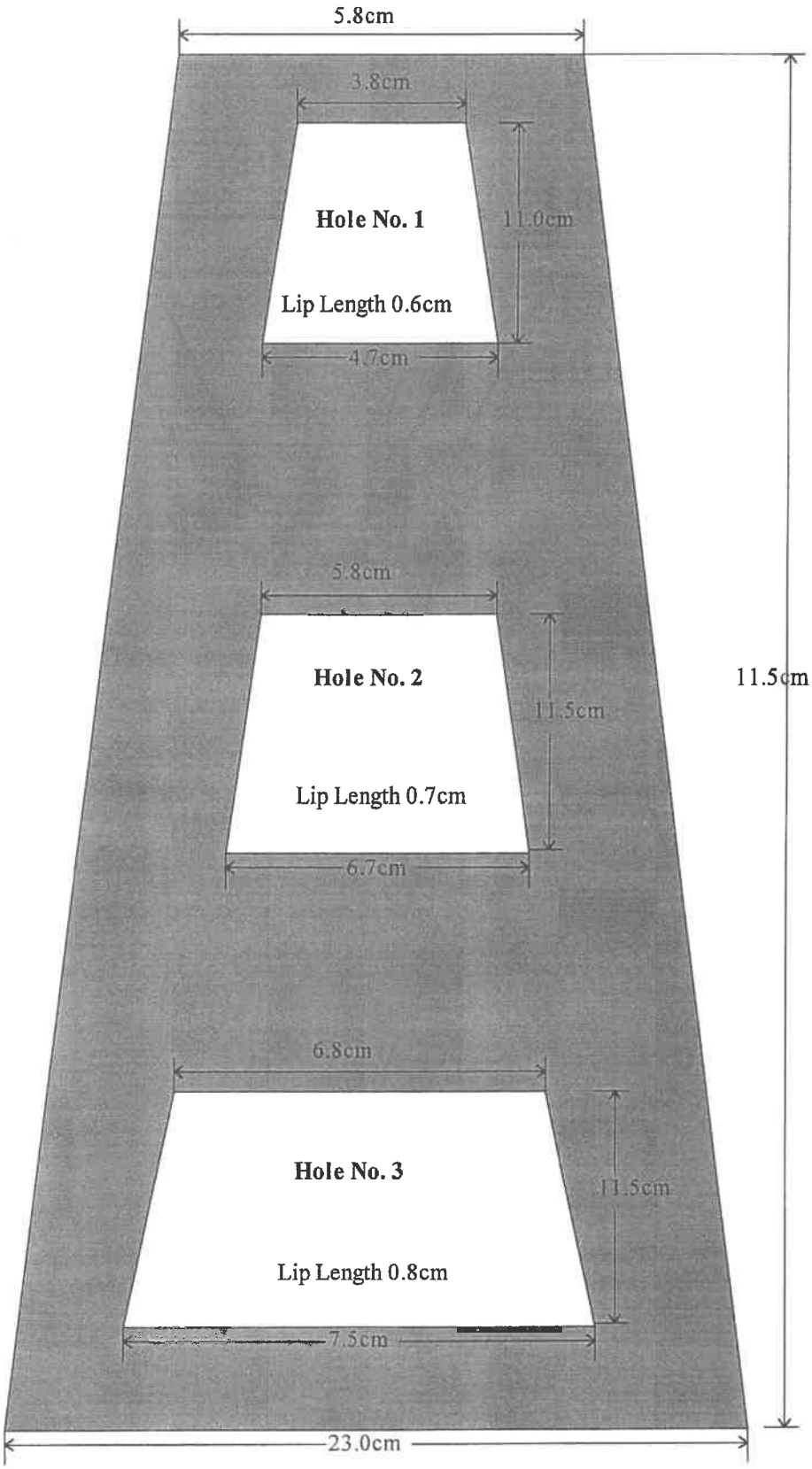

Figure 2.2(b) Holes in Back Plate of Ó Meachair Spruce and Maple Harp.

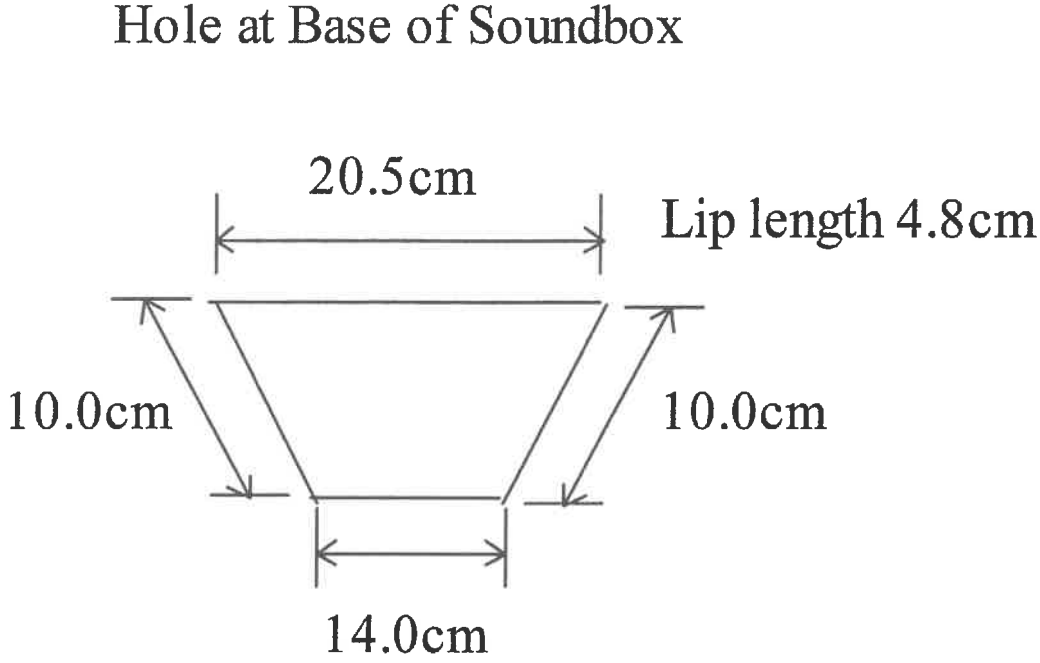

Figure 2.2(c) Dimensions of Ó Meachair Spruce and Maple Harp.

CHAPTER 3

THEORETICAL BACKGROUND AND EXPERIMENTAL PROCEDURES.

3.1 Introduction

In this investigation, the completely strung harp was tested first using the input admittance method. Then the same method was used to test a held and barred soundboard isolated from a harp instrument body. Finally, the held and barred soundboard was investigated by the Chladni powder pattern method. The object of the experiments on the held and barred soundboard was to assist in the analysis of the vibrations of the fully strung instrument and to gather data that may later be useful in the scientifically based construction of Irish folk harps.

In this chapter the theoretical background to the methods used is set out and an account is given of the experimental procedures employed.

3.2 Theory of Flexural Vibrations of a Plate

Though wood is not an isotropic material, it is useful to consider first the flexural vibrations of an isotropic plate. Because the slight lateral expansion that accompanies a compression is constrained in the plane of a flat plate, the speed of longitudinal (compressional) waves, C_L, is slightly greater than in a bar[1], thus

$$C_L = \sqrt{\frac{E}{\rho(1-\sigma^2)}} \qquad (3.1)$$

where E is Young's modulus of elasticity, ρ is density, σ is Poisson's ratio.

The equation of motion for flexural waves of small amplitude in an infinite plate is given by

$$\nabla^4\phi + \left(\frac{12}{h^2}\right)\left(\frac{1}{C_L^2}\right)\frac{\partial^2\phi}{\partial t^2} = 0 \qquad (3.2)$$

or

$$\nabla^4\phi + \frac{12\rho(1-\sigma^2)}{Eh^2}\frac{\partial^2\phi}{\partial t^2} = 0 \qquad (3.3)$$

where h is plate thickness and ϕ is the displacement of the plate perpendicular to the static plane of the plate.

For harmonic solutions,

$$\phi = \Phi(x,y)e^{j\omega t} \qquad (3.4)$$

where ϕ is complex and $\omega = 2\pi f$, where f is the frequency.

By substitution,

$$\nabla^4\Phi - \left(\frac{12\rho(1-\sigma^2)\omega^2}{Eh^2}\right)\Phi = 0 \qquad (3.5)$$

$$\nabla^4\Phi - k^4\Phi = 0 \qquad (3.6)$$

$$\text{where } k^2 = \frac{\omega\sqrt{12}}{h}\left(\sqrt{\frac{\rho(1-\sigma^2)}{E}}\right) = \frac{\omega\sqrt{12}}{hC_L} \qquad (3.7)$$

Such flexural waves are dispersive, that is, their phase speed v varies with frequency, thus

$$v = \frac{\omega}{k} = \sqrt{1.8\,fhC_L} \qquad (3.8)$$

The solution of the differential equation for $\Phi(x, y)$ is generally achieved by separation of variables. Initial conditions and boundary conditions must then be taken into account in each particular case to get an exact solution.

In all cases, the set of solutions involves discrete frequencies. These are the resonant frequencies or modes of the plate.

For an isotropic rectangular plate with simply supported (hinged) edges, Rossing[1] gives the solution as

$$\Phi(x,y) = A\sin(m\pi x / L_x)\sin(n\pi y / L_y) \qquad (3.9)$$

where L_x and L_y are the length and width, respectively, and m and n are integers each beginning with zero.

The resonant frequencies are given by

$$f(m,n) = 0.453\, C_L h\left[\left(\frac{m}{L_x}\right)^2 + \left(\frac{n}{L_y}\right)^2 + \frac{2mn}{L_x L_y}\right] \qquad (3.10)$$

The manner in which the soundboard is affixed to the soundbox of the harp approximates to the clamped edge situation. In some experiments in this project, a separate soundboard, isolated from the harp soundbox, was clamped all around the edges.

Due to the extra stiffness created by the clamping at the edges, the resonant frequencies are expected to be somewhat higher in the clamped case than in the unclamped or hinged case[2]. This difference between resonant frequencies for the clamped case and hinged case is greatest for the low frequency modes and generally declines progressively as resonant frequencies increase.

Rossing[1] presents the nodal patterns for a square isotropic plate which is clamped all around the edges. These are shown in figure 3.1. He also presents the relative frequencies for the four lowest frequency modes of a clamped rectangular isotropic plate for different ratios L_x / L_y. These are shown in table 3.1.

When a plate bends concavely downwards in one direction, the upper layers stretch and the lower layers contract in that direction, as in a bending beam. This causes a contraction in the perpendicular direction in the upper layers and an expansion in the perpendicular direction in the lower layers, an effect known as the Poisson Effect. If the frequencies of different modes are close together or identical, the above process can cause significant Poisson coupling between them[1]. In the square isotropic plate, the coincidence in frequency of the (1,3) and (3,1) modes and the Poisson coupling between them causes the plate to resonate at two separate frequencies, that of the cross-mode being lower than that of the ring-mode. This is due to a different phase relationship in the coupling. So, in the (3,1) - (1,3 case, the separate vibrations aid each other but in the ring-mode they oppose each other. This adds a little stiffness to the ring-mode, thereby raising its frequency.

Rossing[1] points out that in a quarter-sawn rectangular spruce plate, in which Young's modulus is 16 times greater along the grain than across the grain, the coincidence of frequency that leads to the appearance of the cross mode and the ring mode occurs if the length of the plate is twice its breadth. In the harp soundboard, however, the quarter-sawn spruce or cedar pieces are edge-jointed so that the grain runs across the board. This means that there is no length to breadth ratio in this case for which modes such as (3,1) and (1,3) would coincide in frequency. Mode splitting associated with this type of coincidence of frequency is therefore not to be expected in the harp soundboard.

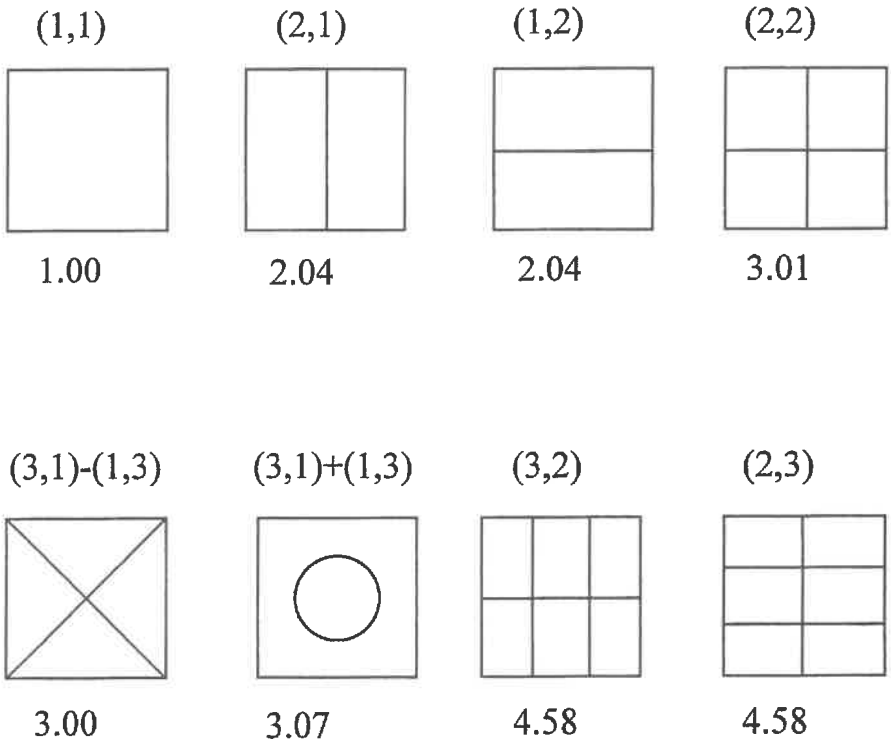

Figure 3.1 Nodal patterns for the first eight modes of a square plate with clamped edges. Relative frequencies are given below the patterns.(after Rossing)[1]

Mode	$L_x/L_y = 1$	1.5	2	2.5	3	∞
(1,1)	1.00	0.75	0.68	0.66	0.64	0.62
(1,2)	2.04	1.88	1.82	1.79	1.78	1.72
(2,1)	2.04	1.16	0.88	-	-	-
(2,2)	3.01	2.27	2.02	1.91	1.86	1.72

Table 3.1 Relative Vibrational Frequencies of Rectangular Plates with Clamped Edges (after Rossing)[1]

3.3 Wooden Plates

Wood is an orthotropic substance. Its Young's modulus has three different values, E_x (along the grain), E_y (across the grain and perpendicular to the tree rings) and E_z (along the tree rings).

Caldersmith[3] takes twisting elasticity, as well as bending elasticity, into account in finding an expression for the resonant frequencies of the hinged wooden plate. Account is also taken of the significantly differing values of Poisson's ratio along the two axes of the wooden plate. The resonant frequencies may then be written

$$f^2(m,n) = \frac{h^2}{4.86\,\rho}\left[\frac{D_x m^4}{L_x^4} + \frac{D_y n^4}{L_y^4} + 2D_{xy}\frac{m^2 n^2}{L_x^2 L_y^2}\right] \qquad (3.11)$$

where $D_x = E_x/(1 - \sigma_x\sigma_y)$, $D_y = E_y / (1 - \sigma_x\sigma_y)$ and D_{xy} is the twisting modulus, given by $D_{xy} = D_x\sigma_y + 2G$, where G is the shear modulus.

As pointed out earlier, the resonant frequencies expected for a clamped plate are higher than those for a hinged plate with the differences getting progressively less as one moves to higher modes.

The harp soundboard is not rectangular but trapezoidal in shape. In relation to the narrower end of the board the equivalent rectangular plate would have $L_x / L_y \approx 9$ and in relation to the wider end of the board $L_x / L_y \approx 2.5$ for the equivalent rectangular plate.

Furthermore, a piece of wood as well as having three orthogonal values of Young's modulus, has three values of shear modulus and six values of Poisson's ratio. According to McIntyre[4] there are also nine separate internal damping coefficients. If a theoretical vibrational analysis of a harp soundboard

is to be carried out, all these factors, in addition to the effects of the edge-jointing, of the trapezoidal shape of the board and of the tapered thickness, must be taken into account. The data accumulated here should be of some assistance in such a process.

Further complications are added when the cover and strain bars made of another stiffer wood are firmly glued to the central axis of the board.

3.4 Mechanical Resonance

When the board is impulsively excited by plucking a string attached to it, the board will vibrate with all its resonant frequencies simultaneously. The resonant modes will die out over time, but generally at different rates depending on the degree of damping associated with each mode. It should be possible to find these modes through a Fourier analysis of the onset transient response of the board to the plucked string.

Except at high frequencies where the resonant frequencies effectively merge into a continuum, if a sinusoidal force is applied at the same frequency as that of a resonant mode, that resonance will occur, giving rise to large amplitude vibrations of the board. If the point of application of the driving force is near a node for the resonant mode concerned, the vibrations will be much smaller than if the point of application were in an anti-nodal region. If other resonances, either of the board itself or of structures to which the board is attached, are coupled to the particular mode concerned, such resonant modes will also be set in motion.

Such a resonance can be treated broadly by analogy with a single degree of freedom under-damped spring-mass system driven sinusoidally. Hussey[5] gives the following treatment of the topic.

The equation of motion is

$$F(t) - b\dot{x} - kx = m\ddot{x} \qquad (3.12)$$

where F(t) is the applied sinusoidal force, b is the damping coefficient, m is the mass attached to the spring, k is the stiffness of the spring and x is the displacement of the mass.

Dividing each term by m, one obtains

$$\ddot{x} + 2\alpha\dot{x} + \omega_o^2 x = g(t) \qquad (3.13)$$

where $g(t) = \frac{F(t)}{m}$, the so-called coefficient of decay $\alpha = \frac{b}{2m}$ and $\omega_o^2 = \frac{k}{m}$

where $f_0 = \frac{\omega_0}{2\pi}$ is the undamped resonant frequency of the system.

If $F(t) = F_o \cos \omega t$, then $g(t) = G_o \cos \omega t$ and $G_o = \frac{F_o}{m}$.

The solution to the differential equation can be written for the steady state, in the case of under-damping, as

$$x = A\cos(\omega t - \gamma) \qquad (3.14)$$

A and γ can be found by substitution in equation (3.13), thus

$$A = \left(\frac{1}{\sqrt{(\omega_o^2 - \omega^2)^2 + (2\alpha\omega)^2}} \right) G_o \qquad (3.15)$$

and

$$\gamma = \tan^{-1}\left(\frac{2\alpha\omega}{\omega_o^2 - \omega^2}\right) \tag{3.16}$$

The amplitude A is a function of the applied frequency $f = \frac{\omega}{2\pi}$, and becomes a maximum (and resonance occurs) when $\omega = \sqrt{\omega_o^2 - 2\alpha^2}$

When damping is very slight $\omega \approx \omega_0$. Then the maximum value of the displacement amplitude A may be written in a number of ways.

$$A_{max} = \frac{G_o}{2\alpha\sqrt{\omega_o^2 - \alpha^2}}$$

$$= \frac{G_o}{2q\omega_o^2\sqrt{1-q^2}}$$

$$= \frac{G_o}{2\alpha^2\sqrt{4Q^2 - 1}} \tag{3.17}$$

where the damping ratio $q = \frac{b}{b_c} = \frac{\alpha}{\omega_o} = \frac{b}{2\sqrt{km}}$, b_c being the damping coefficient at critical damping.

The quality factor $Q = \frac{1}{2q} = \frac{\sqrt{km}}{b} = \frac{\omega_o}{2\alpha}$

A high value of Q is indicative of a system with low coefficient of decay α and low damping ratio q. In such a system the value of A_{max} is high and the resonance is said to be high. Also due to the low decay coefficient, the resonance amplitude declines slowly when the driving force is removed.

3.5 Impedance

The mechanical impedance Z of the damped mass/spring system is defined as the ratio of the driving force to the resulting velocity of the mass.

$$Z = \frac{F(t)}{\dot{x}} \tag{3.18}$$

and it has units of kg/s.

For a thorough analysis of impedance, it is instructive to use the complex solution to equation (3.13) for the underdamped case in the steady state, thus

$$x = Ae^{j(\omega t-\gamma)} \tag{3.19}$$

The real part of this solution is equation (3.14). Then

$$\dot{x} = j\omega Ae^{j(\omega t-\gamma)} \tag{3.20}$$

The complex form of the driving force is $F(t) = F_o e^{j\omega t}$

The complex mechanical impedance is then given by

$$Z = \frac{F_o e^{j\omega t}}{j\omega Ae^{j(\omega t-\gamma)}}$$

$$= \frac{m}{\omega}\left[2\alpha\omega - j\left(\omega_0^2 - \omega^2\right)\right]$$

$$= b - j\left(\frac{k}{\omega} - m\omega\right) \tag{3.22}$$

putting $\omega_0^2 = \frac{k}{m}$ and $2\alpha = \frac{b}{m}$.

The magnitude of Z is given by

$$|Z| = \sqrt{\left[b^2 + \left(\frac{k}{\omega} - m\omega\right)^2\right]} \qquad (3.22)$$

and the phase angle is given by

$$\phi = \tan^{-1}\frac{\left(\frac{k}{\omega} - m\omega\right)}{b} = \frac{\pi}{2} - \gamma \qquad (3.23)$$

The complex mechanical impedance Z can therefore be written

$$Z = |Z|\, e^{-j\phi} \qquad (3.24)$$

When $f = f_0 = \frac{\omega_0}{2\pi}$, the undamped natural frequency, the imaginary part of the impedance is zero and the impedance reduces to b, the damping coefficient, and the phase angle ϕ becomes zero. The impedance is then a minimum, the velocity of the mass and the driving force are in phase and resonance occurs.

At frequencies less than f_0, the stiffness of the spring predominates over the inertia of the mass and the system is said to be stiffness controlled. The phase angle ϕ is then positive. At frequencies greater than f_0, the mass predominates over the stiffness, the system is said to be mass controlled and the phase angle ϕ is negative.

3.6 Admittance

The admittance is the inverse of the impedance.

The magnitude of the admittance B is given by

$$B = \frac{1}{|Z|} = \frac{1}{\sqrt{\left[b^2 + \left(\frac{k}{\omega} - m\omega\right)^2\right]}} \tag{3.25}$$

Since the impedance is a minimum at resonance, the admittance is a maximum at resonance.

If B_0 be a chosen reference value of admittance, one can define an amplification ratio or gain, (G) thus

$$G = \frac{B}{B_o} \tag{3.26}$$

The admittance B varies with the position of the driving point and with frequency. As B_0 is a constant, G is thus a function of driving point position and of frequency.

It is customary to express the G on a logarithmic scale

$$\log_{10} G = \log_{10} \frac{B}{B_o} \tag{3.27}$$

$$= \log_{10} B - \log_{10} B_o \tag{3.28}$$

On a decibel scale, this expression becomes

$$20\log_{10} G = 20\log_{10} B - 20\log_{10} B_0 \tag{3.29}$$

Hence, if measured admittance is expressed on the dB scale, relative gain and relative admittance are identical and can be found by subtracting the two admittances concerned when expressed on the dB scale.

3.7 Power in the Resonant System.

The time averaged vibrational power delivered to the system is given by

$$P = \frac{F_0^2}{4\alpha m}\left[\frac{(2\alpha\omega^2)}{(\omega_0^2-\omega^2)^2+(2\alpha\omega)^2}\right]$$

$$= P_0\left[\frac{(2\alpha\omega^2)}{(\omega_0^2-\omega^2)^2+(2\alpha\omega)^2}\right] \qquad (3.30)$$

where P_0 is the value of P at $\omega = \omega_0$.

P is plotted against ω in figure 3.2.

Finding the values of ω at the half-power points from equation (3.30), one finds

$$\omega_1 = \sqrt{(\omega_0^2+\alpha^2)}-\alpha \qquad \text{and} \qquad \omega_2 = \sqrt{(\omega_0^2+\alpha^2)}+\alpha.$$

The resonance width $\Delta\omega = \omega_2 - \omega_1 = 2\pi\,\Delta f = 2\alpha$.

The quality factor Q, may therefore be written in the alternative versions, thus

$$Q = \frac{\omega_0}{2\alpha} = \frac{\omega_0}{\Delta\omega} = \frac{f_0}{\Delta f} \qquad (3.31)$$

When the damping is increased, for instance from α_1 to α_2 in figure 3.2, the maximum of the curve is reduced and the width between the half-power points is increased. In this case Q is reduced and the sharpness of the resonance curve is also reduced.

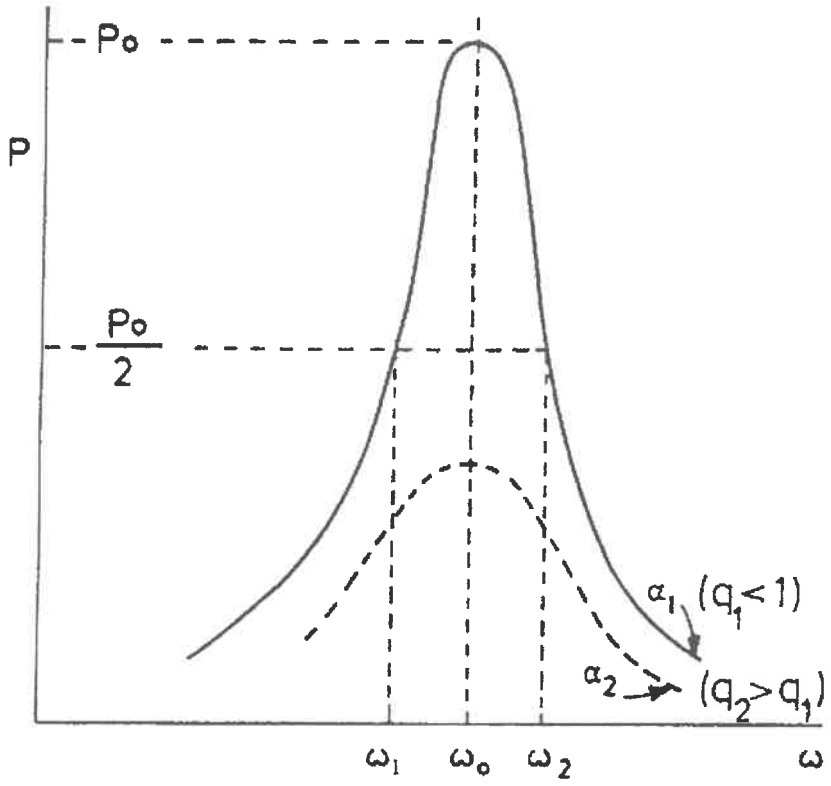

Figure 3.2 Average power (P) dissipated in the damped harmonic oscillator as a function of driving frequency f [=ω/(2π)]

Substituting the basic system parameters for ω_0^2 and 2α in equation 3.30.

$$P = \tfrac{1}{2}\frac{bF_0^2}{|Z^2|} = \tfrac{1}{2}bF_0^2B^2 \qquad (3.32)$$

Where B is the magnitude of the admittance.

3.8 Resonant Modes of a Distributed Mass System

By analogy with the above treatment, which applies to a discrete point mass connected to a discrete spring, one can consider resonant modes of a distributed mass/spring object, such as a soundboard. One can attribute to the mode at each driving point an effective mass, an effective stiffness, as well as an effective damping coefficient. The impedance/admittance is likely to vary, not only with the frequency, but also with the point of application of the force. If this point is near to a node on the soundboard, the admittance will be expected to be reduced.

The resonant frequency of such a mode is given by

$$f_0 = \frac{\omega_0}{2\pi} = \frac{1}{2\pi}\sqrt{\frac{k}{m}}$$

where m is the effective mass of the mode and k is the effective stiffness of the mode.

Both the effective mass and the effective stiffness tend to have minimum values at driving points which are anti-nodes for the mode concerned and tend to increase to maximum values as the driving point approaches points which are nodes for the mode concerned.

A small additional mass placed on the soundboard brings about the greatest change in resonant frequency when placed at a point on the board which is an anti-node for the resonant mode concerned.

For a given point on the soundboard, the effective stiffness k being constant, the rate of change of resonant frequency with effective mass is given by

$$\frac{df_0}{dm} = \frac{1}{2\pi} k^{\frac{1}{2}} \left(-\frac{1}{2}\right) m^{\frac{-3}{2}}$$

$$\frac{df_0}{dm} = -\frac{1}{2}\frac{f_0}{m} \qquad (3.33)$$

The fractional change in resonant frequency brought about by a small change in mass Δm at the driving point is, therefore, given by

$$\frac{\Delta f_0}{f_0} \approx -\frac{1}{2}\frac{\Delta m}{m} \qquad (3.34)$$

Clearly, the effect of loading the board with additional mass, is to reduce the resonant frequencies of the modes.

Equation (3.34) enables the effective mass of a mode to be estimated experimentally by loading the point with a small additional mass and by measuring the resulting fractional change in resonant frequency.

Increasing the relative stiffness at a fixed point on the sound board would, of itself, tend to increase the resonant frequency. But this cannot be readily carried out without increasing the effective mass also. The stringing of a musical instrument tends to increase both the effective mass and the effective stiffness of resonant modes. Its effect on resonant frequency cannot therefore be readily predicted.

Work on this project shows that when the strings of the harp are tightened the frequencies of resonant modes of the soundboard are generally increased.

The removal of a small quantity of material from a point on a soundboard changes both the effective mass and the effective stiffness of the resonant

modes of the board. The above considerations have implications for the adjustment of the frequencies of resonant modes or so called plate tuning.

The Q-factor of resonant a mode of a soundboard can be defined by analogy with that of a discrete spring/mass system given by equation 3.31.

$$Q = \frac{f_0}{\Delta f}$$

where f_0 is the resonant frequency of the mode and Δf is the frequency separation of the half power points on a plot of power dissipated in the system versus driving frequency at constant driving force amplitude. As shown in equation 3.32, power at constant driving force amplitude is proportional to the square of the admittance. The term Δf therefore, corresponds to the frequency separation of the two points on either side of a resonance peak on a plot of 20×logarithm of admittance versus driving frequency where the admittance is 3.0 dB below that at the resonance peak.

The approximate frequency above which resonance modes will significantly overlap can be found from the rough approximation $f_0 \approx Q\,\Delta f_0$. For example, resonant modes with a Q-factor of 50 whose resonant frequencies differ by 50 Hz would tend to overlap above a frequency of 2.5 kHz and merge into a continuum of resonance.

3.9 Experimental Arrangement for the Measurement of Input Admittance

A block diagram of the experimental arrangement is shown in figure 3.3. A sinusoidal signal from the signal generator is amplified by the power amplifier which provides a sinusoidal current to the coil. The coil drives a tiny magnet which is affixed with wax to the point to be driven on the surface of the soundboard. The accelerometer (Brüel & Kjaer, Type 4374) may be attached to the opposite side of the soundboard, again with wax, but must be at the position of the driving point. Alternatively, the magnet and accelerometer may be affixed together with wax and the surface then driven by the accelerometer casing.

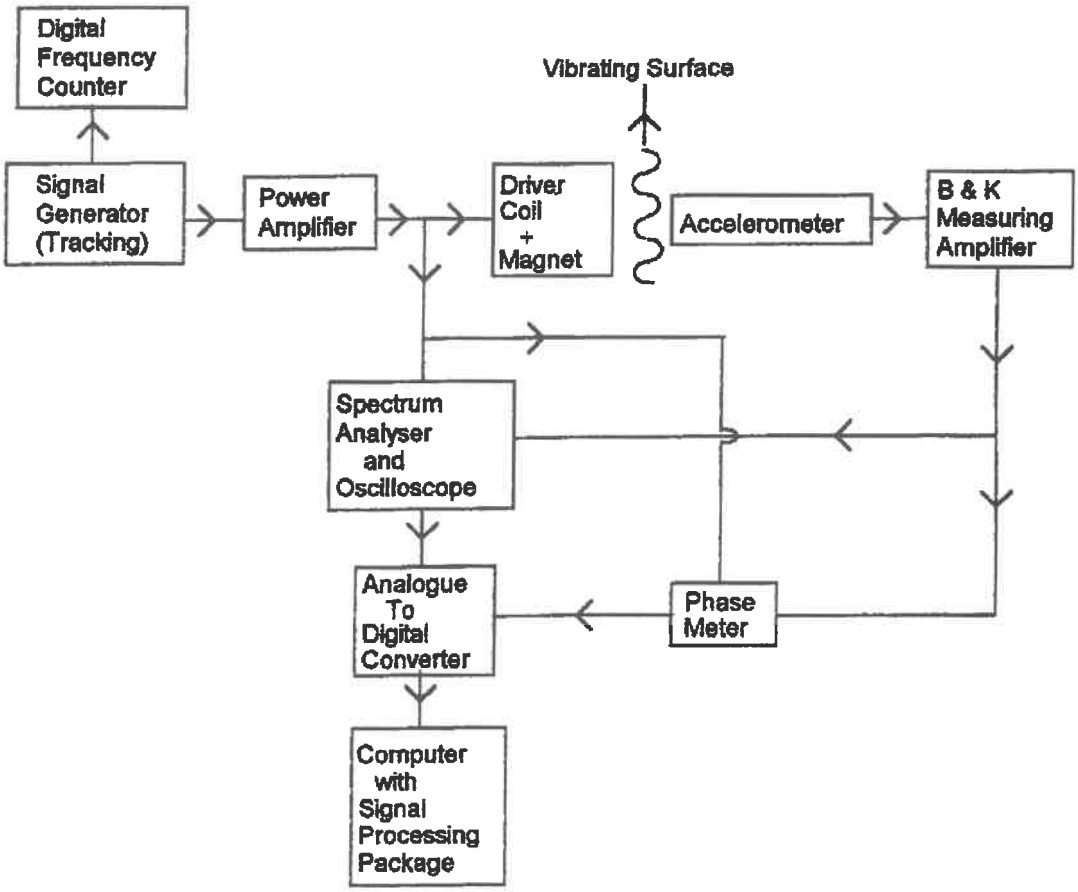

Figure 3.3 Experimental Arrangement for the Measurement of Input Admittance

The accelerometer signal, produced by its piezoelectric crystal, is amplified by a measuring amplifier (B & K, Type 2606) which has a flat and linear response over the range 2 Hz - 200 kHz. The amplified signal is then sent to the spectrum analyser and oscilloscope. The signal generator, spectrum analyser and oscilloscope are contained in a single Tektronix instrument. The instrument contains the 7L5 Option 25 spectrum analyser and tracking signal generator together with the 7603/R7603 Oscilloscope. The Option 25 tracking generator provides a 10 Hz to 5.0 MHz sweeping signal source that tracks the tuned input frequency of the spectrum analyser.

The spectrum analyser employs a set of narrow-band filters. After the signal has passed through these, the amplitude of each frequency component of the signal is displayed and measured on the oscilloscope screen. In these experiments, 10 Hz bandwidth filters were employed up to a frequency of 4000 Hz and 30 Hz bandwidth filters were employed at higher frequencies. Spurious signals outside the filter bandwidth are suppressed by at least 40dB. The sweep time can be varied, the slowest sweeping rate being approximately 500 Hz in 100 s. At this rate, the signal frequency increases in increments of 2 Hz. Tests showed that this rate of sweep was sufficiently slow to enable vibrations of the mechanical system at the previous exciting frequency to have died away and a resonance to build up and its average amplitude to be measured.

In the experiment on the completely strung harp, the strings were immobilised with a cotton ribbon to prevent undue persistence of the string vibration. The trace on the oscilloscope screen, which represents the average signal amplitude at each frequency, is seen to change as the sweeping rate is increased. This is particularly marked at resonant frequencies and anti-resonant frequencies. In these experiments, a full sweep from 0 to 20 kHz took approximately 12 minutes.

To measure the average amplitude of the driving force at each frequency, a signal was taken from the driving circuit and input to the spectrum analyser. This signal was taken out across a 1 Ω resistance in series with the driving coil and was thus proportional to the current in the coil. Unfortunately, this spectrum analyser does not provide for simultaneous measurement of two signals, which would be desirable. It was, therefore, necessary to first measure the signal proportional to the driving force current. The accelerometer response was measured and then the force current signal was re-measured to ensure, as far as possible, that no change in driving current had taken place and that no change had taken place in the relationship between the outputs of the tracking signal generator and the spectrum analyser filter.

The trace on the oscilloscope, in fact, represents the logarithm to the base 10 of the average amplitude of the incoming signal. In the case of the signal from the accelerometer, the signal is proportional to the average amplitude of the acceleration at the driving point.

Preparatory to calculating admittance at each frequency it was necessary to derive velocity from acceleration. For sinusoidal quantities this derivation requires the amplitudes of the acceleration to be divided by the angular frequency, ω. Therefore it was necessary to have a signal proportional to the frequency and this was provided by an output port on the Tektronix instrument.

A phasemeter (Universal Ad-Yu Electronics Inc., Model No. 406L) was also used to measure the phase difference between the driving force current and the accelerometer signal to indicate the expected reversal of phase as the frequency passed through a resonance. The phasemeter provided an output voltage proportional to the phase difference.

Three signals - one proportional to the amplitude of the acceleration of the driving point, one proportional to the driving frequency and one proportional to the phase difference between driving point acceleration and the driving force - were sent simultaneously to the computer (PC, Prompt 2, 286) via a Data Translation Analogue to Digital Converter (Data Translation Inc., DT2812A(SE)). A two pole switch was used to choose either the acceleration amplitude signal or the driving force current signal, to be measured.

The A/D converter has 16 channels with a maximum sampling rate of 100 kHz in single channel operation. As the high frequency signals were not being directly sent to the computer, but were being processed first by analogue devices, high sampling frequencies to prevent aliasing were not necessary. A sampling frequency of 37.5 Hz per channel was used. As the voltage range with this converter could not be varied from channel to channel, it was necessary to use potential dividers to reduce the phasemeter signal and the signal proportional to frequency from the spectrum analyser.

Figure 3.4 shows the computer with A/D converter, the Tektronix spectrum analyser and the digital frequency counter (Philip Harris Digicounter). Figure 3.5 shows the power amplifier (LING Dynamic Systems, Model PA100) with metal box, containing potential dividers, resting on top, beside the phasemeter with the measuring amplifier resting on top.

The accelerometer signal was connected to channel CH00, providing a signal named CH00 for the Global Lab signal processing package in the computer. The voltage proportional to frequency was connected to channel CH01 and the signal proportional to phase difference was connected to channel CH02.

All connections were by coaxial cable and an earthed metal box enclosed the potential dividers in order to reduce pick-up of ambient interference voltages.

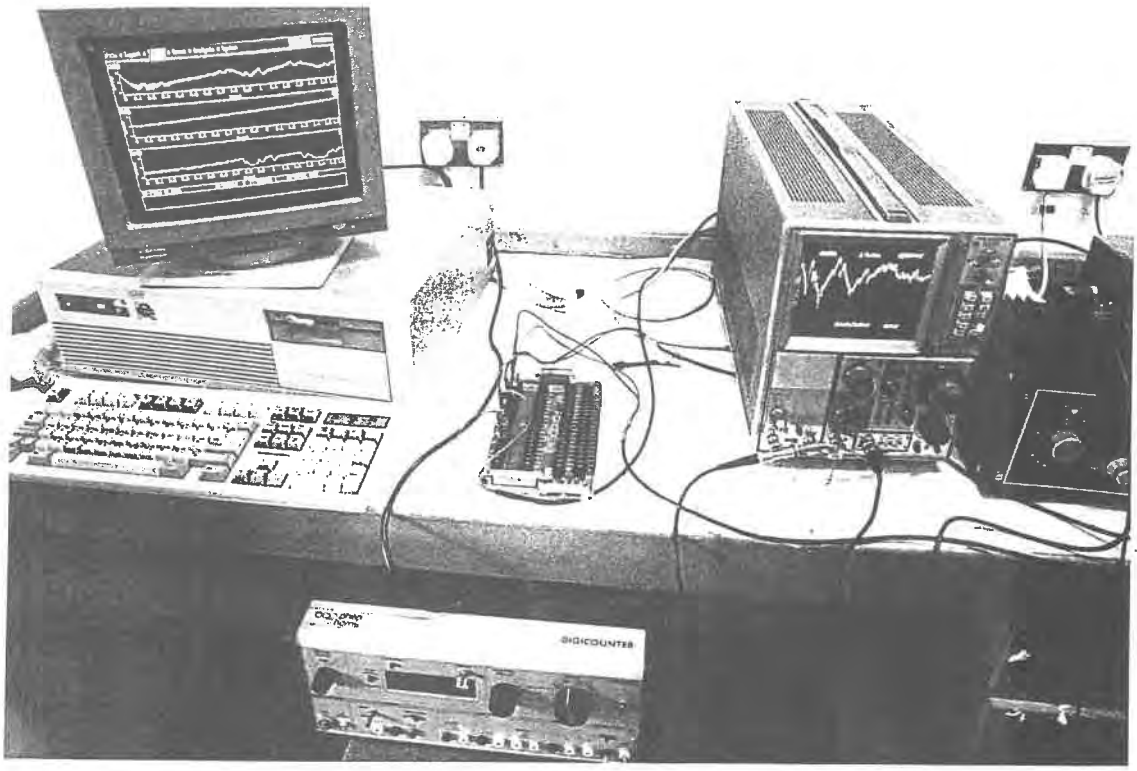

Figure 3.4 (Left to Right on Bench) Computer, A/D Card, Spectrum Analyser. (Centre Foreground) Digital Frequency Counter.

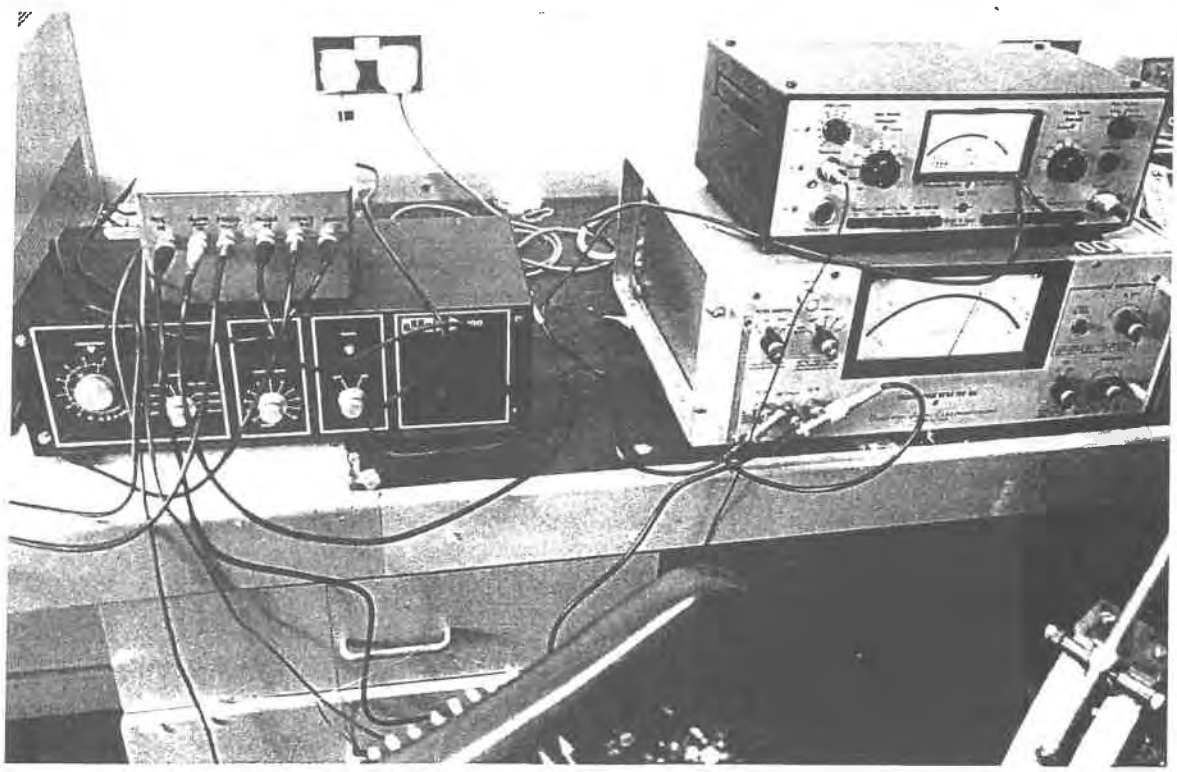

Figure 3.5(Left to Right) Power Amplifier with Junction Box on top, Phasemeter with Measuring Amplifier on top.

The two-pole switch within the metal box enabled the accelerometer signal to be replaced by the driving force current signal for input to the spectrum analyser and thence to the computer via the A/D converter. Thus, depending on the setting of the switch, the signal named CH00 on the computer may represent the driving force current amplitude or the accelerometer signal amplitude. Figure 3.6 shows the computer screen displaying a typical accelerometer signal, a frequency signal and a phase difference signal. In figure 3.7 the accelerometer signal is replaced by the driving force current signal.

The A/D module of the signal processing package allowed the time interval for signal capture to be specified. Accordingly, the sweep time across the oscilloscope screen was measured with a stopwatch fifty times and an average of 96.05 s was found with a standard deviation of 0.20 s. A duration of capture of 96.0 s was therefore specified.

To conduct a signal capture, the following procedure was adopted.

The signal generator was first put in manual sweep mode. The dot which traverses the top of the screen as the generator sweeps, was fixed on the first vertical line on the oscilloscope screen. A digital frequency counter was used to measure the frequency. The dot was then fixed on the last vertical line and the frequency was measured. These readings were entered in the data book.

The signal generator was then put in single sweep mode. The signal processing package was used to put the computer and A/D converter in a state where the pressing of any key would initiate the capture.

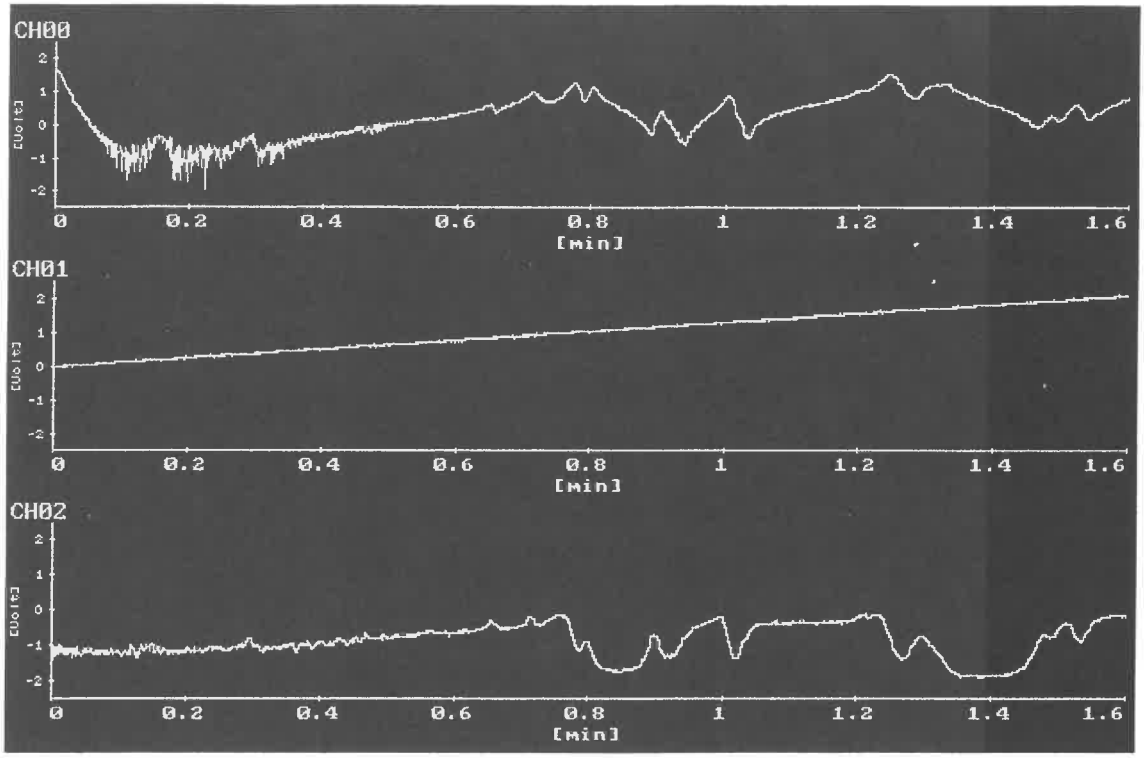

Figure 3.6 Computer Screen Displaying 3 Signals:

CH00 is Accelerometer Signal

CH01 is Signal Proportional to Frequency

CH02 is Signal Proportional to Phase Difference*

***(between driving force current and accelerometer signals)**

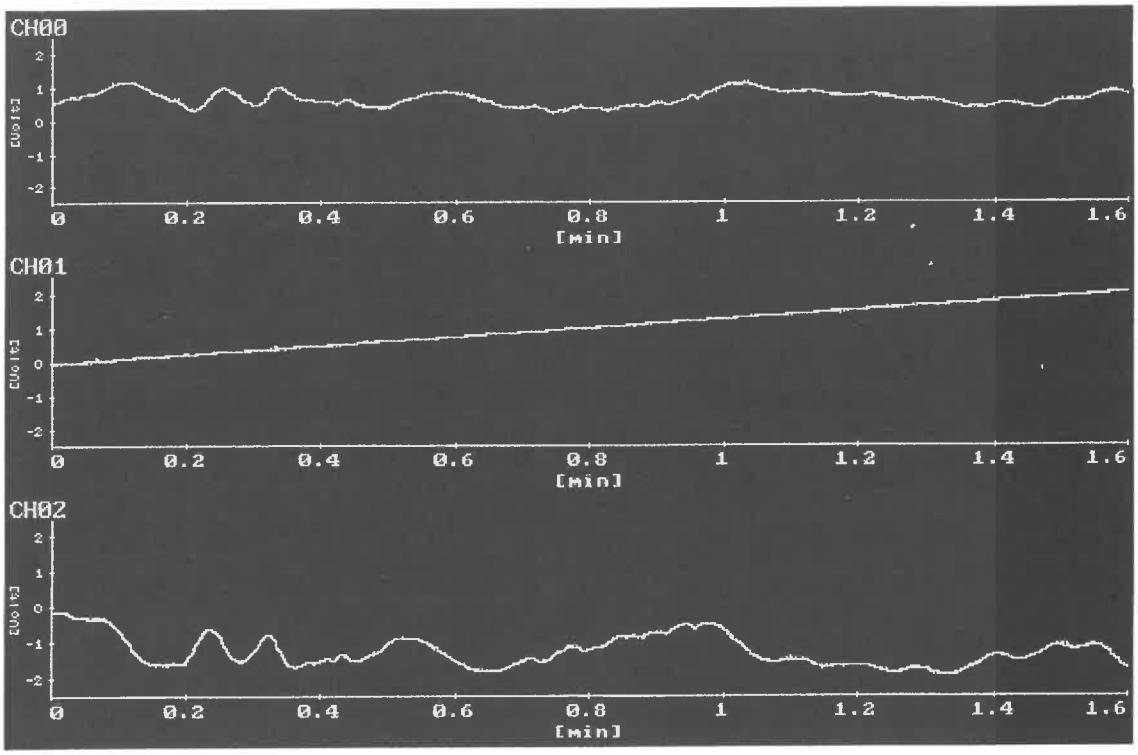

Figure 3.7 Computer Screen Displaying 3 Signals:

CH00 is Signal Proportional to Coil Current Amplitude

CH01 is Signal Proportional to Frequency

CH02 is Signal Proportional to Phase Difference*

***(between driving force current and accelerometer signals)**

The sweep, which takes about five seconds to reach the first vertical line on the screen, was initiated by the single sweep button on the Tektronix instrument. As the dot reaches the first vertical line on the screen, a computer key is pressed and the capture begins. The computer terminates the capture automatically after 96.0 s. The termination was seen to coincide with the traversing dot reaching the last vertical line on the screen.

Repeated experiments using this method showed that the position of a resonance peak near 250 Hz for a particular driving point never varied by more than ±1 Hz. Loading effects and couplings give rise to much larger frequency variations for the same resonance as the driving point position is changed.

3.10 Signal Processing

At a given frequency the magnitude of the admittance $B = \frac{V_o}{F_o}$ where V_0 is the velocity amplitude at the frequency concerned and F_0 is the force amplitude at the same frequency.

The acceleration amplitude $A_0 = (2\pi f V_0)$.

From this,

$$V_o = \frac{A_o}{2\pi f} \qquad (3.35)$$

Hence, from the signal in which voltage is proportional to A_0 and the signal in which voltage is proportional to f, dividing the first by the second gives a voltage signal which is proportional to the velocity amplitude.

However, the accelerometer signal is exported on a logarithmic scale by the Tektronix instrument and the frequency signal is exported on a linear scale. Therefore from equation (3.35)

$$\log_{10} V_0 = \log_{10} A_0 - \log_{10}(2\pi f)$$

$$= \log_{10} A_0 - \log_{10} f - \log_{10} 2\pi \qquad (3.36)$$

$\text{Log}_{10}\, 2\pi$ is a constant for all frequencies and all driving points. To find $\log_{10} f$, the following procedure was adopted. Using the measuring facility on the Global Lab package, the voltage difference between the beginning and the end of the sweep on the signal proportional to frequency CH01 is measured using a cursor on the computer screen. The frequency span for the sweep concerned is found in the data book having been measured on the digital frequency counter. From these data f and $\log_{10} f$ were calculated.

Taking the example of string point C2 on the completely strung harp for a sweep of span 504 Hz beginning at 503 Hz and ending at 1007 Hz, where the voltage difference on CH01 was 2.10 V, the calculation was the following.

$$\log_{10} f = \log\left\{503 + \frac{504}{2.10}(\text{H1\_C2A2.CH01})\right\}$$

H1_C2A2.CH01 is the full designation in the Global Lab package of the signal proportional to frequency captured at this driving point over the stated frequency range.

To compute a signal (y) proportional to $\log_{10} V_0$, the following operation is carried out using equation 3.36.

$$y = \text{H1\_C2A2.CH00} - \log_{10} f$$

where H1_C2A2.CH00 is the designation in the computer package of the signal proportional to the logarithm of the amplitude of the acceleration.

Finally, since the driving force amplitude is proportional to the current amplitude in the coil and this current amplitude signal is exported by the spectrum analyser on a logarithmic scale, a signal proportional to the logarithm of the admittance is found thus,

H1_C2E2 = y - H1_C2C2.CH00

where H1_C2C2.CH00 is the designation in the computer package of the logarithmic driving force current signal.

H1_C2E2 is the designation given to the signal representing the variation of admittance (on a logarithmic scale) with frequency. In order that the admittance axis be scaled in dB, the H1_C2E2 file was edited. The admittance axis was multiplied by 20 and an offset of 80dB was used for the highest setting used on the measuring amplifier. This offset was required to give all relative admittance readings on the dB scale a positive value. Measurements were carried out to determine the adjustments to the offset required at the amplifier settings. Finally, the horizontal axis was edited so that it read frequency directly, rather than time in seconds. The frequency span (504 Hz in the above example) was divided by the number of data points in the signal and this figure was used as the multiplier of the horizontal frequency axis. The starting frequency of the sweep, read from the data book, was then used as an offset on this frequency axis.

At constant frequency acceleration amplitude is directly proportional to velocity amplitude. Hence, when driving force amplitude is unchanged, admittance differences at a particular driving frequency are the same as differences read from plots of 20×log(acceleration amplitude) versus frequency.

3.11 Linearity

In order to investigate if the relationship between driving force amplitude and acceleration amplitude at the driving point was linear over the 0 - 20 kHz range, sweeps were carried out at three different output settings on the power amplifier at a single driving point on the cedar and mahogany harp. The sweep over the frequency range 0 - 20 kHz was subdivided into 6 sections: 0 - 500 Hz, 500 - 1000 Hz, 1 kHz - 2 kHz, 2 kHz - 4 kHz, 4 kHz - 9 kHz and 9 kHz - 19 kHz. The acceleration amplitude versus frequency plots for the first two sections are set out in figures 3.8 and 3.9. Plots of current amplitude versus frequency for the same frequency ranges at the three output settings of the power amplifier showed that the system was linear.

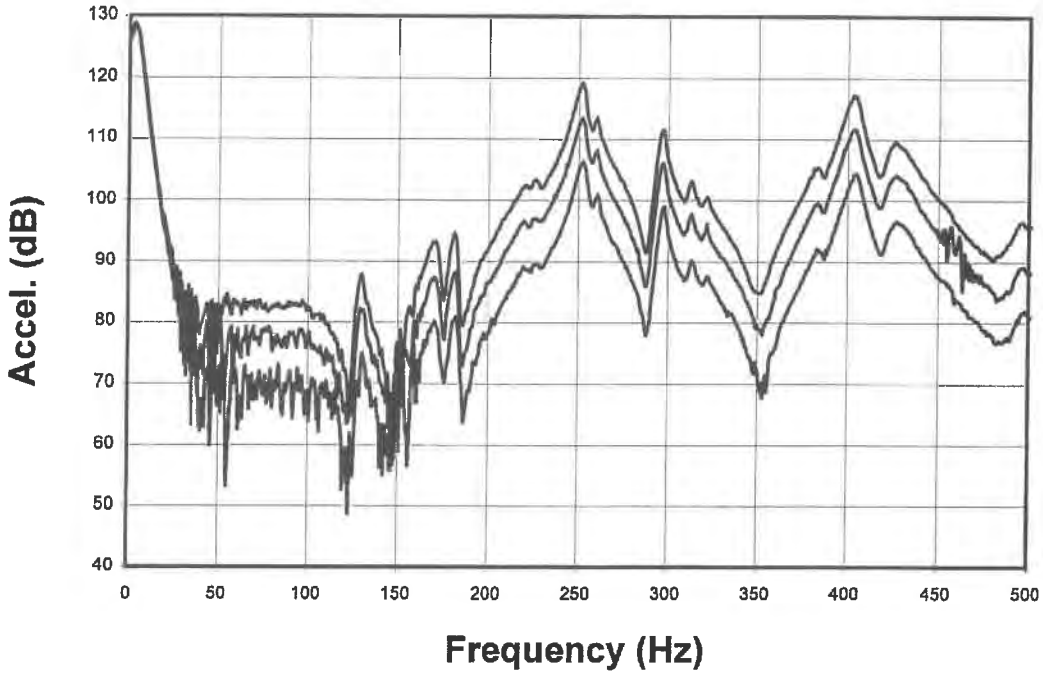

Figure 3.8 Acceleration Amplitude versus Frequency at the Same Driving Point for three Settings on the Power Amplifier

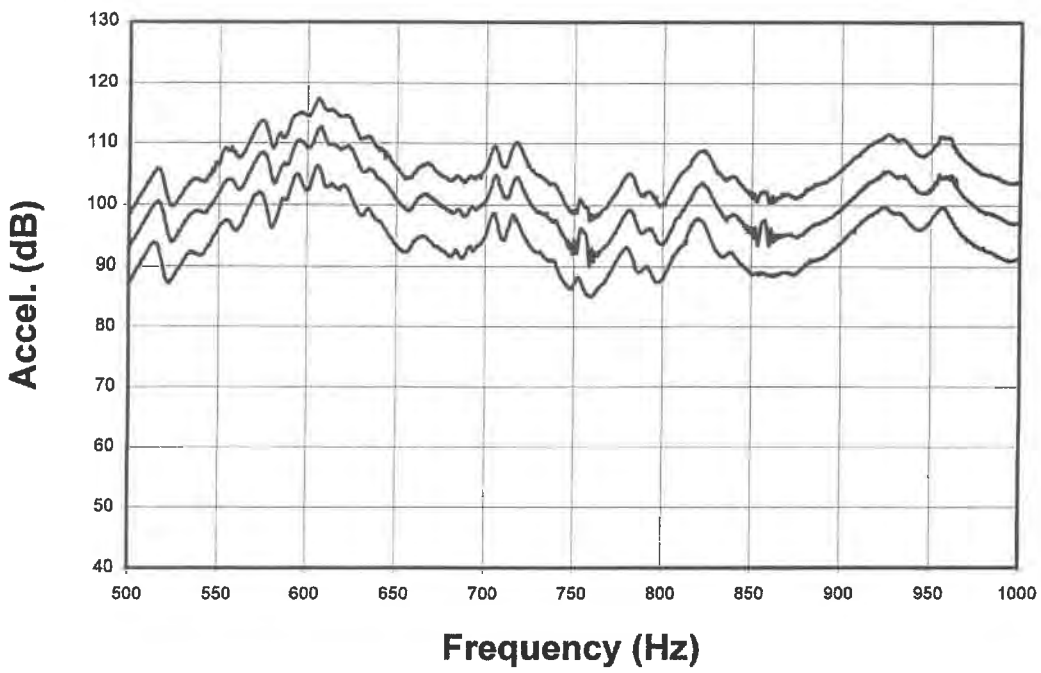

Figure 3.9 Acceleration Amplitude versus Frequency at the Same Driving Point for three Settings on the Power Amplifier

As the driving coil and magnet are not repositioned at any time during this experiment and the displacements of the tiny magnet on the soundboard are very small in comparison to the length of the cylindrical coil (1.5 cm), it is assumed that the driving force is proportional to the driving current. The driving current declines with increasing frequency broadly as expected in an a.c. circuit containing an inductance and resistance.

Table 3.2 shows measurements of acceleration amplitude and corresponding current amplitude at three frequencies made on a computer screen using a cursor. A1, A2 and A3 are the acceleration peak amplitudes at power amplifier output settings 1, 2 and 3 respectively. C1, C2 and C3 are the corresponding driving current amplitudes. From figures 3.8 and 3.9 and table 3.2 it can readily be seen that when the driving current amplitude increases, the accelerometer current amplitude increases proportionally at each frequency.

In table 3.3, frequency values at peak acceleration at the three settings on the power amplifier are recorded. In all 18 separate sub-sweeps, there is no case in which the acceleration-peak frequency is shifted by more than ±0.5% by changing the driving force amplitude.

The measuring system is therefore broadly linear over the 0 - 19 kHz frequency range. Also, the position of the acceleration peak on the frequency scale is not appreciably shifted by changing the driving current and hence the driving force amplitude over the range and at the frequencies used in these experiments.

3.12 Flatness of Response with Frequency of the Spectrum Analyser

The flatness of response of the spectrum analyser across the spectrum was investigated by connecting the output of the tracking generator directly to the input of the spectrum analyser, with the settings on the spectrum analyser identical to those used in the measurements. The output d.c. signal from the spectrum analyser is captured through the A/D converter card by the computer using the Global Lab signal processing package. The plots of signal amplitude versus frequency are displayed on the computer screen.

Mean Peak Frequency (Hz)	A3 dB	C3 dB	A2 dB	C2 dB	A1 dB	C1 dB
252	118.8	118.8	113.0	113.2	105.8	106.0
718	109.8	118.0	103.8	112.4	98.0	105.8
1198	113.8	116.6	107.6	110.6	101.8	104.2

Table 3.2 Acceleration Amplitudes (A) and Corresponding Current Amplitudes (C) for a single driving point for three settings on the Power Amplifier.

Power Amplifier Setting	Resonant Peak Frequency (Hz)
1	252
2	252
3	252
1	717
2	717 → 718
3	719
1	1197
2	1202
3	1197

Table 3.3 Resonant Frequency Values at three Power Amplifier settings

The experiment showed that measuring errors due to the tracking generator - spectrum analyser - computer system are less than 0.4 dB and well within the requirements of the experiments in this work, for the frequency range 0 - 22 kHz.

3.13 Amplifier Flatness

The flatness of response of the measuring amplifier over the frequency range 0 - 22 kHz was investigated by reducing the signal amplitude from the tracking generator and connecting it to the input of the measuring amplifier. The output of the amplifier was connected to the input of the spectrum analyser. The output of the spectrum analyser was captured in the computer as before. The scale setting on the measuring amplifier was 1 mV, the setting always used when measuring the accelerometer signal from the cedar and mahogany harp. The plot of signal amplitude versus frequency showed a flatness less that ±0.5 dB, well within the requirements of the experiments in this work.

3.14 Amplifier Settings

As on occasion it was necessary to use the 3 mV and 10 mV measuring amplifier settings, sweeps from 0 to 20 kHz were carried out at these settings in the same manner as described in section 3.13 above. In addition to establishing flatness of response with frequency at these settings, it was necessary to determine the offsets on the signal amplitude scale required to make measurements comparable when the amplifier setting was changed.

Measurements of signal amplitude at the frequency indicated at each of the three setting of the measuring amplifier are recorded in table 3.4. The values shown indicate that the flatness of response of the measuring amplifier at each scale setting is well within ±0.2 dB and so within requirements of these experiments. The procedure of averaging the offset on the signal amplitude scale over the range 100 Hz to 20 kHz and using this to correct for amplitude settings in this frequency band, is also satisfactory.

Frequency (kHz)	1 mV Scale A1 (dB)	3 mV Scale A2 (dB)	10 mV Scale A3 (dB)
0.100	111.6	102.0	92.6
1.00	111.6	102.0	92.6
2.00	111.6	102.0	92.6
4.00	111.8	102.0	92.8
6.00	111.6	102.0	92.6
8.00	111.8	102.0	92.6
10.00	111.6	102.0	92.6
12.00	111.8	102.0	92.6
14.00	111.8	102.0	92.8
16.00	111.8	102.0	92.6
18.00	111.8	102.0	92.6
20.00	111.8	102.0	92.6

Table 3.4 Signal Amplitudes at the Frequency Indicated at 3 Settings on the B & K Measuring Amplifier

3.15 Accelerometer

The principal accelerometer used in this work was the B & K Type 4374. It employs a piezoelectric sensing element and provides an output voltage proportional to the acceleration of the surface to which it is attached. The manufacturers' specifications are set out in the Appendix. A typical mounted resonance frequency of 85 kHz is quoted and a very flat response over the frequency range 200 Hz to 20 kHz is shown.

However, this very satisfactory behaviour of the accelerometer only fully applies when it is affixed with great rigidity to the surface to be tested. In this work the accelerometer was affixed to the soundboard surface with wax.

To examine the behaviour of the accelerometer under these mounting conditions the driving point admittance of a large concrete block was measured using the same driving system as was employed in measurements carried out on the harp soundboard. As the strain bar was of polished mahogany, a piece of this material was attached to the surface of the concrete block with an epoxy resin. The accelerometer was attached to the mahogany surface with wax and the tiny magnet was attached to the accelerometer casing with wax also. The concrete block was inclined to the ground at approximately the same angle as the harp soundboard and it leaned against another concrete block when being driven.

The driving point admittance of the concrete block over the range 20 Hz to 1000 Hz is set out in figure 3.10. The admittance of the harp soundboard in the completely strung instrument at string point G2 over the same frequency range is shown for comparison in figure 3.11. The admittance of the two lowest frequency soundboard resonances is more than 30 dB above that of the concrete block at the same frequencies. At approximately 1000 Hz, in a frequency region far from a resonance, the soundboard admittance is more than 20 dB above that of the concrete block at the same frequency. The corresponding driving admittance plots over the frequency range 1 kHz to 4 kHz are displayed in figures 3.12 and 3.13.

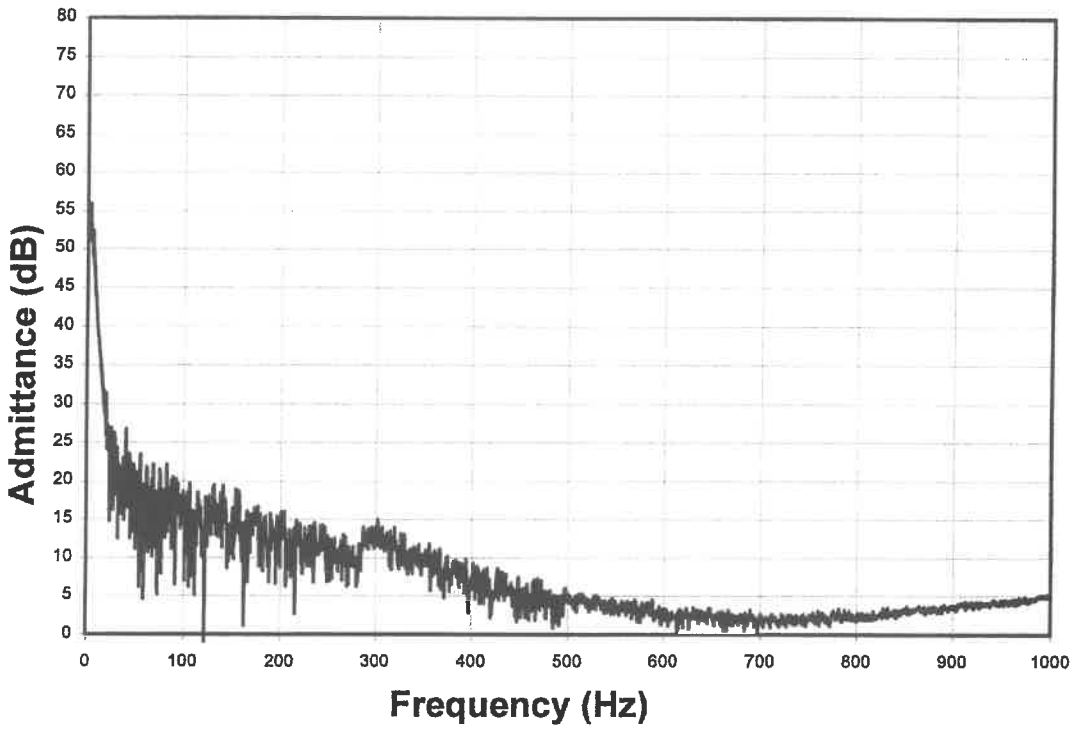

Figure 3.10 Driving Point Admittance of Concrete Block over Frequency Range 20 Hz to 1000 Hz.

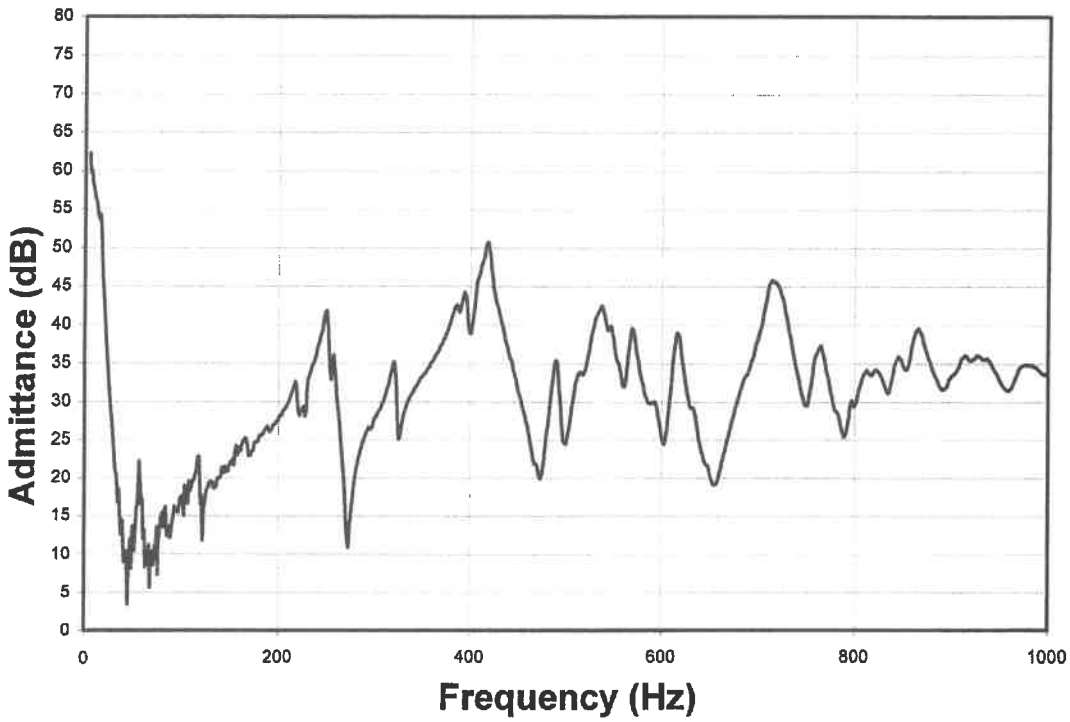

Figure 3.11 Driving Point Admittance of Soundboard in Completely Strung Harp at String Point G2 over Frequency Range 20 Hz to 1000 Hz.

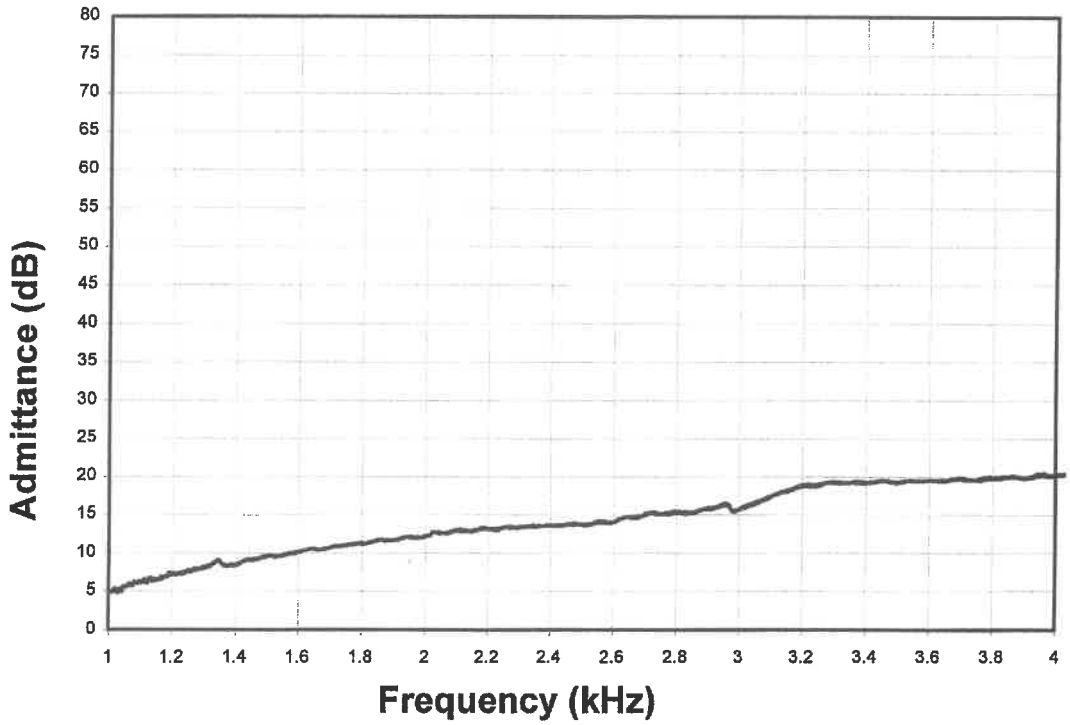

Figure 3.12 Driving Point Admittance of Concrete Block over Frequency Range 1 kHz to 4 kHz.

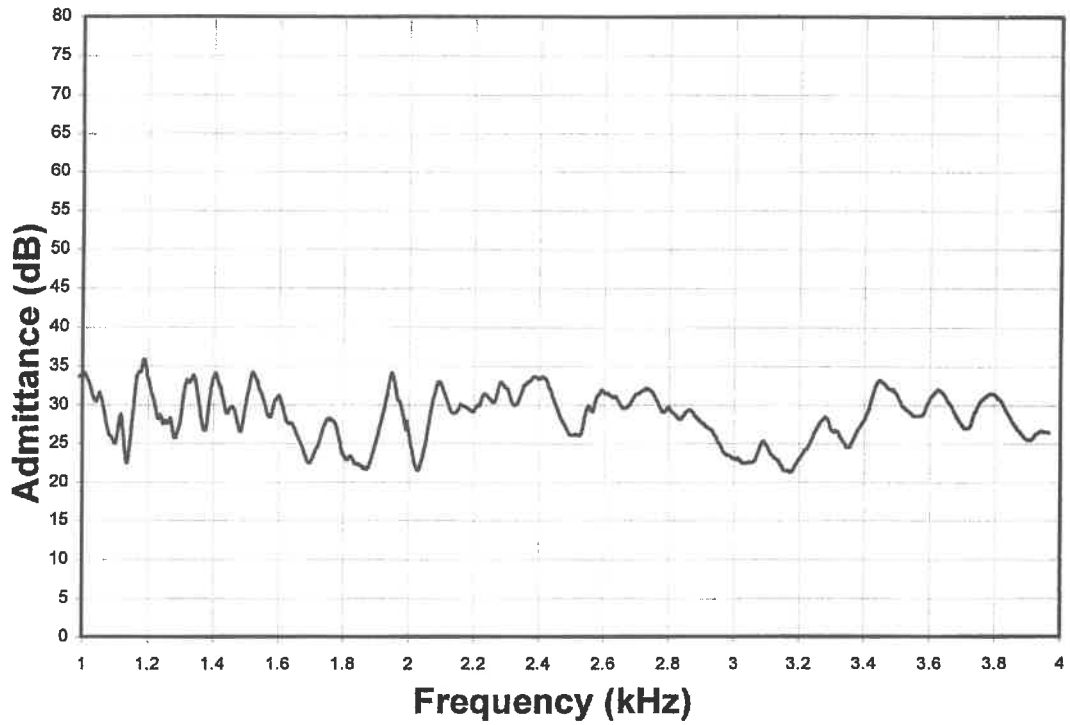

Figure 3.13 Driving Point Admittance of Soundboard in Completely Strung Harp at String Point G2 over Frequency Range 1 kHz to 4 kHz.

Up to a frequency of 2.5 kHz the admittance peaks at string point G2 are approximately 20 dB above that of the concrete block.

Above this frequency the measured admittance of the concrete block rises more steeply than heretofore and reaches a peak at approximately 15 kHz where the peak admittance is comparable to that of the first two soundboard resonances. The tiny accelerometer and magnet emit a high pitched whistle as they vibrate. This is due to the compliance of the wax. It is therefore unsafe to use this measuring system above a frequency of approximately 2.5 kHz.

The manufacturers' frequency response curve does not extend below 200 Hz. Work done by a colleague[6], under the supervision of this investigator, shows that it is acceptable to use the accelerometer for resonance peak identification down to a frequency of approximately 100 Hz. However, below this frequency, large departures from the flat response occur.

In experiments to measure the effective mass of resonant modes of the soundboard which will be reported in Chapters 4 and 5 it will be shown that shifting of resonances along the frequency scale, due to the additional combined mass of the accelerometer and magnet, is negligible.

3.16 Adjustment of Coil and Magnet

Reliability and precision of measurements are clearly satisfactory once the coil and magnet have been placed in position. Relative admittance levels at various frequencies at the same driving point can then be determined very accurately. The frequency at which each peak occurs can also be determined to well within an error of ±1%.

However, when it is required to compare the admittance of the same mode of vibration at difference driving points, the coil and magnet must be repositioned. The procedure adopted was to adjust the coil in relation to the magnet at a fixed frequency which gives a relatively large response until that response reaches a maximum value when viewed on the screen of the spectrum analyser

and also on an oscilloscope where the actual oscillations can be viewed. Repeating the adjustment process from the beginning shows that differences of response can be confined to ±0.4 dB if care is exercised. This degree of precision is adequate for the investigations reported in this work.

References

[1]Rossing, T.D. and Russell, D.A., American Journal of Physics, Vol. 58, No. 12, pp 1152 - 1162, (Dec 1990).

[2]Benade Arthur, H., Fundamentals of Musical Acoustics, Chapter 9, p 133; Oxford University Press, New York (1976).

[3]Caldersmith, G.W., Acustica, Vol. 56, pp 143 - 152 (1984).

[4]McIntyre, M. et al., On Measuring Wood Properties, JCAS, Vol. 43, pp 18 - 24 (1985).

[5]Hussey, M., Fundamentals of Mechanical Vibrations. Macmillan Press Ltd., London (1983).

[6]Keane, J., Detection of Small Vibrations using the Speckle Interferometry of Laser Light and hence the Calibration of a Small Accelerometer in the Low Frequency Range. Final year project report submitted to Dublin Institute of Technology in examination for the Diploma in Applied Physics.

CHAPTER 4

THE CLAMPED, BARRED BOARD

4.1 Introduction

An unfinished cedar soundboard was supplied by Colm O` Meachair, harp maker. It had an untapered thickness of 6 mm. As outlined in figure 2.1, the soundboard in the completed instrument has a length of 894 mm, a width of 360 mm at the broad end and a width of 98 mm at the narrow end. Its thickness tapers from 4.5 mm at the broad end to 1.5 mm at the narrow end. However, because of the manner in which the board is clamped on the sound box in the completed instrument and the position of the foot of the pillar on the soundboard, the effective vibrating distances are less than those indicated above.

The board was tapered and clamped to replicate, as far as possible, conditions in the completed instrument. The effective vibrating length was 820 mm and the effective vibrating width tapered from 335 mm to 85 mm. The cover and strain bars were attached along the centre on the two sides of the board with wood glue. The board was held around its edges by pairs of heavy slats of wood bolted together.

The board thus clamped and barred, was investigated using the input admittance technique described in Chapter 3 and also the Chladni powder pattern method.

4.2 Input Admittance Method

Each end of the holding frame was placed on a trestle. Three separate 1 kg weights were placed along the frame at the bass end and two such weights were placed along the frame at the treble end. The test driving positions on the central cover bar were as indicated in table 4.1. Holes were bored at these points which correspond to string positions on the completed instrument.

Testing Position	1	2	3	4	5	6	7	8	9	10
Distance from Treble End (mm)	67	155	215	305	370	441	535	625	675	725
Corresponding String	G1	C1	G2	C2	G3	D3	G4	C4	A5	F5

Table 4.1 Clamped, Barred Soundboard

Frequency of Detected Admittance Peak (Hz)	Resonant Frequency Detected by Phasemeter (Hz)	Q-Factor Measured
180	181	51
277	280	60
323	326	61
342	343	66
488	490	61
577	562	43
587	588	47
646	646	35
765	766	59
841	841	60
886	892	23
939	945	33
994	-	-

Table 4.2 Data at String Point C2 on Clamped, Barred Soundboard

The tiny magnet (mass 0.5 g) was attached with wax to the accelerometer and the accelerometer was then attached with wax to the driving position. The current carrying coil was next placed over the magnet and adjusted to give a maximum acceleration signal at a fixed frequency. Tests were carried out at each driving position over the frequency range 0 - 1 kHz.

Figure 4.1(a) shows a plot of relative admittance versus frequency over the frequency range 0 - 500 Hz at driving position C2. Figure 4.1(b) shows the corresponding variation of phase angle between driving force and driving point velocity. Figures 4.2(a) and 4.2(b) display the same information over the frequency range 500 -1000 Hz.

The frequency of each admittance peak at this driving position (C2) was measured and each Q-factor was also determined. The resonant frequency detected by the phasemeter was also recorded. These data are displayed in table 4.2. These measurements and calculations were repeated at each driving point. A summary of these measurements at five driving points on the cover bar (C1, C2, G4, C4, F5) is given in table 4.3.

The Q-factors of some admittance peaks are not measurable because a clear 3.0 dB decline in admittance at both sides of the peak cannot be measured. This may occur because the peak does not correspond to a resonance or due to low admittance at a particular driving point for the frequency concerned or because of the presence of an adjacent admittance peak at a slightly different frequency. At these testing positions there is a low incidence of Q-factor measurability and resonance detection by phasemeter within the frequency range 650 Hz to 1000 Hz. The admittance peak at 765 Hz, alone in this frequency range has a high incidence of detection by phasemeter and of Q-factor measurability.

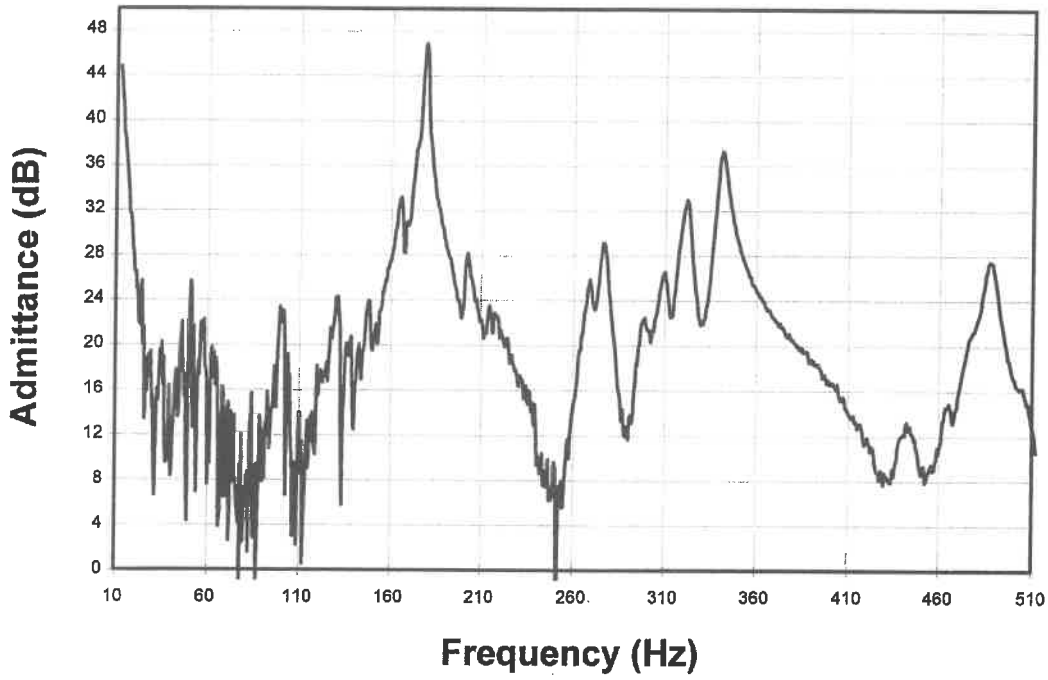

Figure 4.1(a) Relative Admittance v Frequency at String Point C2 on Held Barred Board.

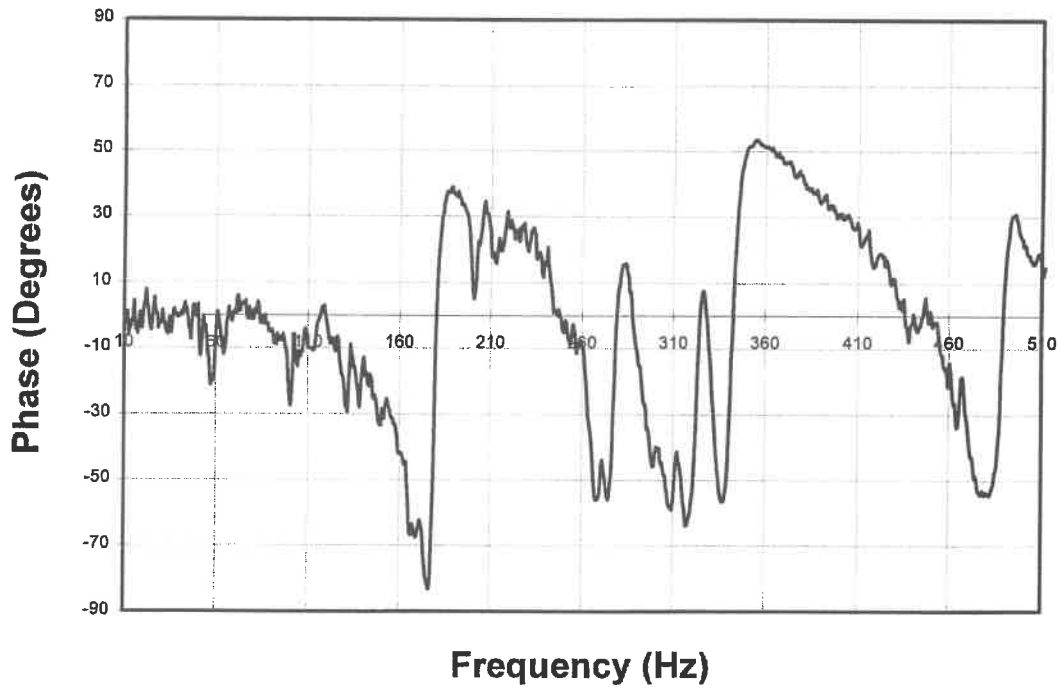

Figure 4.1(b) Phase Difference v Frequency at String Point C2 on Held Barred Board.

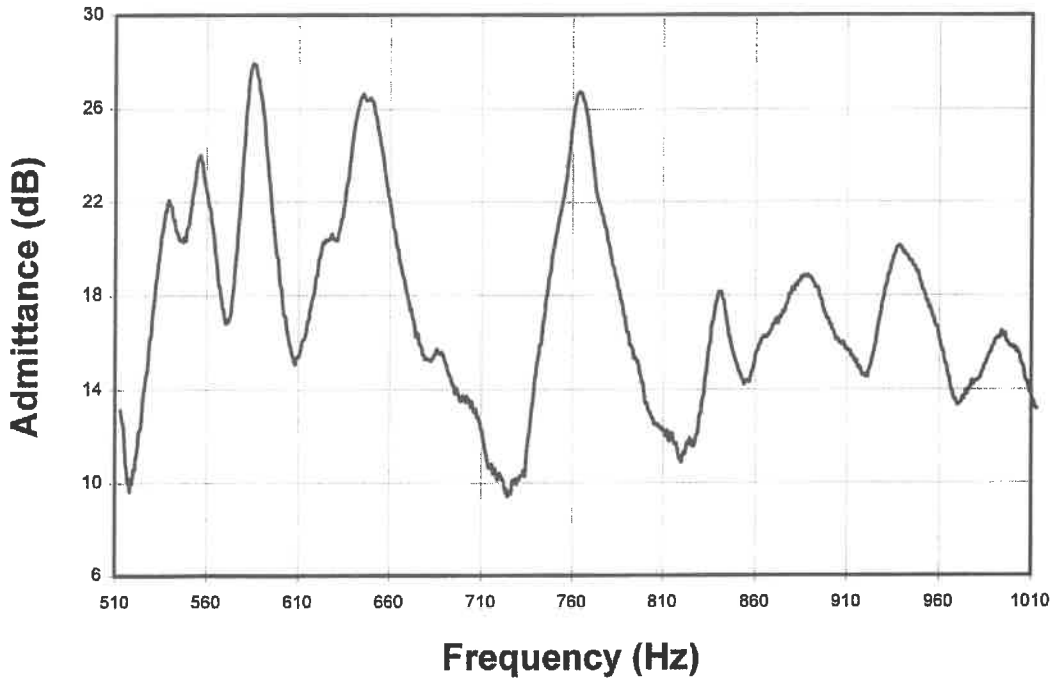

Figure 4.2(a) Relative Admittance v Frequency at String Point C2 on Held Barred Board.

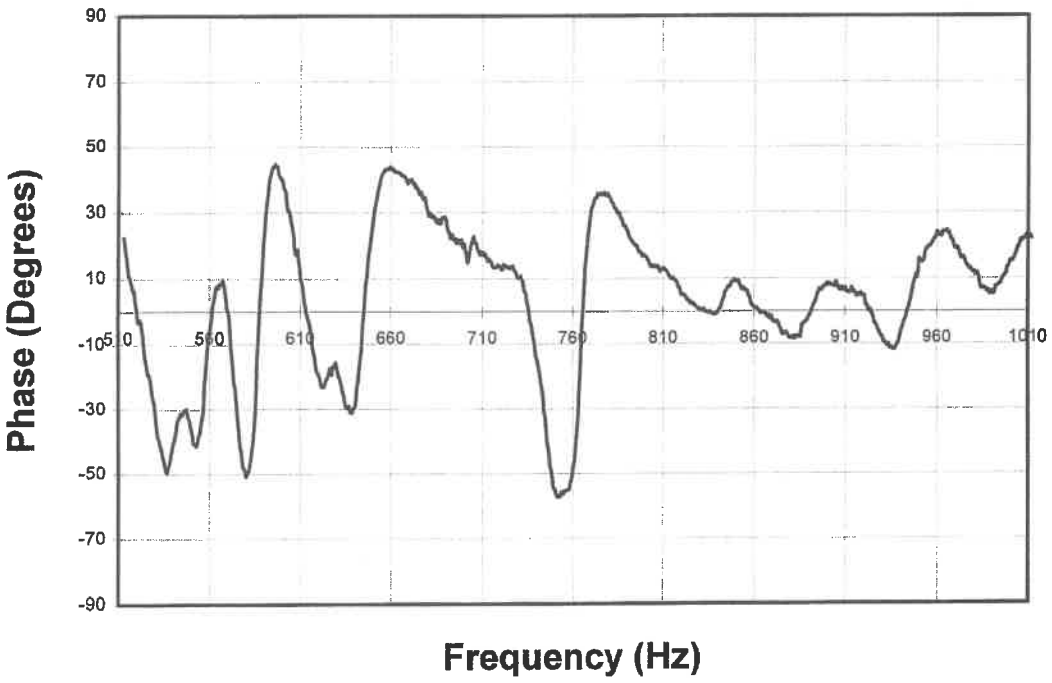

Figure 4.2(b) Phase Difference v Frequency at String Point C2 on Held Barred Board.

Detected Admittance Peak Frequencies (Hz)	Resonant Frequencies Detected by Phasemeter (Hz)	Maximum Q-Factor Measured
180(5)*	181(5)	69(5)
277(5)	280(3)	60(5)
322(5)	325(4)	68(5)
342(5)	343(5)	68(5)
443(3)	442(1)	28(2)
479(5)	490(1)	61(4)
501(4)	502(1)	50(2)
552(4)	556(3)	61(3)
586(5)	587(4)	65(5)
648(4)	645(3)	44(4)
686(2)	708(1)	51(2)
729(1)	733(1)	69(1)
765(5)	766(4)	59(4)
811(1)	820(1)	-
839(2)	841(1)	60(1)
885(2)	892(1)	23(1)
937(2)	945(1)	33(2)
987(3)	992(1)	36(1)

Table 4.3 Summary of Measurements at Five Driving Points on Cover Bar of Clamped, Barred Soundboard.

*** The figures in brackets in the first two columns refer to the number of detections. The corresponding figures in the third column refer to the number of driving points at which Q-factor was measurable.**

The value of Q-factor measured throughout this work and quoted in tables must be treated with caution. The smallest frequency increment which could be produced by the tracking signal generator when sweeping was 2 Hz. Resonances of high Q-factor occurring at frequencies below 300 Hz have a typical bandwidth of approximately 4 Hz. An estimated error of up to ±25% could, therefore, be expected on individual measurements. The error declines as the frequency at which resonance occurs increases.

4.3 Chladni Powder Pattern Method.

The Chladni powder pattern technique is based on the existence of nodal and anti-nodal regions on the board when it vibrates at one of its resonant frequencies. The displacement amplitudes are relatively large at the anti-nodes and very small or zero at the nodes. Dry tea leaves are sprinkled on the board and at resonance the tea leaves slide away from the anti-nodes and congregate at the nodes.

Richardson`s notation is used to classify the modal shapes. S(m,n) is a mode having m separate anti-nodal regions across the width of the board and n separate anti-nodal regions along the full length of the board. Adjacent anti-nodal regions vibrate in anti-phase in accordance with stationary wave theory.

The Chladni method provides insight into the structure and shape of the resonant modes, features which are not readily obtained from admittance measurements on the soundboard. Modal shapes can also be identified using holographic interferometry[1].

4.4 Experiment

The clamped, barred and tapered board was placed on a metal scaffolding designed to facilitate the driving of the board from below. The wooden slats holding the board were firmly affixed to the metal frame with wires. Care was taken to avoid unduly affecting the degree of clamping of the soundboard by

excessive tightening. The foot of the scaffolding was then held firmly in place by a number of 10 kg weights.

A shaker (LING Dynamic Systems Vibrator, Model 400) was powered by a power amplifier (LING Dynamic Systems Amplifier PA100). A light brass rod passing through a hole in the cover bar was connected to the steel drive bar by an adapter. A digital frequency counter (Philip Harris Digicounter) was used to measure the frequency of the driving current.

The total mass of the drive bar, attached brass rod and nuts was 78.3 g. This could be expected to have an appreciable loading effect, thus reducing the frequency of resonant modes. However, the driving point chosen was near the bass end of the board at string hole F5 far from the expected positions of the anti-nodal maxima of the first two resonant modes of the board. The effective mass of a mode is least at its anti-nodal maximum.

In the Chladni patterns, regions of accumulation of tea leaves indicate the nodes and clear regions indicate anti-nodes. The observed patterns are displayed in figures 4.3 to 4.12. The mode displayed in figure 4.3 appears to be the S(1,1) mode which was detected at a driving frequency of 163 Hz. Figure 4.4 shows what appears to be the S(1,2) mode, detected at a frequency of 303 Hz. What appeared to be the S(1,3), S(1,4) and S(1,5) modes were detected at frequencies of 411 Hz, 606 Hz and 644 Hz respectively. These are displayed in figures 4.5, 4.6 and 4.7 respectively. What appears to be the first of the S(2,n) series detected is displayed in figure 4.8. The accumulation of tea leaves along the cover bar, particularly at the bass end of the board, appears to commence at this resonant frequency which is sixth in order of ascent. The frequency of the mode was found to be 746 Hz. The mode shape appears to be S(2,5) or S(2,6). Further mode shapes belonging to the S(2,n) series were detected at 830 Hz, 911 Hz, 986 Hz and 1098 Hz respectively. These are displayed in figures 4.9, 4.10, 4.11 and 4.12.

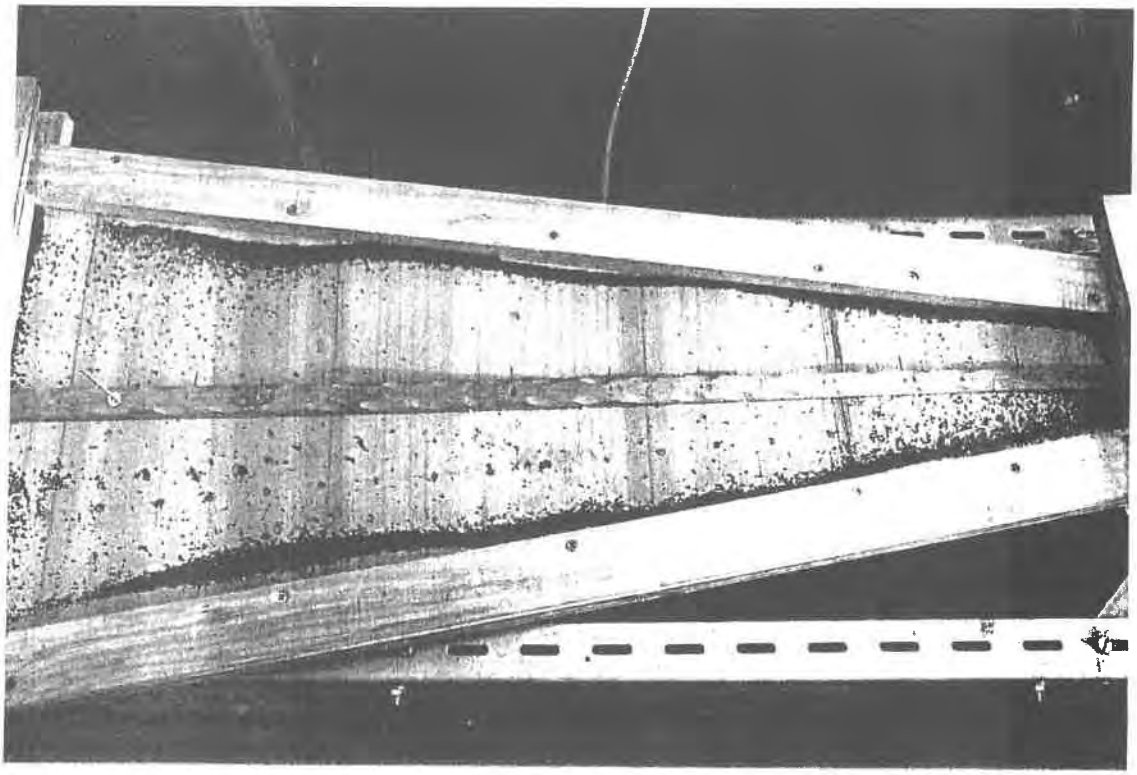

Figure 4.3 Modal Pattern S(1,1) Resonant Frequency 163 Hz

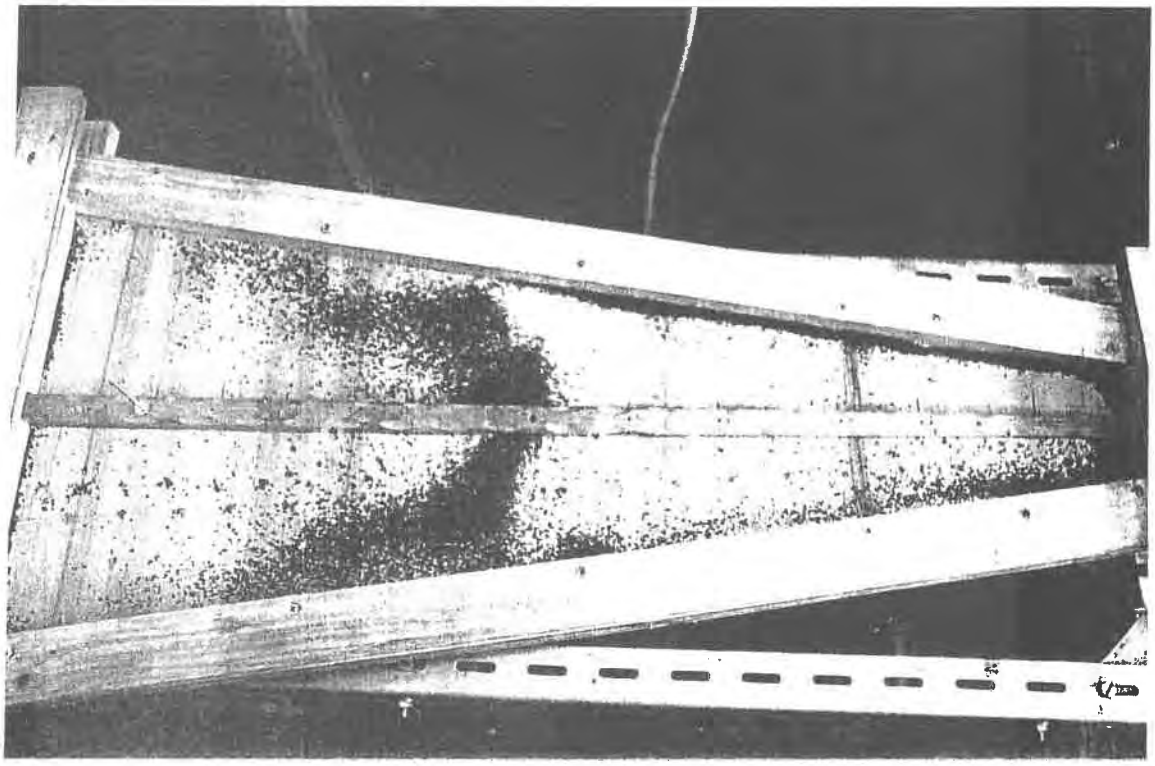

Figure 4.4 Modal Pattern S(1,2) Resonant Frequency 303 Hz

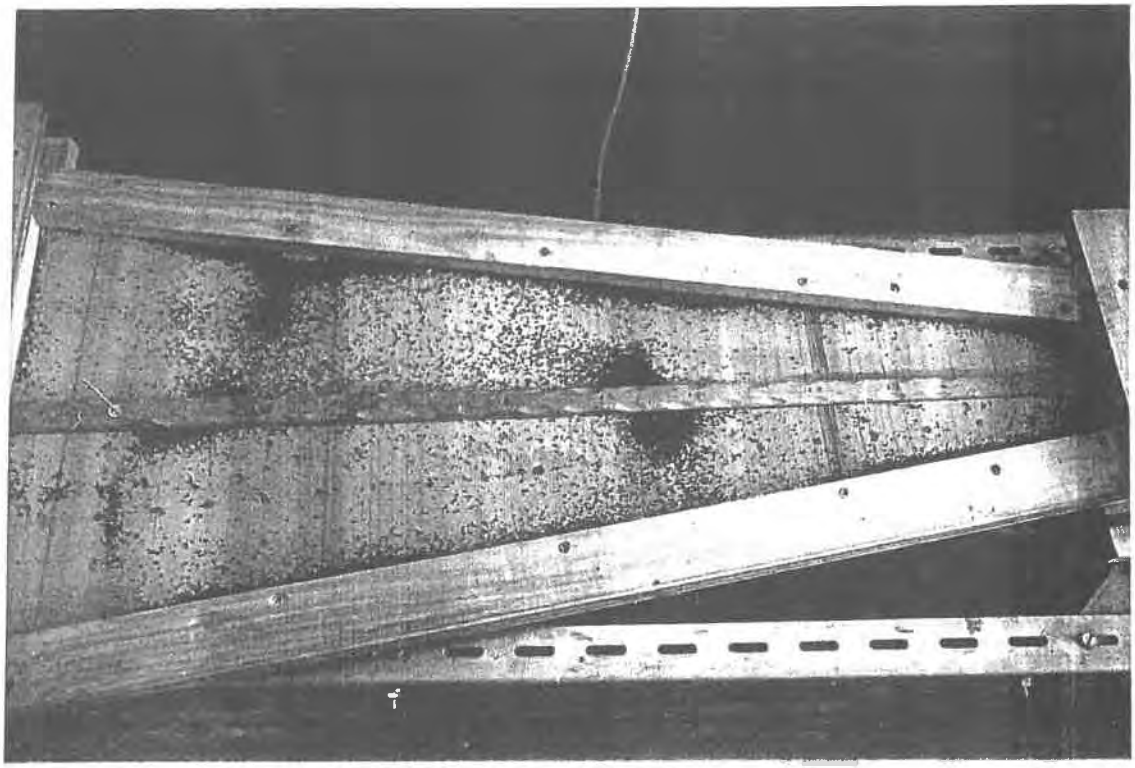

Figure 4.5 Modal Pattern S(1,3) Resonant Frequency 411 Hz

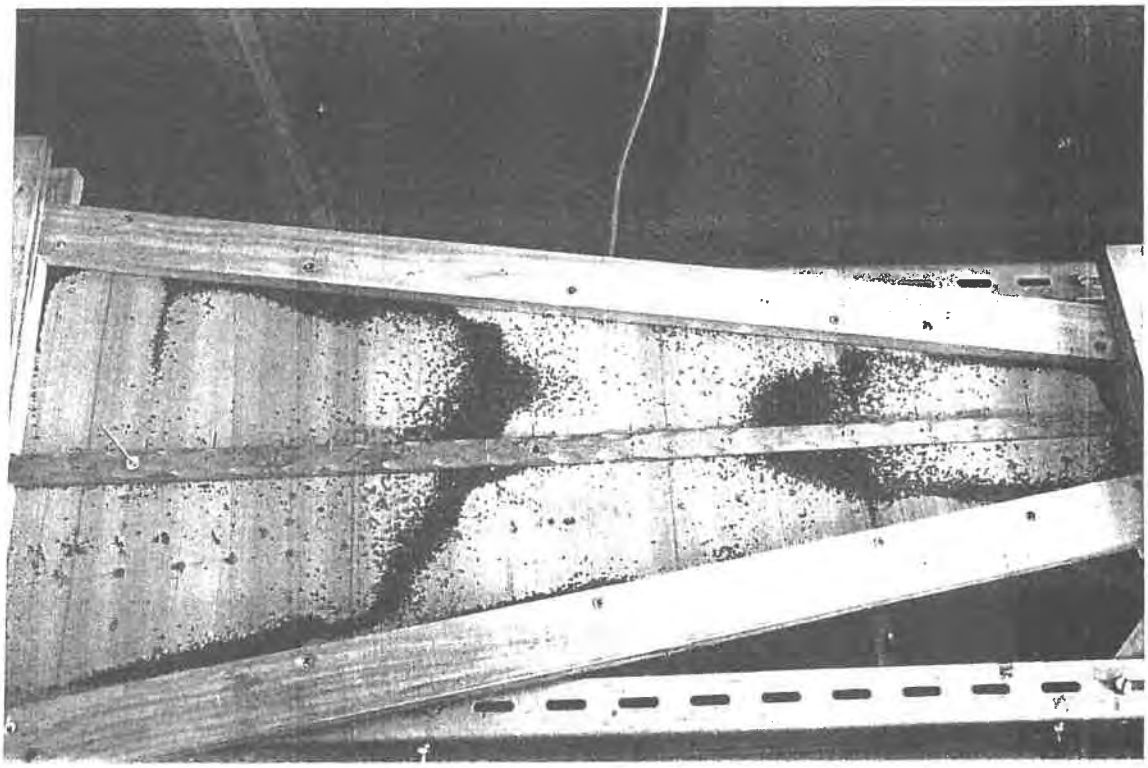

Figure 4.6 Modal Pattern S(1,4) Resonant Frequency 606 Hz

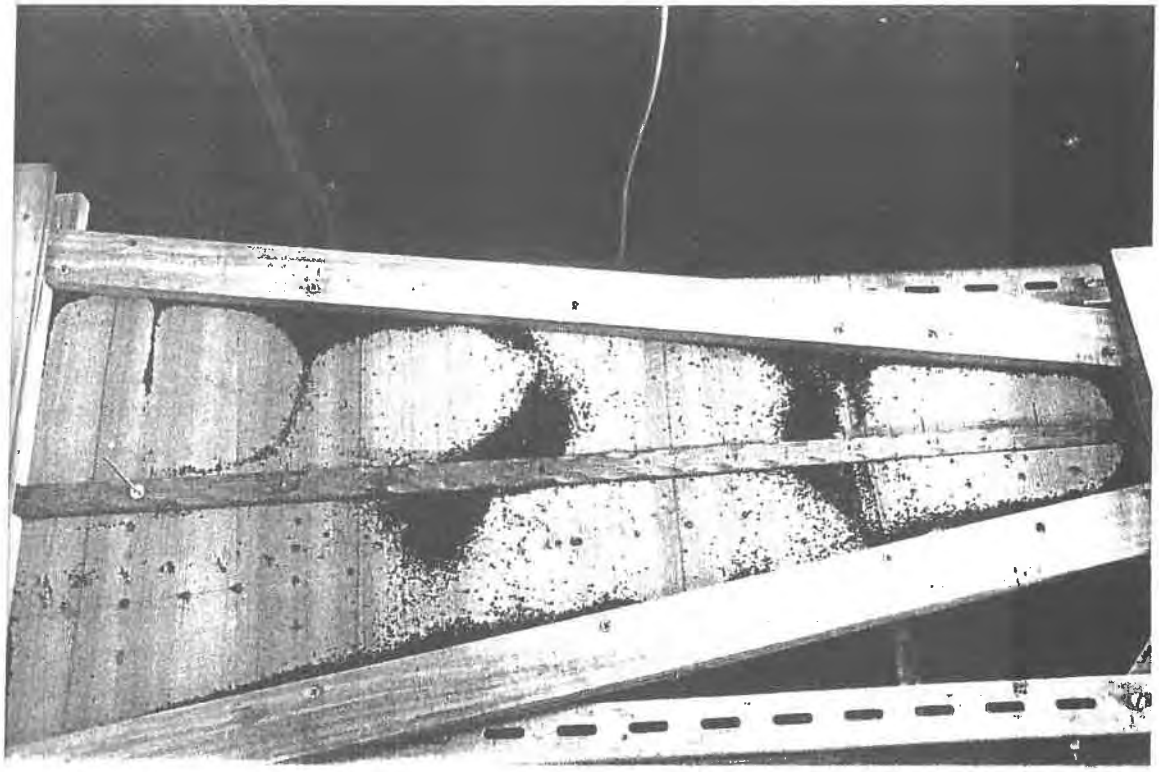

Figure 4.7 Modal Pattern S(1,5) Resonant Frequency 644 Hz

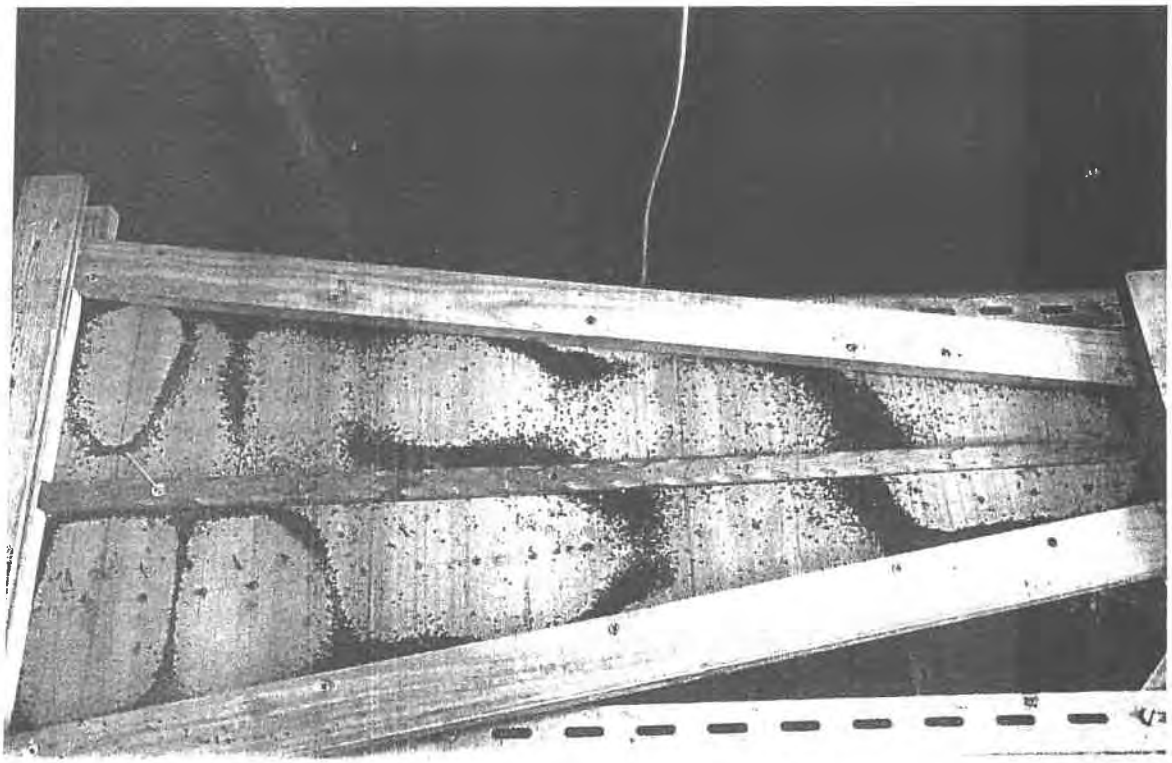

Figure 4.8 Modal Pattern S(2,5) Resonant Frequency 746 Hz

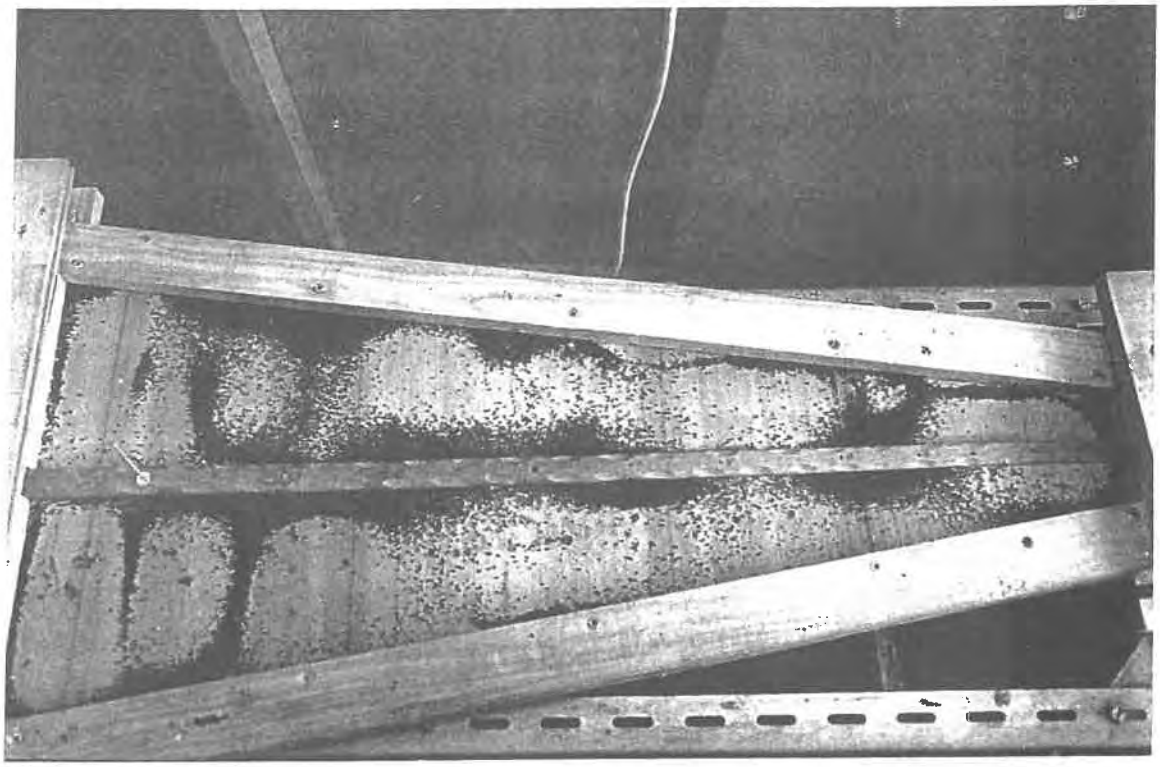

Figure 4.9 Modal Pattern S(2,6) Resonant Frequency 830 Hz

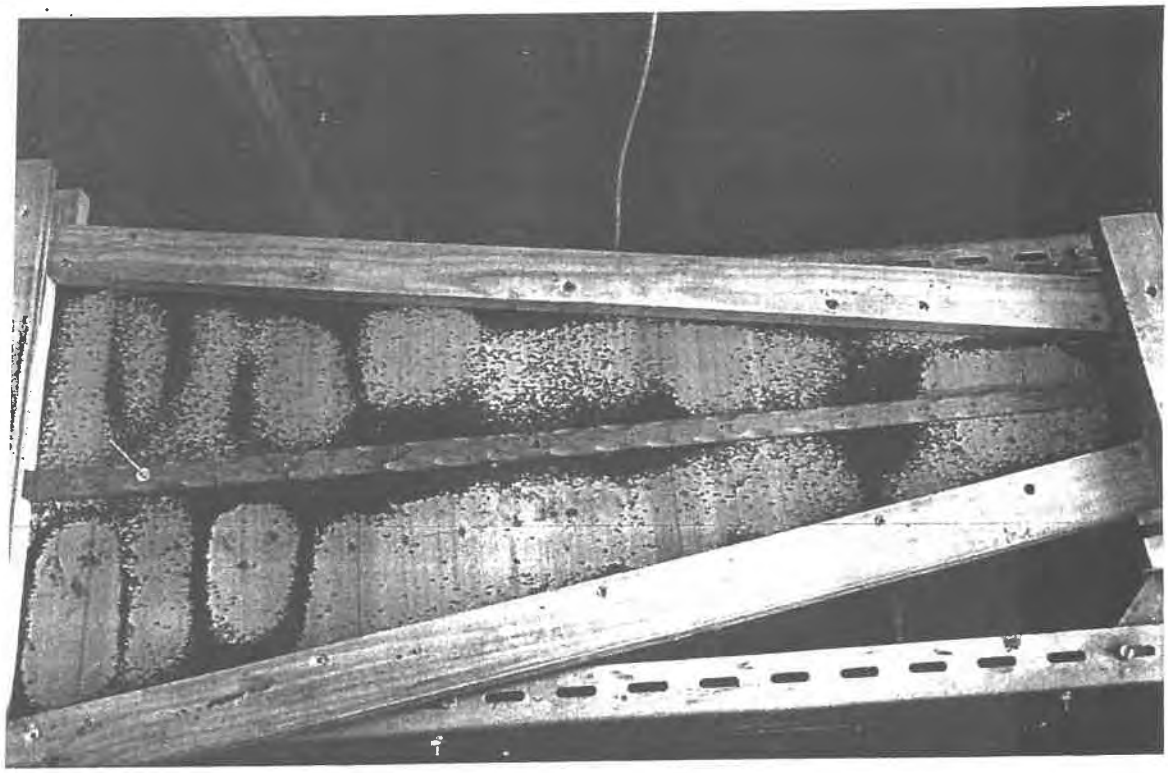

Figure 4.10 Modal Pattern S(2,7) or S(2,8) Resonant Frequency 911 Hz

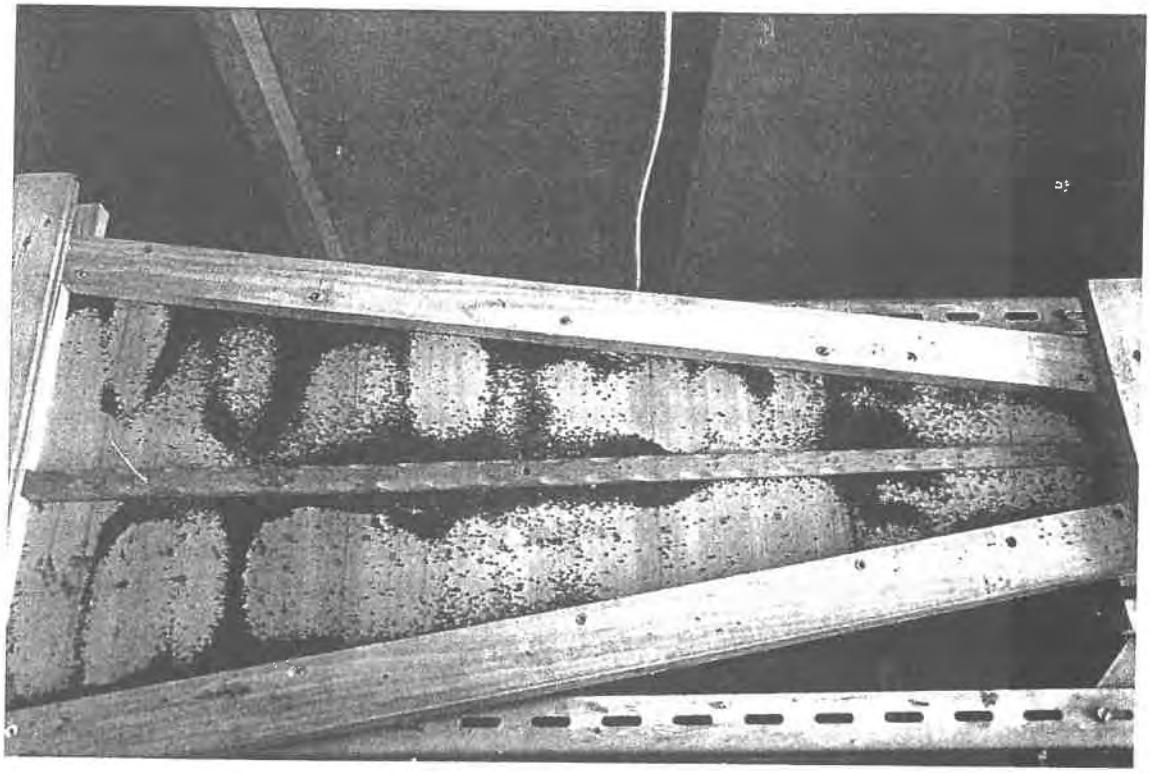

Figure 4.11 Modal Pattern S(2,12) or S(2,13) Resonant Frequency 986 Hz

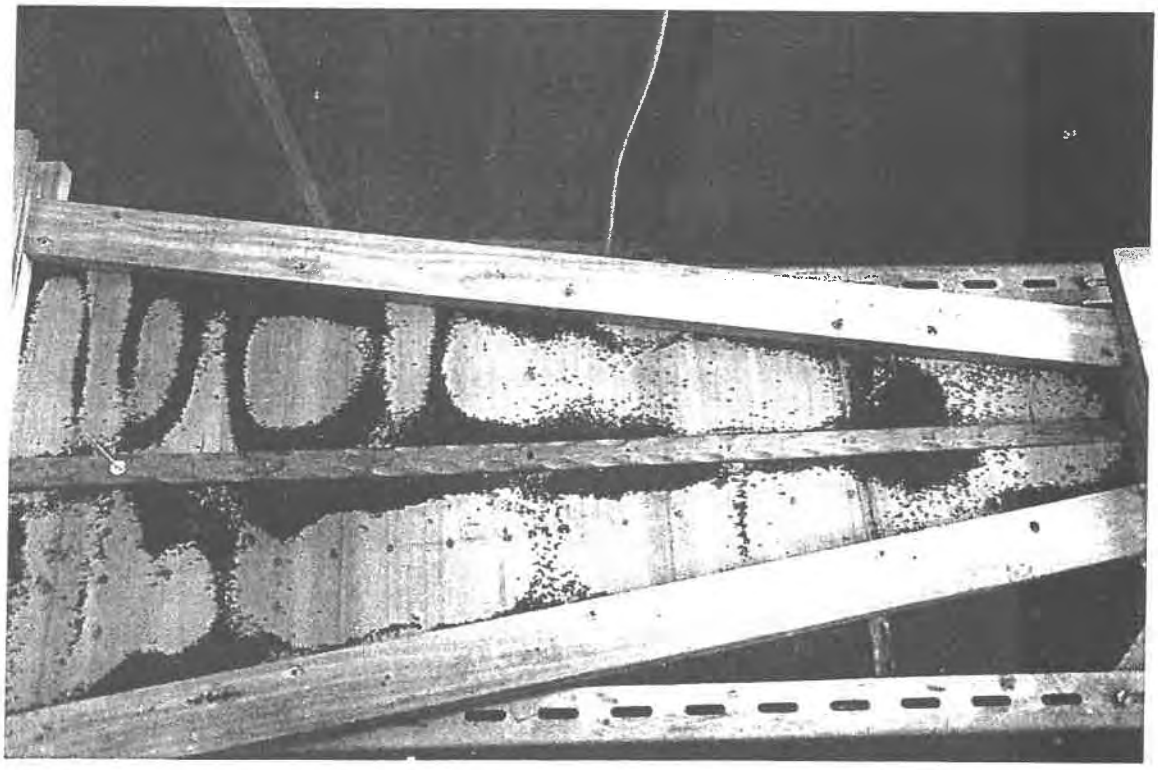

Figure 4.12 Modal Pattern S(2,13) or S(2,14) Resonant Frequency 1098 Hz

The vigorous agitation of the tea leaves persisted for a frequency interval of approximately 5% above and below the resonant frequencies quoted in this section. Attempts to detect modal shapes in the S(2,n) series below S(2,5) by using other driving points were not successful.

4.5 Loading Effects on Frequencies of Resonant Modes.

In order to estimate the loading effects of the accelerometer and the driving mechanism employed in the Chladni powder pattern experiment, the effective mass of the first board mode at its position of maximum admittance on the soundboard was determined. Using the input admittance method the frequency of the first mode peak was found at driving point D3, using both a large and small accelerometer. The total mass of the small accelerometer (B & K Type 4374) together with one attached magnet, excluding the cable was 1.2 g. The total mass of the large accelerometer (B & K Type 4332) together with mounting screws and magnet was 38.3 g excluding the cable. The measured peak frequencies were 179 Hz and 163 Hz respectively. An approximate effective mass of the mode of 180 g was calculated using equation 3.34. The mass of the small accelerometer placed at this driving point would have a very small effect on the peak frequency of this mode (a reduction of less than 0.5%). The large accelerometer and attachments shifts the peak frequency downwards by almost 10%. If the driving mechanism employed in the Chladni powder pattern experiment had been placed at this driving point the loading effect of its mass (78.3 g) would be considerable. If the approximation involved in applying equation 3.34 retains its validity, the depression of the resonant frequency would be in excess of 20%. The driving mechanism was in fact placed very far from the point of maximum admittance on the board and the apparent depression of the resonant frequency was almost 10%. Clearly, the resonant frequencies measured in the Chladni experiment should be treated with caution. However the results are of assistance in establishing the probable hierarchy of modes which are strongly supported and in visualising the vibrational behaviour of the board at resonance.

4.6 Admittance Measurements off the Cover Bar.

To take account of the fact that the position of the central bar on the soundboard is expected to be nodal in the S(2,n) series of resonant modes, it was decided to make further measurements of this input admittance along a line running along the length of the board midway between the cover bar and the side rim of the soundboard and also along lines running across the board perpendicular to the cover bar. For these measurements, the holding frame was placed in a similar orientation to that occupied by the soundboard in the completed instrument. This facilitated the use of a steel jig which was constructed to carry the bar and which holds the driving coil in experiments on the completed instrument. Repositioning and readjusting of the driving coil are more easily and more precisely carried out using this jig.

The holding frame of wooden slats was used as in the previous experiments. In this experiment however, the holding frame leaned against concrete blocks at its centre. Its bass end was prevented from slipping forward by placing of 10 kg weights on the floor against it. Near the treble end, the frame was held by a retort stand, the base of which was weighted down. Great care was taken not to unduly tighten the clamping of the actual soundboard while immobilising the holding frame. The frequency of the first soundboard resonance was used as a guide. In the actual experiment its frequency was approximately 5% above that measured in the experiment conducted with the holding frame on trestles.

The small accelerometer (B & K, Type 4374) was used in these experiments. To facilitate access to the driving points three tiny magnets were attached to the accelerometer casing. This increased the loading mass from 1.2 g to 2.2 g. Consequently, resonant frequencies were expected to be generally slightly depressed. As the proportionality between force and driving current is changed by the addition of these two extra magnets, only admittances measured using this driving arrangement are comparable to each other.

4.7 Admittance Measurements Across the Board.

A plot of acceleration at constant force versus frequency for a driving position on the cover bar near string hole C4 is displayed in figure 4.13. The same plot for a driving point midway between cover bar and side rim is displayed in figure 4.14 and the same plot for a driving point even nearer the rim is displayed in figure 4.15. The admittance peaks at either side of the large peak near 190 Hz are probably due to vibrations of the holding frame and will be discussed later. A first inspection of these three plots might prompt the conclusion that all resonances above 500 Hz are from the S(2,n) series as their admittances are significantly higher at driving points off the cover bar. Indeed, at this position along the length of the board all peaks except the first soundboard mode near 190 Hz are slightly higher near these driving points. This phenomenon was also observed at corresponding driving points on the soundboard in the completed instrument. It is notable that in the plots displayed here the peak near 670 Hz, although its peak admittance off the bar is over 6 dB higher than that measured on the bar, has peak-to-trough height on the bar of approximately 16 dB while its peak-to-trough height at the driving point most distant from the bar is only 5.0 dB. This lends support to the view that this resonance belongs to the S(1,n) series.

In the higher S(1,n) modes in the half of the board towards the bass, the amplitudes of resonant vibrations appear to be greater for driving points off the central bar than for those on it. Further investigation is also required into this phenomenon, which is also found on the soundboard of the completed instrument. This matter will be discussed further in chapter 5.

From the plots displayed in figures 4.13 and 4.15, it is clear that proceeding from the peak near 670 Hz to the peak near 720 Hz, the admittance differences measured on and off the cover bar increase from 12 dB to 25 dB. The same admittance difference for the peak near 780 Hz is approximately 30 dB. This lends support to the view that the peaks near 720 Hz and 780 Hz belong to the S(2,n) series of modes.

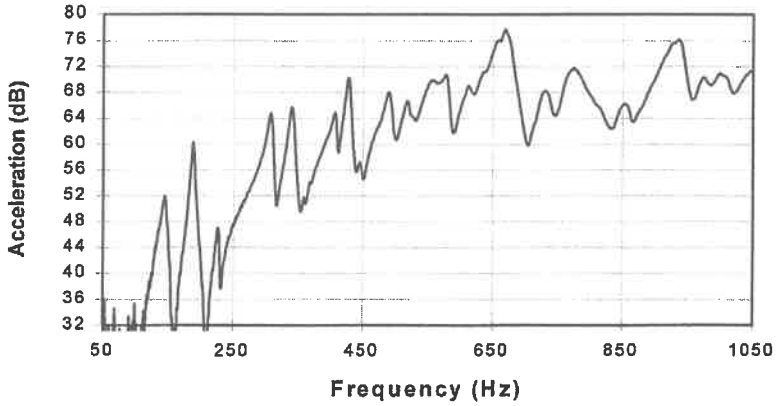

Figure 4.13 Acceleration at constant force Versus Frequency near String Position C4 on Held, Barred Board (on cover bar)

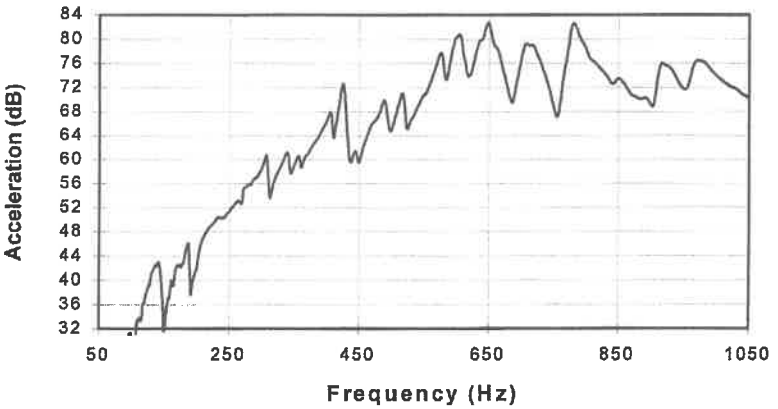

Figure 4.14 Acceleration at constant force Versus Frequency near String Position C4 on Held, Barred Board (midway between cover bar and side rim)

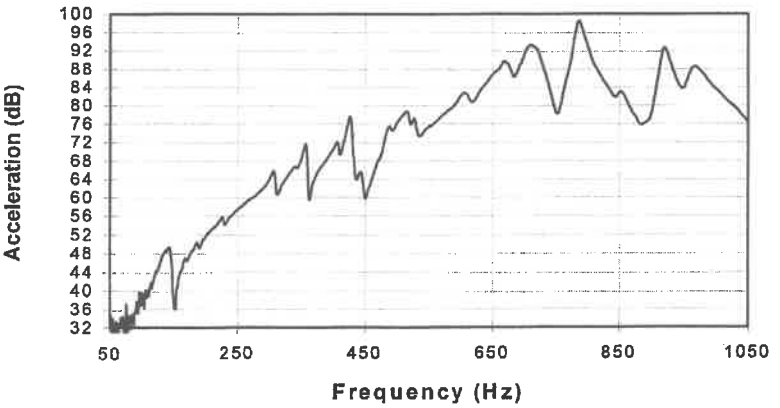

Figure 4.15 Acceleration at constant force Versus Frequency near String Position C4 on Held, Barred Board (nearer side rim than cover bar)

4.8 Measurements Along the Length of the Board off the Cover Bar.

Measurements were carried out at twenty equally spaced driving points from bass to treble ends of the board over a frequency range from 50 Hz to 1000 Hz. The driving points were on a straight line positioned midway between the cover bar and the side rim of the soundboard. A summary of measurements made at six driving points (F5, C4, G4, G3, C2, G2) over the frequency range 550 Hz to 1000 Hz using the driving point admittance and phasemeter methods is shown in table 4.4.

While in the earlier experiment with driving points on the cover bar (summarised in table 4.3) there was a low incidence of resonance detection by phasemeter and Q-factor measurability for admittance peaks above a frequency of 760 Hz, in this experiment there are three peaks above this frequency for which this is not the case. This may be due to the fact that admittance maxima for resonances in the S(2,n) series are off the cover bar. As noted earlier a nodal line runs along the length of the cover bar in this series of modes.

Measurements at driving frequencies below 550 Hz when the board was held in this manner, confirmed the existence of the peaks contained in table 4.3 with two exceptions. The peaks near 280 Hz and 480 Hz were no longer detected. A plot of admittance versus position for the peak at 280 Hz based on data from the first experiment, showed S(1,2) classification. It is probable that this peak corresponds to a vibration of the holding frame and board as a single unit. In the first experiment the frame was held only at the bass and treble ends. In the second experiment the frame was held at a number of points along its length. This may explain the absence of the peaks at 280 Hz and 479 Hz in the second experiment.

Peak Admittance Frequencies (Hz)	Resonant Frequencies Detected by Phasemeter (Hz)	Maximum Q-Factor Measured
572(3)*	570(1)	47(4)
598(2)	-	36(2)
653(3)	-	45(4)
678(3)	689(1)	60(2)
736(3)	744(2)	53(2)
784(4)	795(3)	73(2)
820(2)	833(1)	53(3)
859(2)	870(1)	71(1)
887(2)	886(1)	59(1)
916(4)	915(4)	54(4)
946(2)	954(1)	37(1)
976(4)	968(3)	61(3)

Table 4.4 Summary of Measurements at Six Driving Points off Cover Bar of Clamped, Barred Soundboard over the frequency range 550 Hz to 1000 Hz

*** The figures in brackets in the first two columns refer to the number of detections. The corresponding figures in the third column refer to the number of driving points at which Q-factor was measurable.**

As can be seen from figure 4.13, admittance peaks were also detected at some driving points near frequencies 150 Hz and 220 Hz. For measurements at driving points on the cover bar these peaks were generally of significantly lower admittance than that near 188 Hz which, as will be seen, has a modal classification S(1,1). These peaks are also likely to correspond to vibrations of the holding frame and soundboard as a single unit.

As the frame was supported in this experiment at a number of points along its length at both sides as well as at its ends, the modal classifications of the vibrations at 150 Hz and 220 Hz are likely to be quite different to those of the peaks at 479 Hz and 280 Hz detected in the first experiment. Further work is necessary to identify these. In the experimental arrangements employed here, it was not possible to suppress these modes without altering the clamping conditions of the soundboard.

4.9 Plots of Admittance Along Length of Board.

As peak - to - trough heights were significantly reduced at driving points off the cover bar, admittance measurements were made at twenty driving positions along the cover bar itself from bass to treble end. The experimental arrangements were the same as those for driving points off the cover bar. The increased number of testing positions also facilitated the investigation of modes with a large number of anti-nodal regions along the length of the board. Plots of input admittance versus position along the length of the board for resonant modes identified earlier were made for driving points on the cover bar and off the cover bar.

As the frequency of corresponding admittance peaks detected at different driving positions along the length of the board varied by up to 5%, it was not useful to plot admittance against driving position at constant frequency. The procedure adopted was to plot the peak admittance against position along the board for corresponding peaks irrespective of this 5% variation in frequency.

A plot of admittance versus position along the cover bar for the mode near 190 Hz is displayed in figure 4.16(a). The corresponding plot for positions off the cover bar is displayed in figure 4.16(b). The mode appears to be the first or fundamental resonance of the soundboard having one anti-nodal region along the length of the board. Its modal classification is S(1,1).

A plot of admittance versus position along the cover bar for the mode near 320 Hz is displayed in figure 4.17(a). The corresponding plot for positions off the cover bar is displayed in figure 4.17(b). Similar plots for the resonance detected near 350 Hz are presented in figures 4.18(a) and 4.18(b). Both resonances have the same modal classification. It appears therefore that this S(1,2) mode is split, having two resonant peaks.

The plots for the resonance detected near 440 Hz are displayed in figures 4.19(a) and (b). The plot off the cover bar has lower peak - to - trough heights and is a less definite guide to modal classification than that on the cover bar itself. However S(1,3) modal classification can be inferred with reasonable confidence.

The plots along the length of the board for the mode near 527 Hz are displayed in figures 4.20(a) and (b). Again S(1,4) modal classification can be inferred with reasonable confidence.

The corresponding plots for the resonance near 572 Hz are displayed in figures 4.21(a) and (b). The plot for driving points off the bar is again unclear. The plot for driving points on the bar seems to have the same shape as that for the mode at 527 Hz. It was observed in the Chladni powder pattern experiment that the number of anti-nodes along the length of the board differed by one on either side of the central bar for modes above S(1,4). Because of its position in the hierarchy of modes this resonance probably corresponds to the S(1,5) mode.

The plots for the resonance near 678 Hz are displayed in figures 4.22(a) and (b). The plot along the cover bar indicates the same number of anti-nodal regions as indicated for both resonances immediately below it on the frequency scale. It may be that the transition from S(1,n) to S(2,n) modes takes place at this frequency and that this the S(2,5) mode.

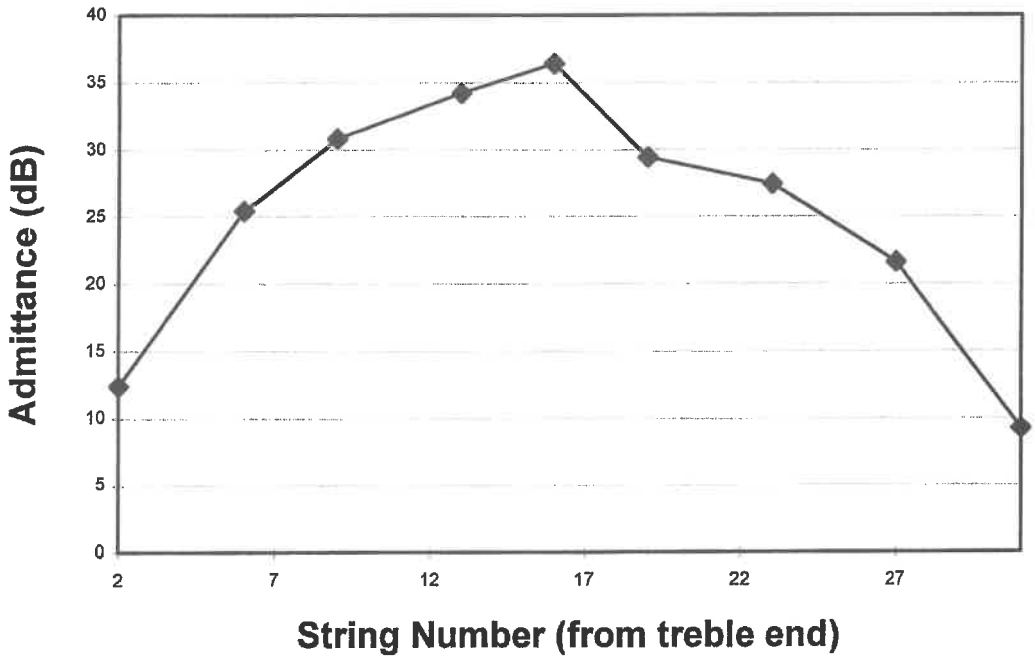

Figure 4.16(a) Relative Admittance v Position along Soundboard from Treble End for Mode near 188 Hz (on cover bar)

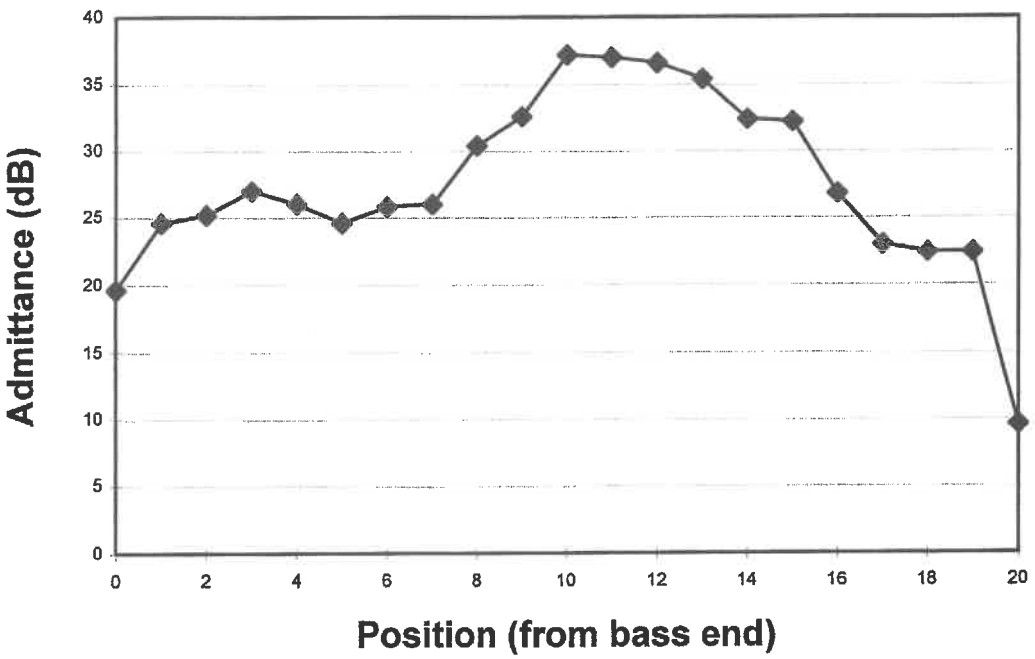

Figure 4.16(b) Relative Admittance v Position along Soundboard from Bass End for Mode near 188 Hz (off cover bar)

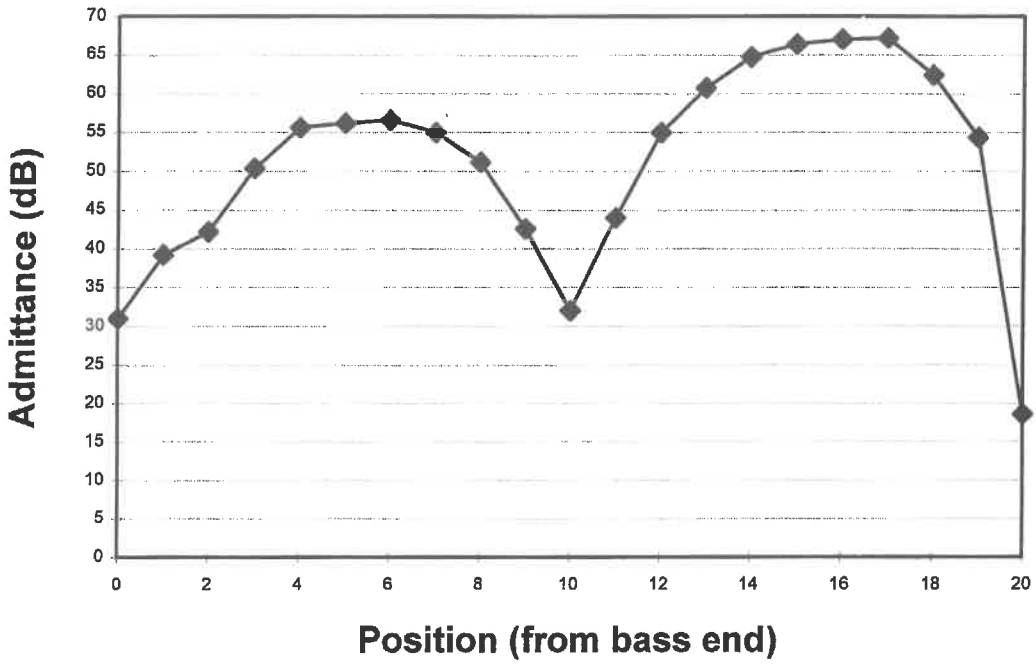

Figure 4.17(a) Relative Admittance v Position along Soundboard from Bass End for Mode near 320 Hz (on cover bar)

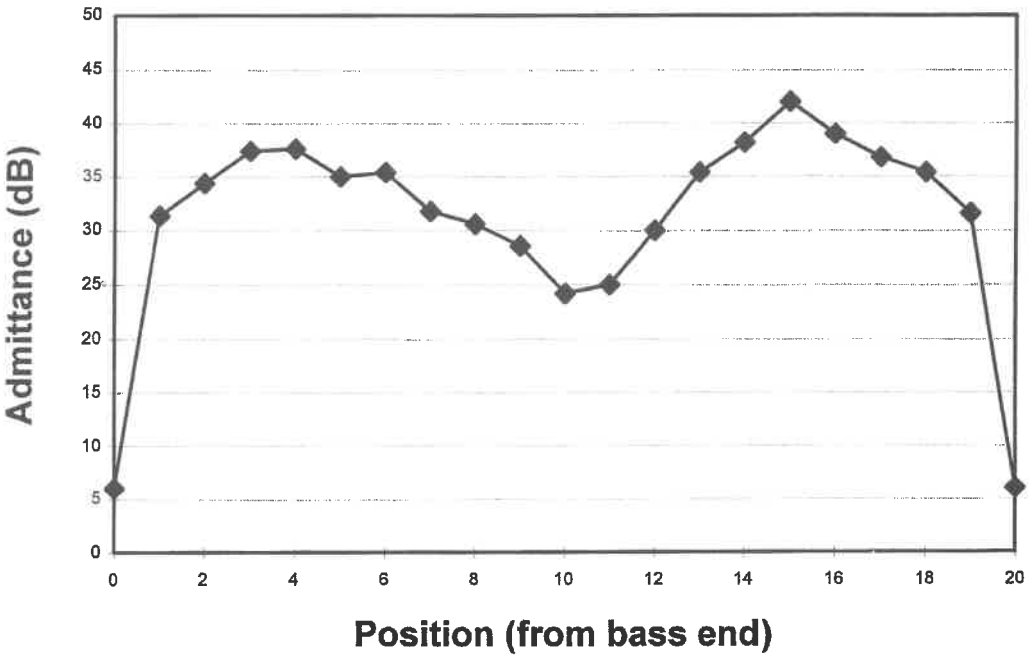

Figure 4.17(b) Relative Admittance v Position along Soundboard from Bass End for Mode near 320 Hz (off cover bar)

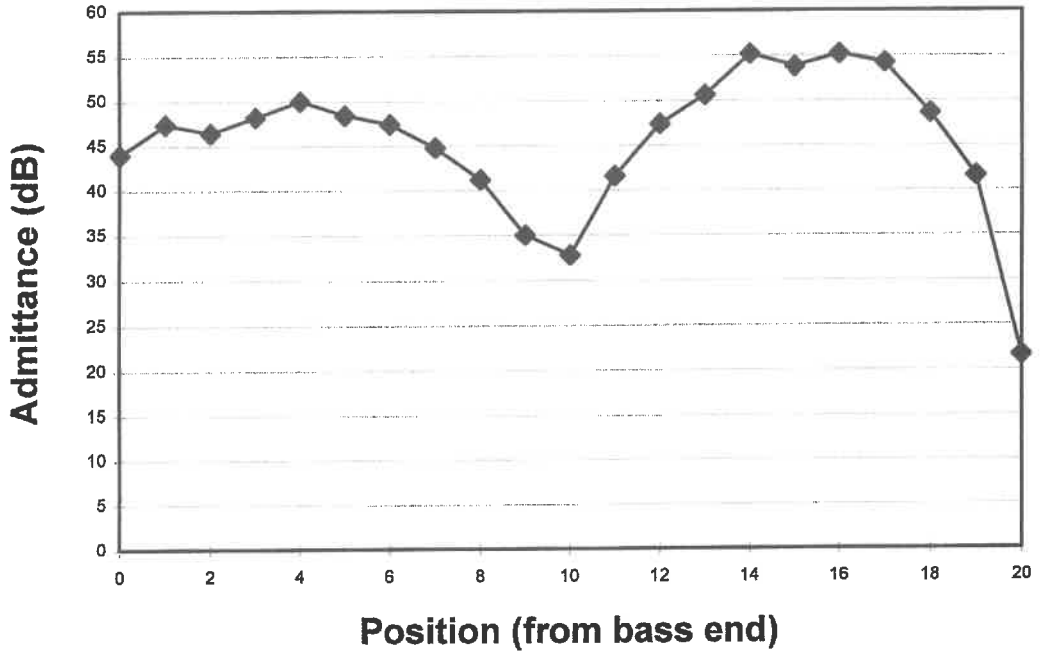

Figure 4.18(a) Relative Admittance v Position along Soundboard from Bass End for Mode near 348 Hz (on cover bar)

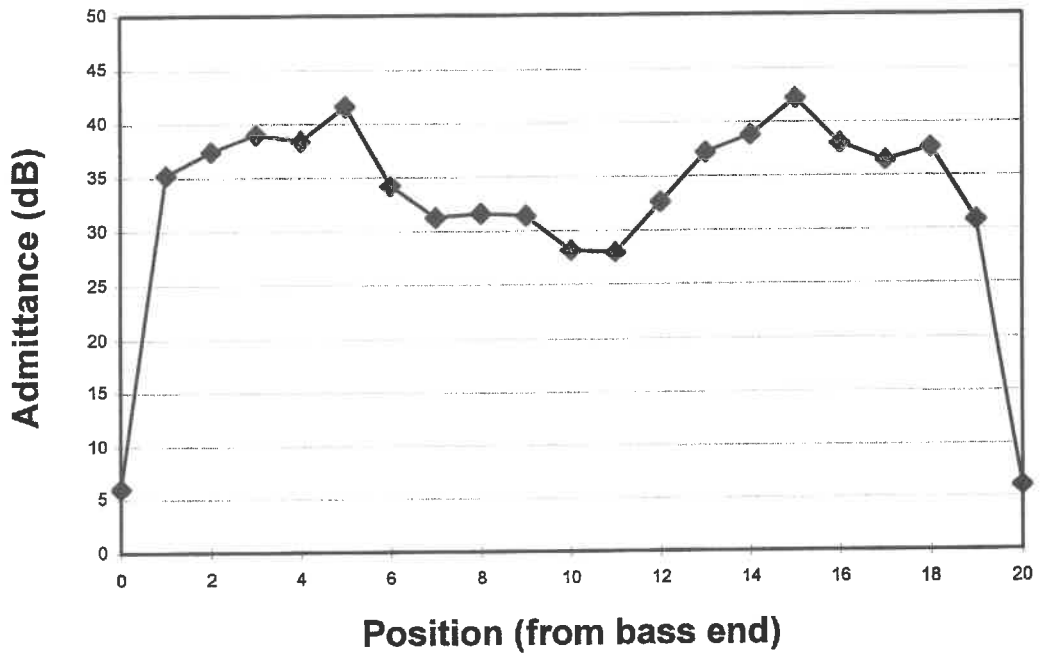

Figure 4.18(b) Relative Admittance v Position along Soundboard from Bass End for Mode near 348 Hz (off cover bar)

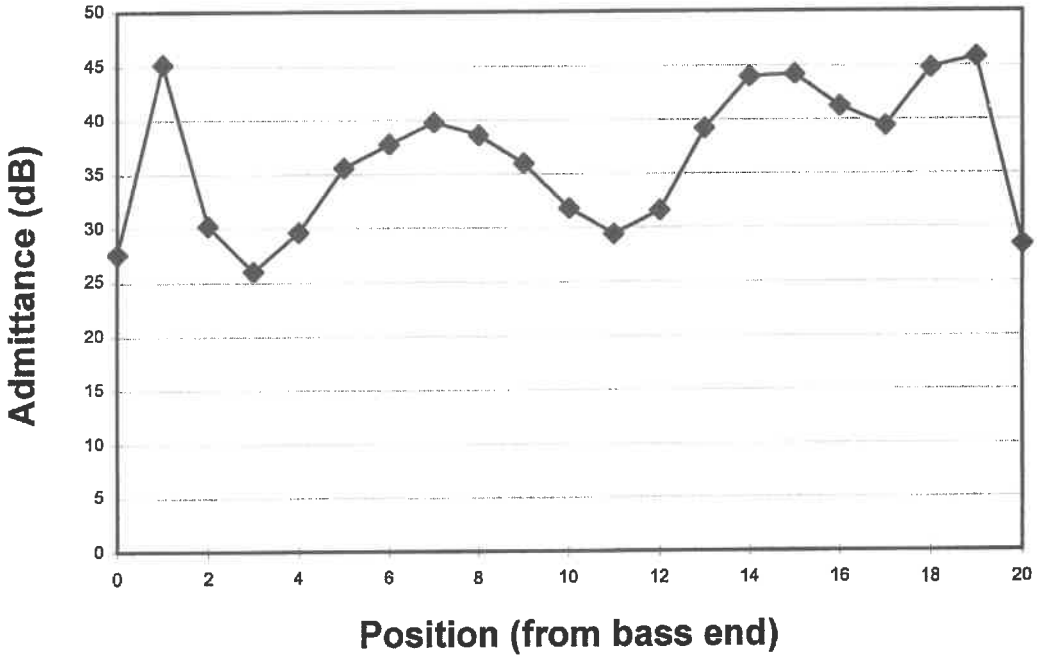

Figure 4.19(a) Relative Admittance v Position along Soundboard from Bass End for Mode near 437 Hz (on cover bar)

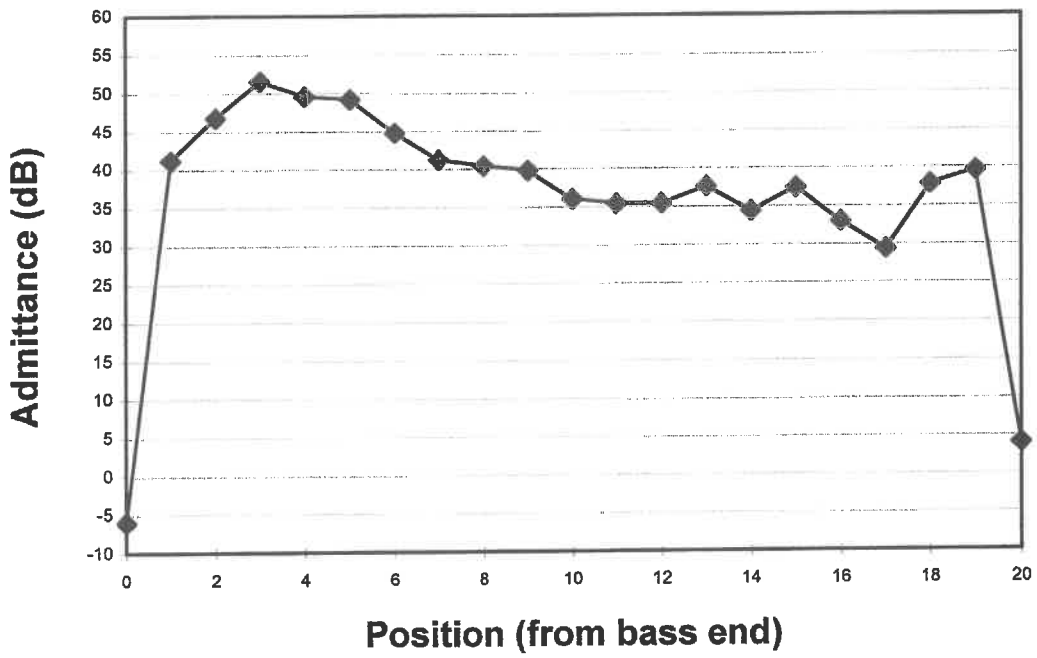

Figure 4.19(b) Relative Admittance v Position along Soundboard from Bass End for Mode near 437 Hz (off cover bar)

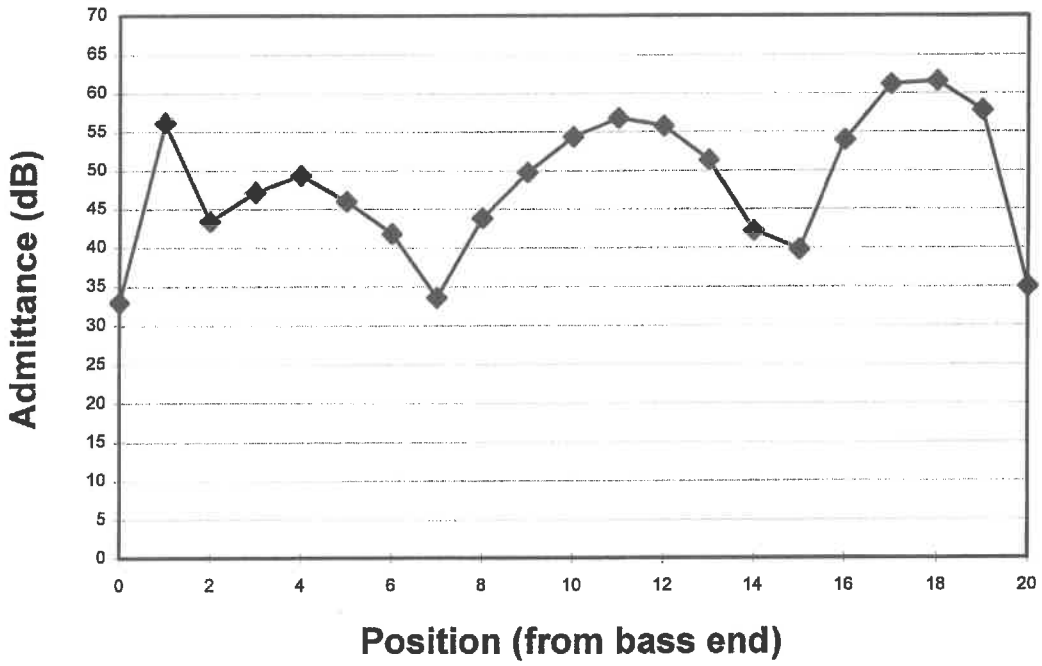

Figure 4.20(a) Relative Admittance v Position along Soundboard from Bass End for Mode near 527 Hz (on cover bar)

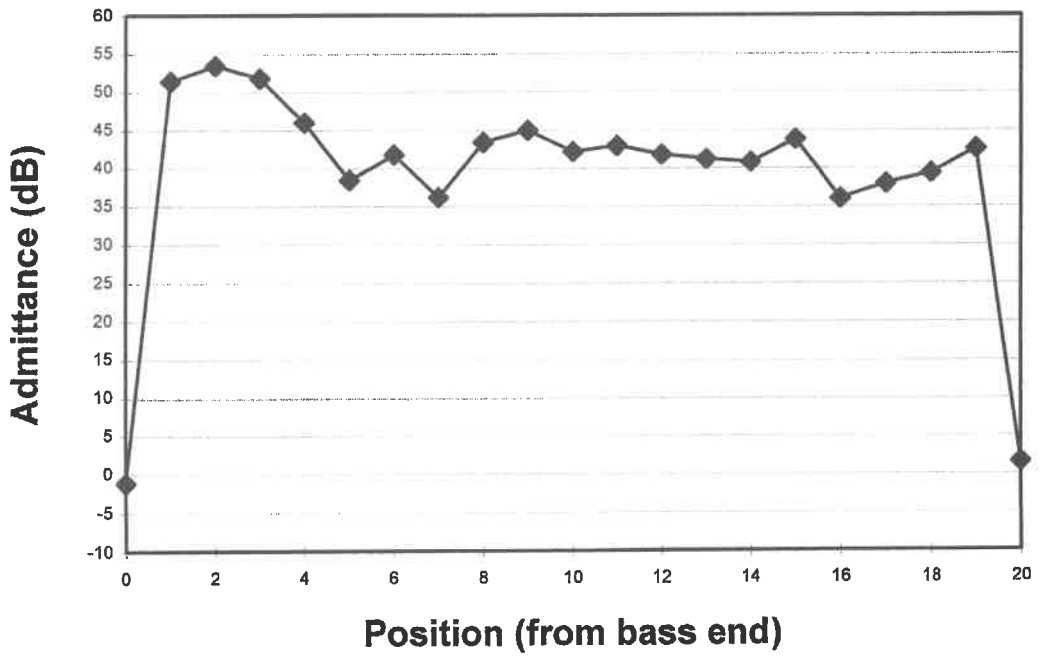

Figure 4.20(b) Relative Admittance v Position along Soundboard from Bass End for Mode near 527 Hz (off cover bar)

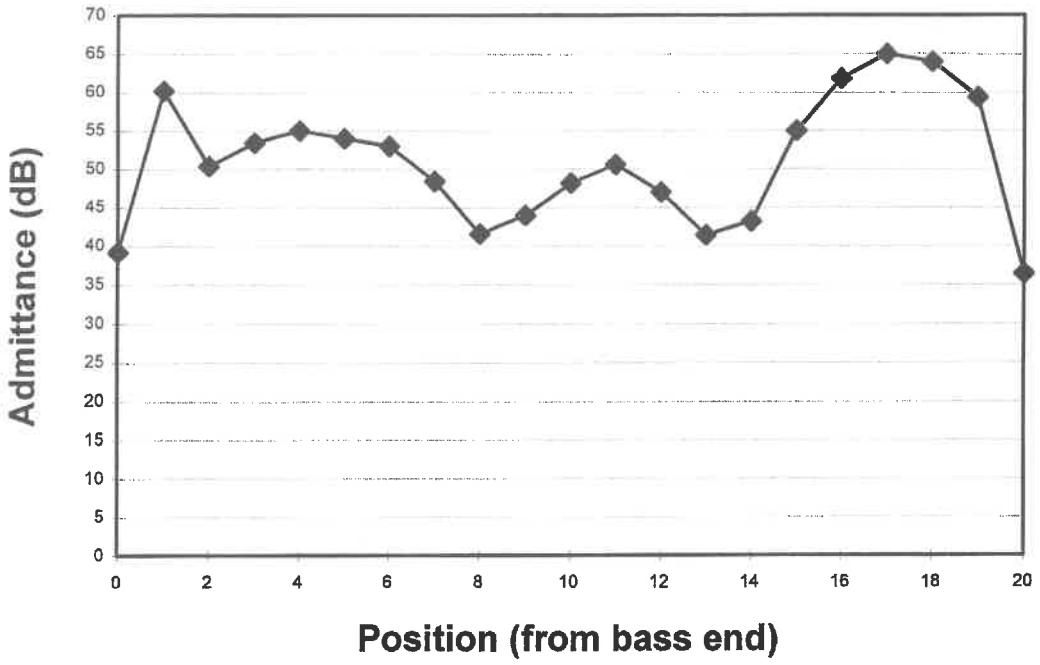

Figure 4.21(a) Relative Admittance v Position along Soundboard from Bass End for Mode near 572 Hz (on cover bar)

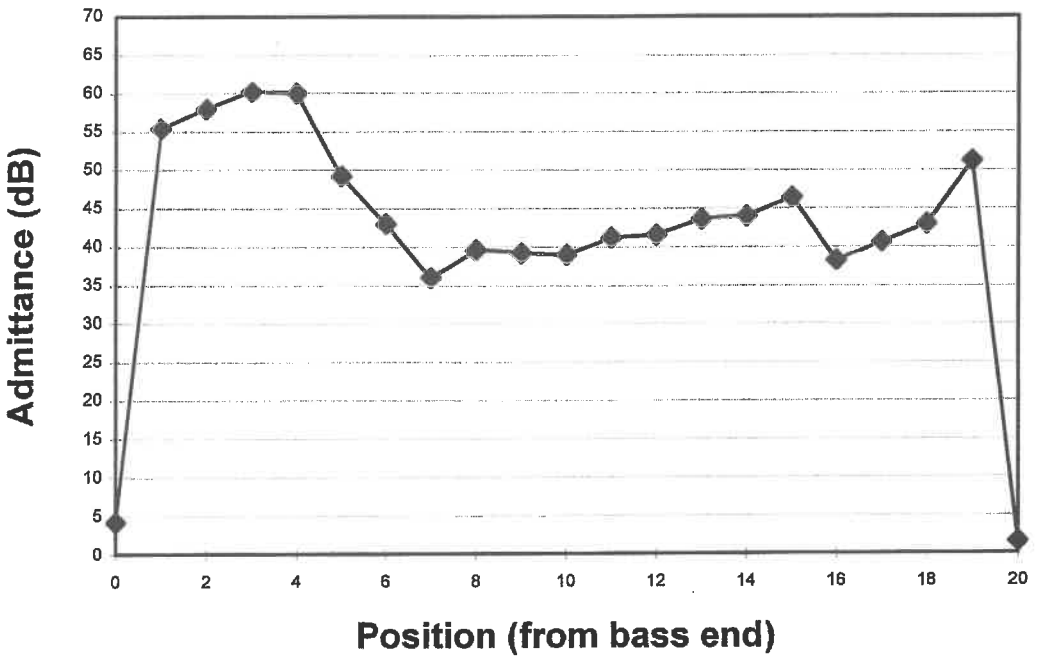

Figure 4.21(b) Relative Admittance v Position along Soundboard from Bass End for Mode near 572 Hz (off cover bar)

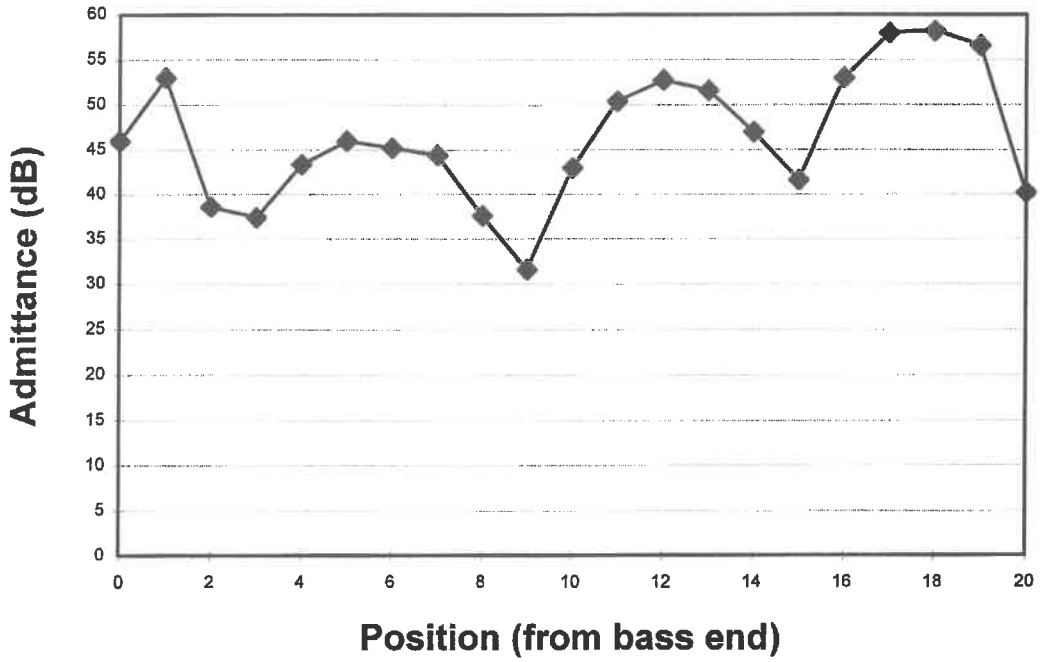

Figure 4.22(a) Relative Admittance v Position along Soundboard from Bass End for Mode near 678 Hz (on cover bar)

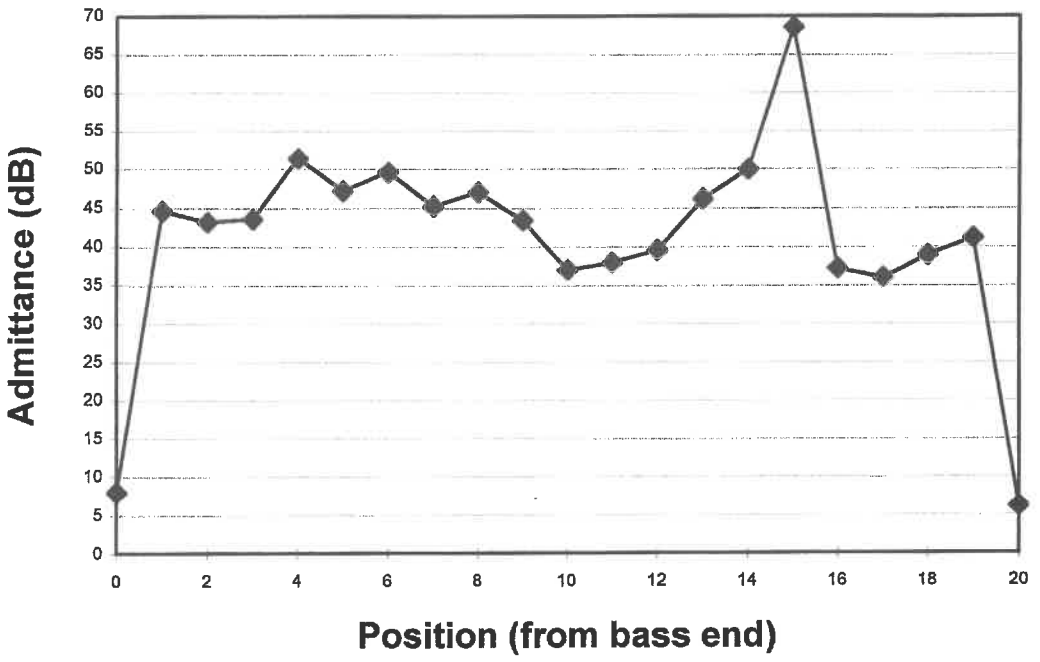

Figure 4.22(b) Relative Admittance v Position along Soundboard from Bass End for Mode near 678 Hz (off cover bar).

The admittances of the modes near 736 Hz and 784 Hz are plotted in figures 4.23(a) & (b) and figure 4.24(a) & (b) respectively. There seems to be little doubt that the transition to S(2,n) modes has actually taken place at 736 Hz based on an inspection of figure 4.23(a). The mode at 784 Hz may also be a higher order S(2,n) mode but the higher number of crests on its plot (figure 4.24(a)) would also be consistent with an S(1,n) classification.

4.10 Discussion

Plots of other admittance peaks in this frequency range along the length of the board have also been made. These show that modes 2, 3, 4 and 5, in ascending order of frequency, all have split peaks. In the case of the S(1,2) mode the peaks are detected as separate resonances. Mode 3 near 527 Hz has two additional peaks with similar admittance profiles along the board. The splitting of the modes seems to be unaffected by supporting the holding frame at different positions and in different arrangements. This splitting of the early resonant modes is also observed on the soundboard of the completed instrument. The fact that this splitting of the early board modes also occurs here on the isolated held and barred board, means that mechanical coupling with other parts of the harp or air coupling with its cavity cannot be adduced as the probable cause of the splitting of the lower frequency soundboard resonances in the harp.

References

[1]Richardson, B.E., Some Factors Affecting the Tonal Quality of the Guitar. PhD thesis, University of Wales (1982).

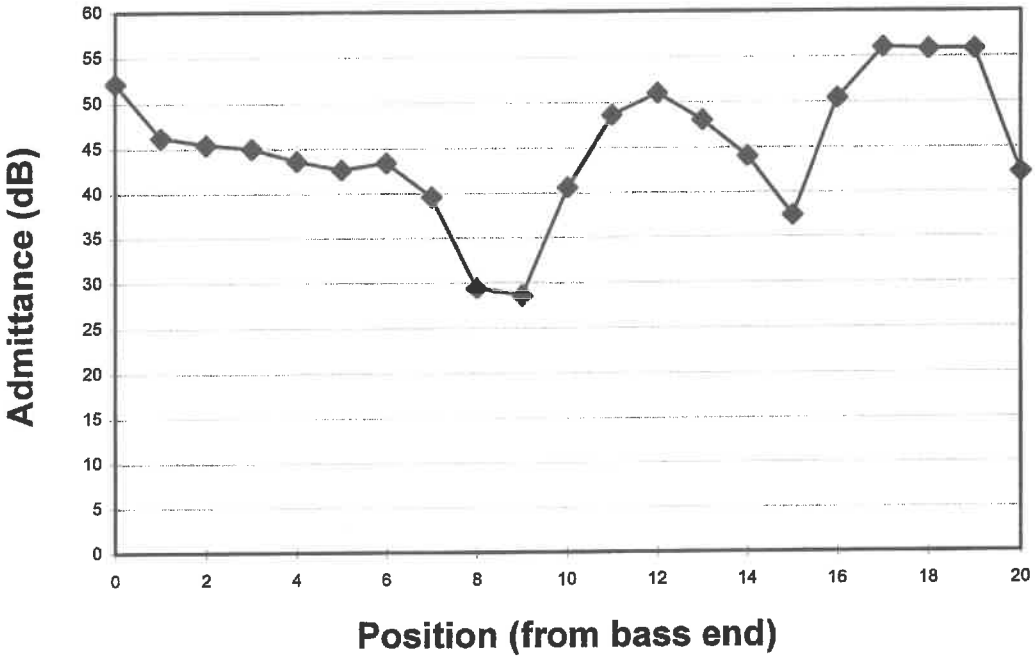

Figure 4.23(a) Relative Admittance v Position along Soundboard from Bass End for Mode near 736 Hz (on cover bar)

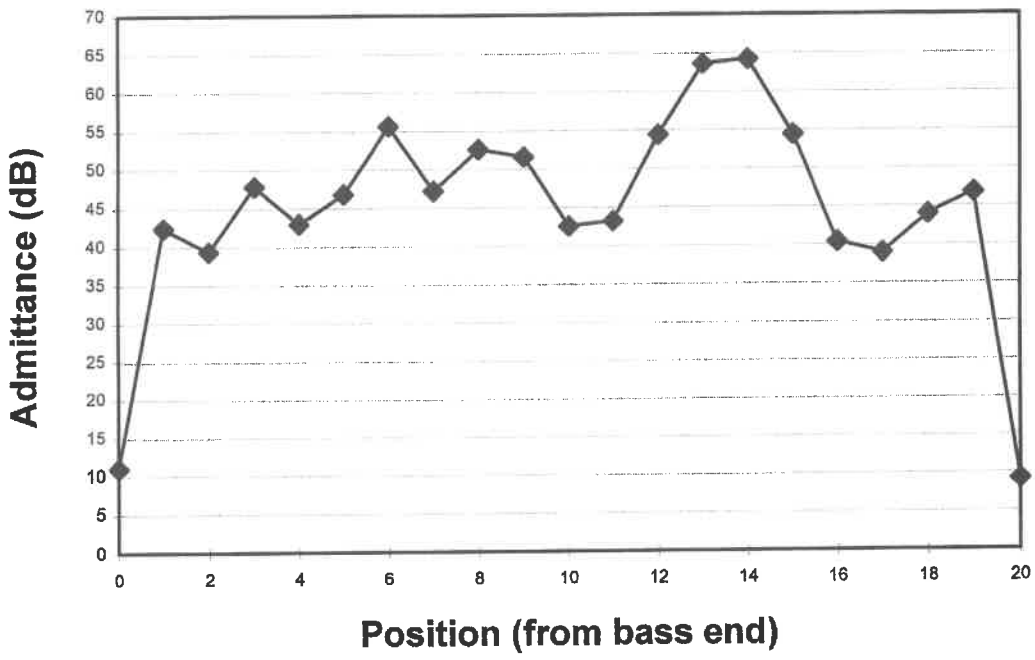

Figure 4.23(b) Relative Admittance v Position along Soundboard from Bass End for Mode near 736 Hz (off cover bar)

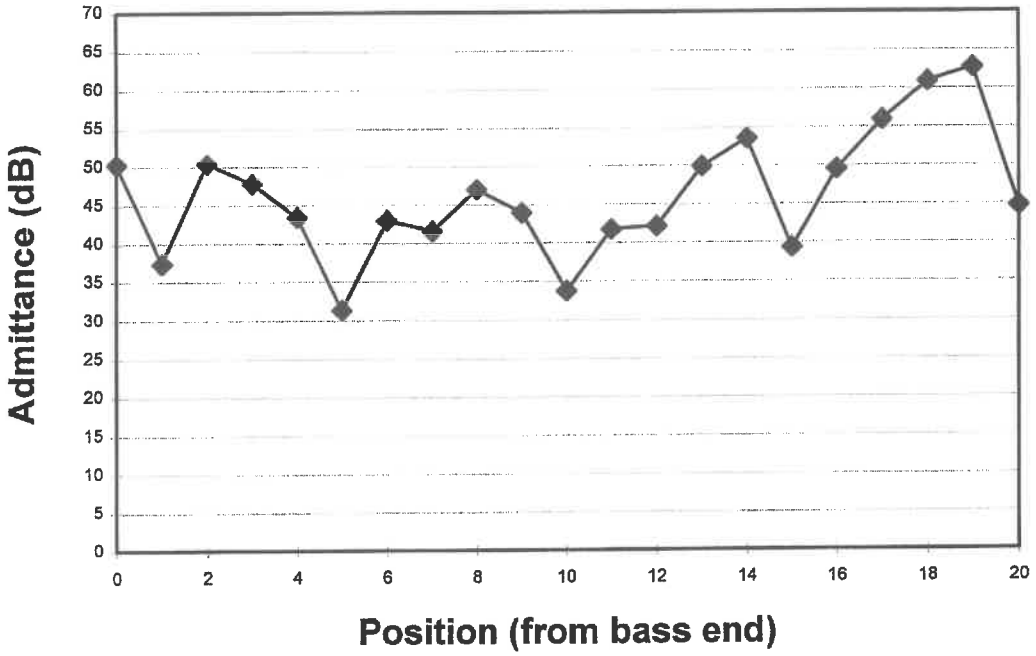

Figure 4.24(a) Relative Admittance v Position along Soundboard from Bass End for Mode near 784 Hz (on cover bar)

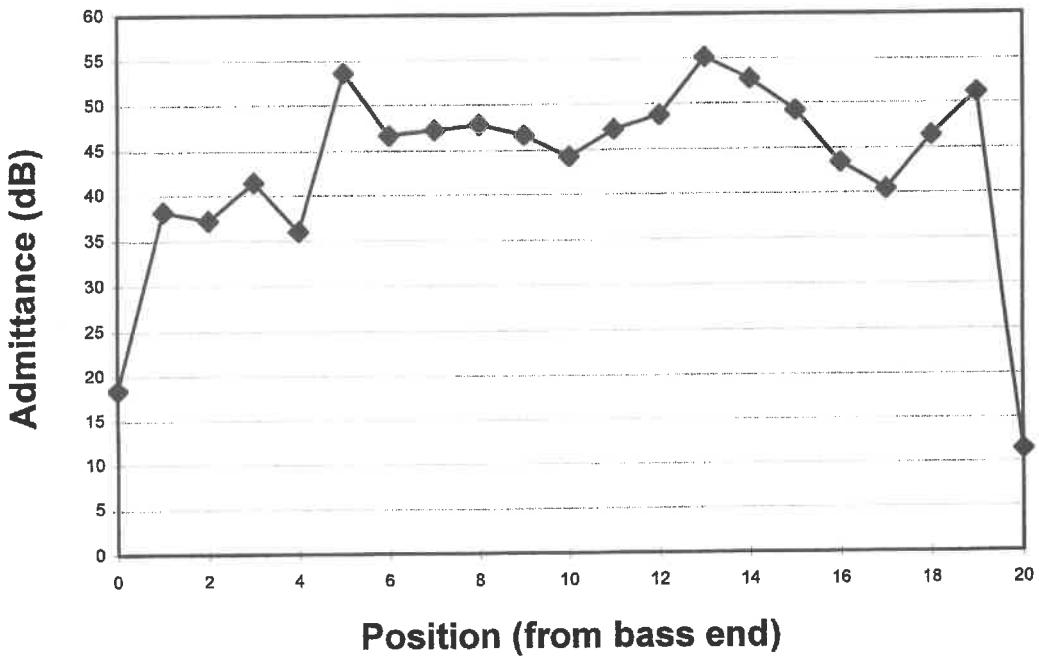

Figure 4.24(b) Relative Admittance v Position along Soundboard from Bass End for Mode near 784 Hz (off cover bar)

CHAPTER 5

THE COMPLETELY STRUNG HARP

5.1 Introduction

In the input admittance experiments on the clamped, barred soundboard described in chapter 4, admittance peaks were detected for driving points on the soundboard which appeared to be due to vibrations of the holding frame. In the completely strung harp, the soundboard with strain bar and cover bar glued along its central axis, is held in a structure whose parts have their own resonant vibrational frequencies. While the material and design of the soundboard is such as to give it relatively high resonant frequencies and relatively large input admittances, in general, in comparison to other wooden pieces in the structure, this is not the case at all driving points on the board and at all frequencies. Exchange of vibrational energy or coupling can take place between the soundboard and other parts of the harp structure. These coupling effects are significant only when the resonant frequencies of the coupled systems are close together. At driving frequencies near the coupled resonant frequencies, interference between the vibrations will occur. Destructive interference can occur at a particular frequency and a split admittance peak will result. In general, both crests of the split peak will be at frequencies different from the separate resonant frequencies. In addition the interference can give rise to changes in input admittance or peak height at a particular driving point from that which would be measured if each resonance occurred in the absence of the other. The coupling effects may be much more marked at some driving points than at others.

Richardson[1] has identified four forms of coupling in stringed instruments. The first is coupling between resonant modes of the soundboard itself. Examples of this have been found in the experiments on the held barred board described in Chapter 4. At higher frequencies for example, the frequency region occupied by the S(1,n) and the S(2,n) series of modes will overlap and close

coincidences of resonant frequencies can occur. Also, modes of the same series which occur separately at some driving points may be coupled together at other driving points, perhaps because at least one of the modes has been moved along the frequency scale due to coupling effects with other parts of the holding structure.

The second form of coupling is air coupling, which is coupling between soundboard modes or so-called plate modes and resonant modes of the air in the enclosed cavity of the instrument. The Helmholtz resonance of the air cavity is known to play an important role in violin and guitar. On the Salvi Orchestra Harp, Bell[2] identified a Helmholtz resonance at 178 Hz. Firth[3] in his earliest work on the Clarsach did not detect such a resonance but identified a number of stationary air modes in the soundbox cavity above 650 Hz.

The third form of coupling identified by Richardson[1] is mechanical coupling. Coupling between the holding frame and the soundboard in the input admittance experiments described in chapter 4 is an example of this form of coupling.

The fourth form of coupling is radiation or acoustical coupling. This involves coupling of resonant modes in which the energy is exchanged through air-borne sound waves. No account of work on this form of coupling in harps has been found.

The input of energy from the plucked string to the instrument body, when the harp is being played is, of course, an example of mechanical coupling. In the input admittance experiment to be described here, the strings were immobilised by drawing a cotton ribbon between them. This had the effect of inhibiting vibration of the strings without significantly changing the tension in the strings. In addition to eliminating coupling effects between soundboard and strings, this was necessary in order to allow vibration of the soundboard to die away quickly. Vibrations of the plucked string in the Irish Folk Harp can persist for up to two seconds and are damped out with the palm of the hand when the instrument is being played.

In the experiment the strings were tuned to pitch. This means that the soundboard, in addition to being coupled to the triangular structure of the harp by being set into it, is also coupled strongly to that structure and in particular to the string arm, through the strings.

The soundboard is most strongly coupled to the soundbox to which it is glued all around the edges. The soundbox, in addition to the cedar soundboard, is made of two mahogany side plates and a mahogany back plate with air holes. There is also a large access hole in the base which is used to install and remove strings from the instrument.

At the treble end of the soundboard, all plates of the soundbox, including the barred soundboard, are held by the string arm at the neck. As the central bars on the soundboard are much reduced in thickness at this end, it is thought that there is little difference between the manner in which the central portion of the board and the remainder of the board is supported at this end. This is not the case at the bass end of the soundboard. The foot of the pillar holds the central bars at some distance from the bass end of the soundbox giving an effective vibrating length of 820 mm. The portions of the board near the two side rims of the soundbox are held at the bass end by the rim of the soundbox. The length of the soundboard from the treble end to the bass end of the soundbox, when the glued-down edges are excluded, is approximately 88 cm. The foot of the pillar, though it is only directly attached to the central portion of the board, does have a supporting effect on the wider reaches of the soundboard. Nevertheless, the height of admittance peaks has been observed to increase as the driving point is moved across the board from the cover bar near the bass end of the board, in cases where the modal classification of the peak is clearly S(1,n). The greatest combined thickness of bars and soundboard in this region is approximately 3 cm, whereas the greatest thickness of the board alone is 4.5 mm. This is also likely to be a factor contributing to the increase in driving point admittance.

The triangular structure of the harp, in which the string arm or so-called harmonic curve is strongly coupled to the soundbox with taut strings, in addition

to being physically connected to it at the neck, can have in-plane and out-of-plane resonant vibrations. These may be detected at driving points on the soundboard and may couple with other vibrations of the instrument.

5.2 Experimental Method.

The input admittance measuring system, described in chapter 4, was employed in these experiments on the completed, strung harp. The phasemeter was also used to measure the difference in phase angle between the driving coil current which is proportional to the driving force and the accelerometer signal voltage which is proportional to the acceleration at the driving point. The harp was tuned to pitch with an electronic tuner (Seiko Chromatic Auto-Tuner ST1000) prior to each frequency sweep.

In the first experiment the cedar and mahogany harp was tested at eighteen driving points. The string near the driving point was removed in order to position the coil over the magnet on the cover bar. In order to avoid the necessity of removing further strings, the accelerometer was placed at the driving position but on the lower side of the central bars and inside the soundbox. The drive position used was 1.0 cm above the string hole (i.e. towards the high pitch end) in each testing position.

As it was intended in this experiment to compare admittances at all the driving points at constant frequency, it was necessary to have the relative positions of coil and magnet as nearly identical as possible at each driving point. Accordingly, the procedure employed for this purpose in the experiments on the held barred board which are described in chapter 4, was also employed in this experiment. In order to replicate playing conditions as closely as practicable, the harp was simply standing on the ground when these measurements were made. No attempt was made to immobilise any part of its structure except its strings.

5.3 Admittance versus Frequency Plots.

A plot of input admittance versus driving frequency at string G3 over the range 20 Hz - 510 Hz is shown in figure 5.1. This is presented because it contains in one plot much of the information that can be gained on the instrument from this experiment when carried out at many driving points. Firstly there are many small peaks of increasing height as the input admittance climbs to a maximum near 250 Hz. There is a separate crest of a slightly lower admittance at a frequency a few hertz higher. This peak is split into at least two parts at almost all driving points. At many driving points one part of the split peak has an admittance which is several dB above the other part, allowing its Q-value to be measured. The maximum Q-value measured was 72. This resonance near 250 Hz will be shown to correspond to the first resonance of the soundboard having a modal classification S(1,1). While the Q-factor is relatively high, the base of this peak is very wide. Over a frequency range of 100 Hz, centred on the resonant frequency the admittance is in excess of 12 dB above that of the adjacent trough. The peak-to-trough height of the resonance is approximately 36 dB. This is fairly typical for driving points at string holes within one octave above or below the middle C string, which is called C3 in this work.

The next admittance peak occurs near a frequency of 290 Hz and is also detected at most driving points on the board. The maximum value of its Q-factor which was measured was 81 but unlike the resonance near 250 Hz, its base is narrower. A second similarly shaped admittance peak is found near 320 Hz. This is also evident at most driving points on the board but at some of these, it is very close to the peak near 290 Hz and they appear as twin peaks. The maximum value measured for the Q-factor of this peak near 320 Hz is 80. A report of an investigation into the nature of these two narrow-based peaks is given later in this chapter.

The next resonance on the ascending frequency scale is in the vicinity of 400 Hz. At most driving points it is twin-peaked but at driving point G3 one of the twins is itself split into two small peaks. At driving point G3, the resonance has a peak-to-trough height of approximately 32 dB.

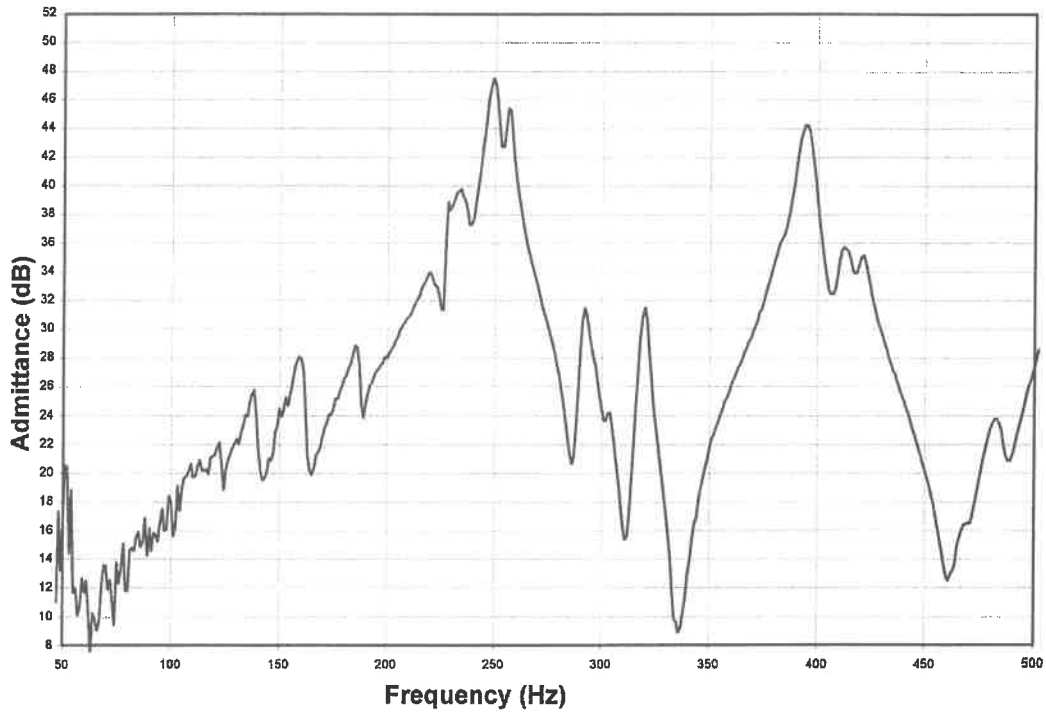

Figure 5.1 Admittance Versus Frequency at String Point G3 on the O`Meachair Cedar and Mahogany Irish Folk Harp.

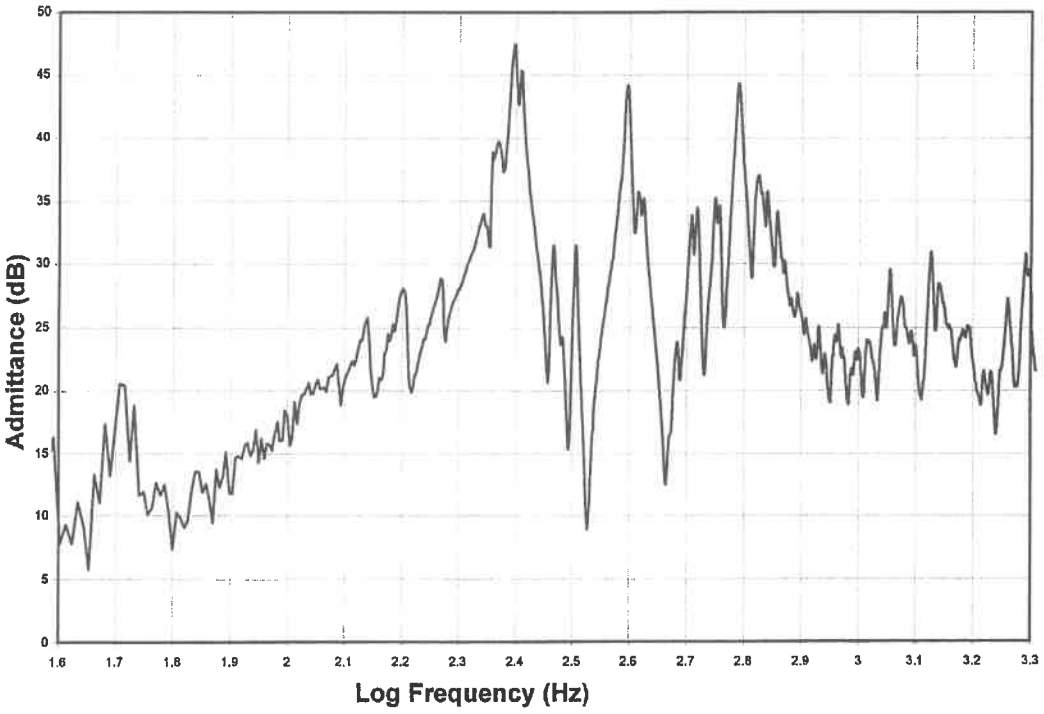

Figure 5.2 Admittance Versus Frequency at String Point G3 on the O`Meachair Cedar and Mahogany Irish Folk Harp (on a logarithmic frequency scale).

This peak-to-trough height declines to approximately 22 dB towards the centre of the board near the C3 string but it increases to approximately 44 dB near the C1 string towards the treble end and near the C4 string towards the bass end of the board. This resonance will be shown to have S(1,2) modal classification. It is found to have two distinct components, one typically occurring at 394 Hz and the other at 416 Hz. The maximum measured Q-factors were 60 at 394 Hz and 66 at 416 Hz.

While at this driving point the admittance at 394 Hz is the greater, at most driving points the admittance near 416 Hz is the higher. The base of this peak is also very wide. Over a frequency range of approximately 100 Hz, centred on the resonant frequency, the admittance is in excess of 12 dB above that of the adjacent trough, as was the case with the peak near 250 Hz.

A plot of admittance versus frequency over the range 100 Hz to 2 kHz is shown in figure 5.2. The frequency axis in this instance, has a logarithmic scale. Peak-to-trough admittance differences begin to decline significantly above 500 Hz. There is a general decline in admittance level from a frequency of 600 Hz upwards at this string point. At some other string points the marked decline begins a little further up the frequency scale, near 700 Hz. This decline is in fact steeper than represented in this plot. As can be seen from figures 3.10 and 3.12 (chapter 3), which display admittance versus frequency plots for a concrete block, the admittance measured by this system is gradually rising in this frequency region, probably due to compliant wax mounting of the accelerometer. Peak-to-trough admittance differences on the frequency plot decline very sharply above the 700 Hz to 800 Hz region. Above 2 kHz, peaks become much broader and there is a general decline in measured Q-factors. As the frequency limit above which resolution of peak frequencies is impossible is given by the rough approximation $f_0 \approx Q.\Delta f_0$ where Δf_0 is the frequency separation of peaks, some low Q-factor resonances are already unresolvable above approximately 1 kHz. The tendency towards the development of a continuum of resonance, already evident above 1 kHz, becomes dominant above 2 kHz.

5.4 Summary of Results.

Admittance peak frequencies measured at driving points just above 9 string holes are presented in table 5.1. The declining separation of peaks on the frequency scale is evident above 800 Hz. As a frequency of 2 kHz is approached, this frequency difference is of the order of 5% or less.

Peak admittance frequencies which were confirmed as resonant frequencies by phase measurement at driving points just above 5 string holes are presented in table 5.2. Above a frequency of 800 Hz the number of detections by the phasemeter falls off rapidly except at that part of the soundboard nearest the bass end.

Peak admittance frequencies with the corresponding values of the Q-factor measured for each peak at driving points just above 6 string holes, are presented in table 5.3. Measured Q-factors significantly below 30 are probably due to merged peaks. At peak frequencies lower than 800 Hz measured Q-factors which are well below the maximum values for that peak are probably due to coupling effects which can vary from one driving point to another. The number of resonant modes above 800 Hz detected by phasemeter and having a high Q-factor is significantly greater towards the bass end of the board. It is recalled that in Chladni Powder Pattern experiments on the isolated held, barred soundboard, the transition from one modal pattern to the next highest on the frequency scale above 1 kHz, typically takes place through the establishment of one additional short anti-nodal region along the length of the board near the foot of the pillar at the bass end, while the pattern on the remainder of the board stays largely unaltered.

Table 5.4 contains a list of peak admittance frequencies, detected as resonances by the phasemeter and also having measurable Q-factors. The maximum measured value of the Q-factor for the resonance in question is also given in the table. All these resonances were detected at driving points on the cover bar just above string holes but, exceptionally, the Q-factor of that at 760 Hz was detected off the cover bar midway towards the side rim of the soundboard.

G1 (Hz)	C1 (Hz)	G2 (Hz)	C2 (Hz)	G3 (Hz)	D3 (Hz)	G4 (Hz)	C4 (Hz)	F5 (Hz)
-	-	-	225	234	236	-	-	-
251	250	250	245	249	249	252	243	-
-	-	258	253	256	-	-	252	259
289	292	-	285	292	293	301	290	290
316	315	321	316	320	321	322	315	321
-	376	394	390	394	386	397	389	-
409	-	418	416	412	398	418	415	413
448	425	-	-	421	418	-	-	-
477	488	490	476	483	493	-	485	486
-	516	512	509	511	511	-	512	512
527	542	536	535	521	544	-	-	-
506	555	567	581	561	578	579	567	559
612	625	614	607	618	612	609	608	616
684	688	-	686	669	672	-	665	677
712	714	711	-	721	721	-	709	720
-	741	-	749	741	751	745	729	743
764	782	766	775	761	783	766	764	761
814	-	819	827	809	821	816	820	823
873	875	864	856	853	-	869	878	876
929 937	939	912 925 935	948	912 923 936	926 933	938	917 932	947
959	960	974	979	974	962	-	970	971
989	997	1007	999	988 998	988	-	-	1007

Table 5.1 Driving Point Admittance Peak Frequencies (Hz) at Nine String Points.

G1 (Hz)	C1 (Hz)	G2 (Hz)	C2 (Hz)	G3 (Hz)	D3 (Hz)	G4 (Hz)	C4 (Hz)	F5 (Hz)
1059	1038	1053	1047	1037	1035	1046	1042	1057
1121	1082 1096 1140	1119	1089 1123	1115 1137	1135	1102	1090 1116	1113
1187	1180 1220 1234	1191	1177 1197 1223	1189	1163 1189 1225	1160 1186 1220	1185	1197 1237
1275	-	1239 1271	-	1241 1263	-	1252	1287	1267
1345	1354	1341	1345	1343	1363	1338	1338	1343
1403	-	1411	-	1387	-	1400 1426	1386 1411	1393
1473	1466	1461	1477	-	1451 1483	1466 1484	1451 1488	1447 1467 1487
1537	1528	1525	1531	1523 1553	1531 1555	1554	1530	1521
1605	1598 1624	1603	1611 1641	-	1631	1584 1638	1578 1597 1624	1567
1687	1688	-	1689	1661 1707	1679 1705	-	1666	1655 1679
1755 1775	1754	1761	1755 1777	-	1733	1716 1764	1731	1719 1765
1829	1824 1860	1825	-	1821	-	1844	1877	1857 1883
1991	1970	1955	1969	1955 1981	1897 1963 1981	1940 1986	1974	1931 1967

Table 5.1(contd.)

C2 (Hz)	D3 (Hz)	C4 (Hz)	A5 (Hz)	F5 (Hz)
245	249	252	-	-
285	293	290	288	-
316	321	-	-	322
390	398	-	-	-
416	418	414	410	413
-	-	-	-	486
-	511	-	513	-
534	-	-	538	-
-	-	-	559	-
581	-	-	581	-
607	612	608	-	-
686	-	-	-	-
-	721	709	-	-
-	783	-	-	-
827	821	-	818	-
-	933	932	-	-
-	962	-	949	-
999	-	-	-	1018
1047	1035	-	1047	1057
-	-	-	-	1113
-	1163	1185	1168	1197
-	-	-	1257	1267
-	-	-	1282	-
1345	-	-	1331	1343
-	-	-	1387	1393
1477	1483	1488	-	1467
1531	-	-	-	-
-	-	-	-	1567
-	-	-	1688	-
-	-	1731	1771	1765
-	-	1877	-	1883
-	-	-	1930	1931

Table 5.2 Peak Admittance Frequencies Confirmed as Resonant Frequencies by Phase Measurement at Five String Points.

G1		C2		D3		C4		A5		F5	
f	Q	f	Q	f	Q	f	Q	f	Q	f	Q
		225	35								
		245	49			244	44				
251	46	253	72	250	41	253	63	256	64		
		285	81	295	65	291	58	287	57		
316	49	316	70	322	52	316	79	318	86	321	60
		390	60	400	50						
409	27	416	35	419	60	415	66	410	59	413	49
449	10										
		476	80	493	76			507	42	486	46
		534	34	510	39	512	28	537	96		
		581	72	576	48			558	53		
		606	71	612	44	613	76	578	12	612	16
684	98	684	26	671	30					688	86
712	36			722	90	716	70	702	78		
		827	41	822	59	849	66	816	19	820	47
				893	46					872	60
				935	39	931	23	947	41	944	67
		999	55	962	60					1008	56
1061	35	1048	55	1038	40	1042	20	1047	28	1057	42
										1114	43
1191	35	1180	30	1189	66	1185	40	1167	34	1192	48
				1226	35	1287	40	1255	96	1267	47
1350	31	1348	31							1343	39
1408	34							1383	76		
				1485	13						
1541	32	1531	41	1631	63	1530	20	1674	36	1567	46
1760	26	1689	50	1736	18	1731	48	1760	34	1768	55
						1880	24				
								1927	39	1932	19

Table 5.3 Peak admittance Frequencies (f) with Measured Q-Factors (Q) at Six String Points.

Peak Frequency f (Hz)	Maximum Measured Q-Factor
250	72
291	81
319	80
394	60
416	66
476	80
511	96
581	72
610	76
687	98
715	90
760	31
821	59
933	67
999	60
1041	55
1113	43
1185	66
1267	96
1345	39
1383	76
1483	13
1531	41
1765	55
1877	24
1931	39

Table 5.4 Peak Admittance Frequencies (f) Detected as Resonant Peaks by Phasemeter, but which also have Measurable Q-Factors (Q).

5.5 Estimation of Effective Mass of Modes.

The effective mass of modes was estimated by replacing the small accelerometer (B & K, Type 4374) with the large accelerometer (B & K, Type 4332) and observing the frequency shift of the resonant mode, as described in section 4.5 of chapter 4. The mass of the accelerometer together with the magnet placed at the driving point was 1.2 g, excluding the effect of the cable. The mass of the large accelerometer together with magnet and attaching screws was 38.3 g, excluding the effect of the cable. The string hole nearest to the admittance maximum of the mode along the length of the board was chosen as the driving point where the estimate was to be made, as the effective mass of modes is least at the anti-nodal maximum displacement and loading effects on frequency measurement are greatest there.

Table 5.5 lists the measured reductions in resonant frequencies when loaded and the estimated effective mass for each mode of the eleven lowest frequency modes examined. The estimated effective modal mass for the resonance near 291 Hz is remarkably high. Measurements carried out at two further string points where admittance is high for this mode showed no significant reduction in the value quoted in the table.

5.6 Variation of Peak Admittance Along the Soundboard.

A plot of peak admittance versus string number beginning at the treble end for the resonant mode near 250 Hz is displayed in figure 5.3. String number 31 is F5 near the bass end. The position with a string number of zero corresponds to a driving position 1 cm from the treble end of the board and above the top string (A1). The measurements were made at the 18 driving positions along the length of the board on the cover bar. Clearly the length of the board corresponds to one anti-nodal region in the mode. Driving point admittance measurements across the board along lines perpendicular to the cover bar at several string points show a decline in admittance from cover bar to side rim at this frequency. It is concluded that the resonant mode near 250 Hz corresponds to the first or fundamental soundboard resonance with modal classification S(1,1) in accordance with Richardson`s notation.

Mode Frequency (Hz)	Resonant Frequency Reduction (Hz)	Estimated effective mass (g)
250	20.0	250
291	2.0	2900
319	15.0	420
394	11.5	680
416	12.0	690
511	22.0	465
610	21.0	580
680	34.0	400
760	24.0	650
820	33.0	500

Table 5.5 Estimated Effective Modal Mass values for modes on the soundboard of the Completely Strung Harp.

Figure 5.4 displays a similar plot for the resonant mode near 416 Hz. There are two anti-nodal regions along the length of the board. Measurements along lines perpendicular to the cover bar show a general decline in admittance from cover bar to side rim in this mode. It is concluded that this resonance is the second soundboard resonance with modal classification S(1,2).

Peak admittance for the resonant frequency at 394 Hz, just below that at 416 Hz, is plotted along the length of the board and is displayed in figure 5.5. While the plot lacks the degree of clarity contained in the corresponding plot at 416 Hz, it is believed to correspond to a resonance with modal classification S(1,2) as was the case for the resonance near 416 Hz. Across-the-board measurements lend support to this contention. This mode appears to be split, having two resonant frequencies. The S(1,1) mode near 250 Hz has at least two peaks on an admittance versus frequency plot but in that case it proved impossible to detect them as two separate resonances using the phasemeter.

Plotting peak admittance versus position along the length of the board above a frequency of 416 Hz is an uncertain process. There are six separately identified admittance peaks between 470 Hz and 610 Hz. All of these have been detected by phasemeter at some driving point along the length of the board.

All of these peaks had measurable Q-factors at some driving point. Plots of acceleration at constant force versus frequency at two string points are displayed in figures 5.6 and 5.7. These plots show the complexity of the situation. While correspondence between peaks is readily apparent at many driving points, this is not so at others. The frequency of clearly corresponding peaks can vary by up to 5% between driving points. The magnitude of this variation is greater than that expected due to loading effects. Clearly extensive coupling is taking place in this frequency region. Where corresponding peaks were reasonably clear from inspection of the plots, these admittance readings were used in the plot along the length of the board.

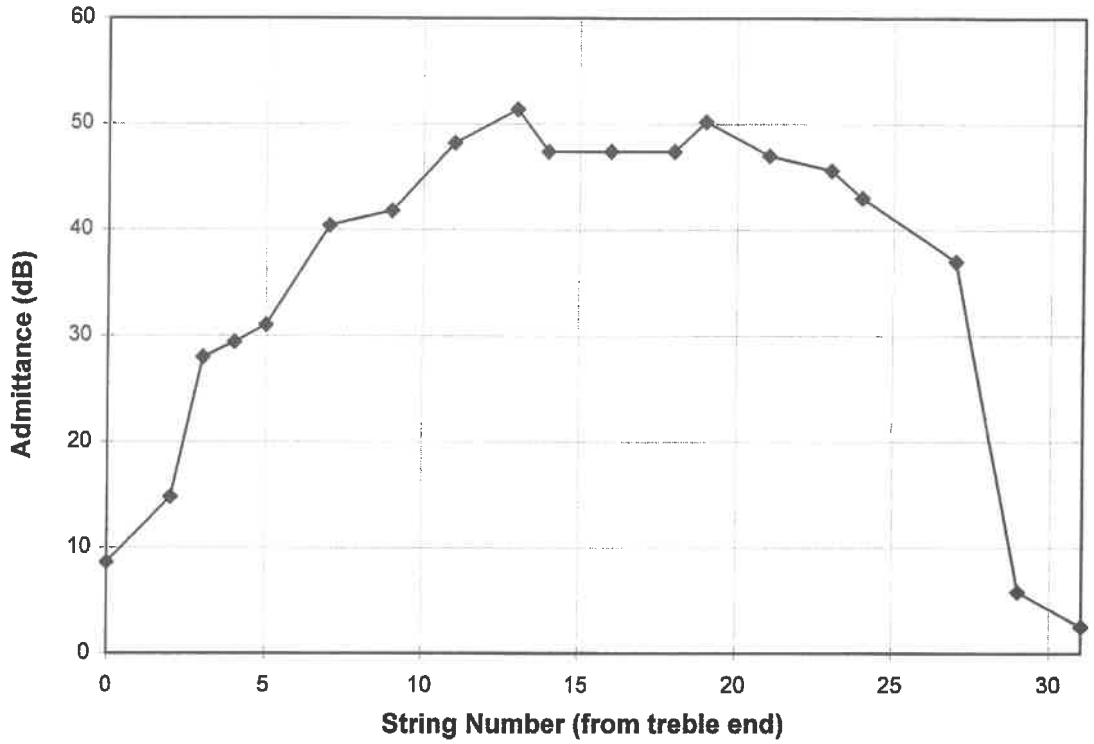

igure 5.3 Relative Admittance v String Number from Treble End for Resonant Mode near 250 Hz (on cover bar).

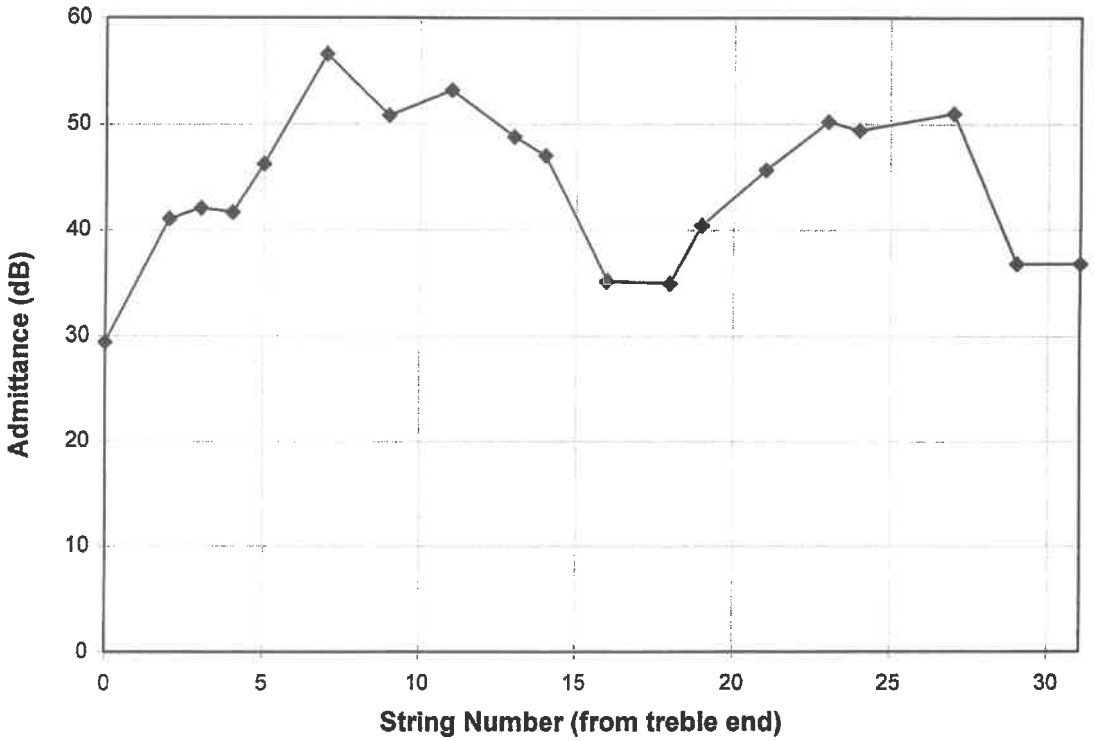

Figure 5.4 Relative Admittance v String Number from Treble End for Resonant Mode near 416 Hz (on cover bar).

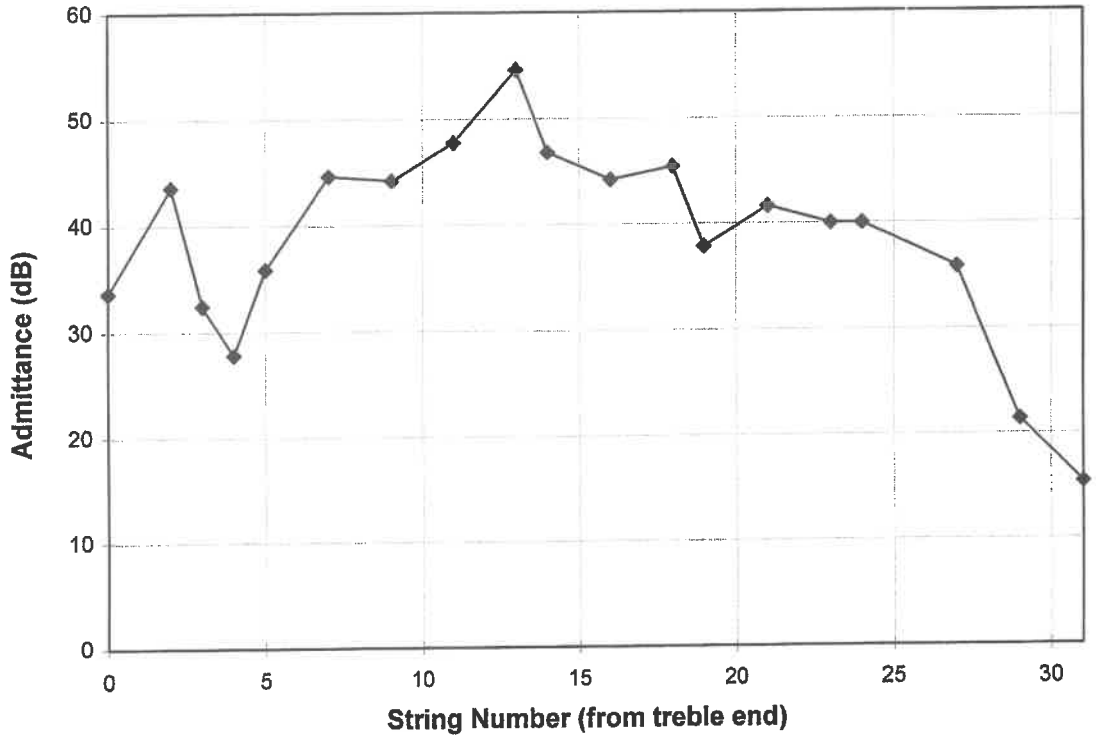

Figure 5.5 Relative Admittance v String Number from Treble End for Resonant Mode near 394 Hz (on cover bar).

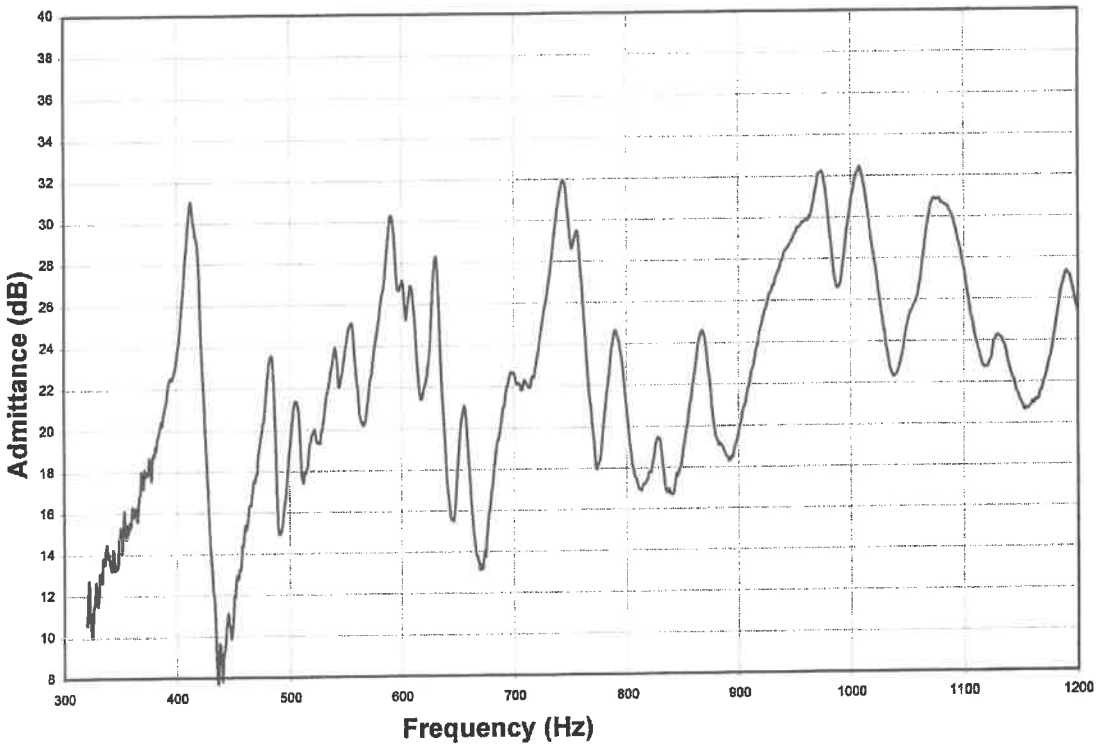

Figure 5.6 Admittance v Frequency at String Point E1 on Completed Harp.

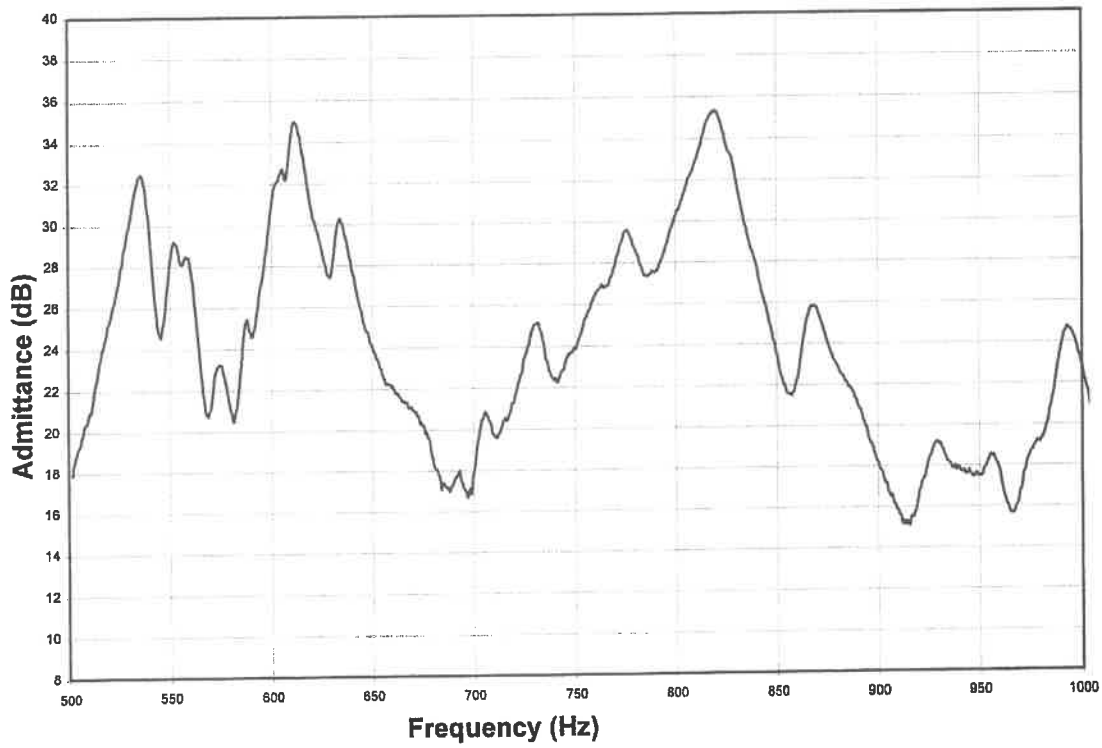

Figure 5.7 Admittance v Frequency at String Point C2 on Completed Harp.

Where an admittance peak seemed to be entirely absent at a driving point, an admittance reading was taken there at the frequency at which the peak occurred at the nearest neighbouring driving point. In some cases, an admittance peak was completely absent, though the admittance level for the frequency concerned was above that at a neighbouring driving point where the peak was clearly detected.

The admittance peak at 511 Hz is detected by phasemeter as a resonance and has a measurable Q-factor at some string points, the maximum measured value being 96. Unlike its neighbours at 476 Hz and 537 Hz, it is detected as a peak at the vast majority of driving points. Its absence at a small number of driving points is attributable to low admittance near a node. A plot of admittance versus position along the length of the board for this peak is shown in figure 5.8. Its admittance declines after string point 31 as the driving point is moved towards the foot of the pillar at C5. Although its modal classification is not clear in the plot, it is considered to be the third soundboard mode with classification S(1,3). Across-the-board measurements largely confirm that this mode is not of S(2,n) classification. The peak at 476 Hz which is detected as a resonance by phasemeter at some driving points, is very weakly detected at the bass end of the board. With the mode at 511 Hz it appears to constitute a split S(1,3) mode with the splitting being evident mainly at the treble end of the board.

The admittance peak near frequency 610 Hz is strongly detected in all regions of the board and has a high incidence of detection as a resonance by phasemeter and of Q-factor measurability at many driving points. A plot of admittance along the length of the board at this resonant frequency is displayed in figure 5.9. The resonance appears to have modal classification S(1,4). Its classification is more clearly apparent from the plot than is the case for the mode at 511 Hz. Across-the-board measurements indicate that this mode has one anti-nodal region across the board and is not of the S(2,n) series. The peak at 581 Hz also appears to have one anti-nodal region across the board and to constitute a splitting of the S(1,4) mode into two resonant frequencies.

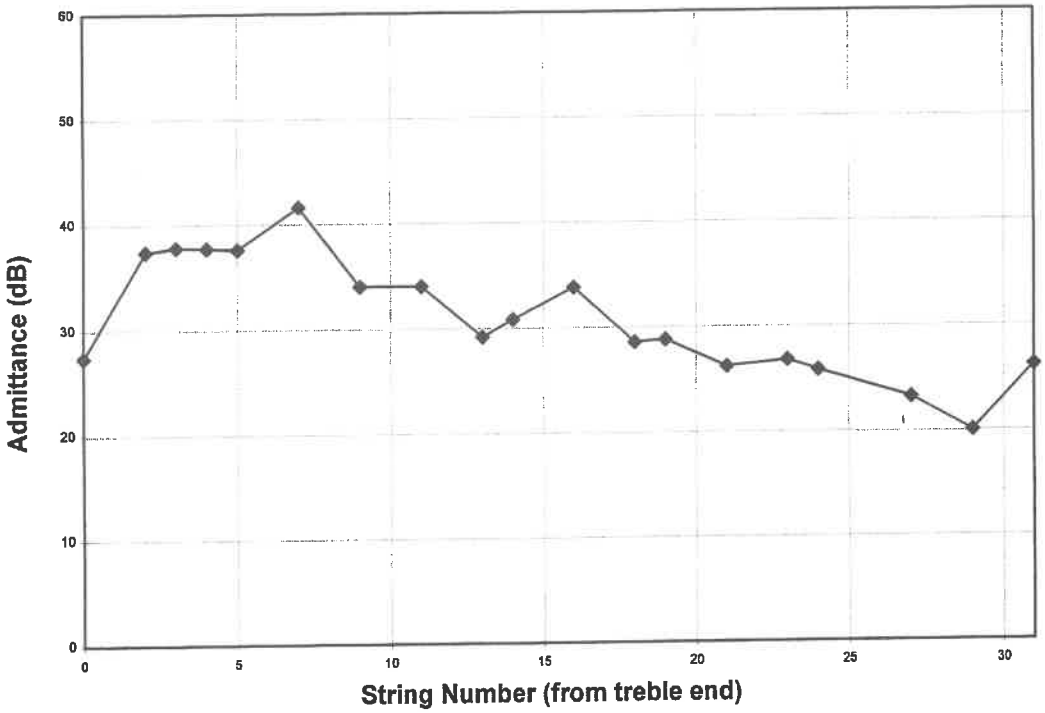

Figure 5.8 Relative Admittance v String Number from Treble End for Resonant Mode near 511 Hz (on cover bar)

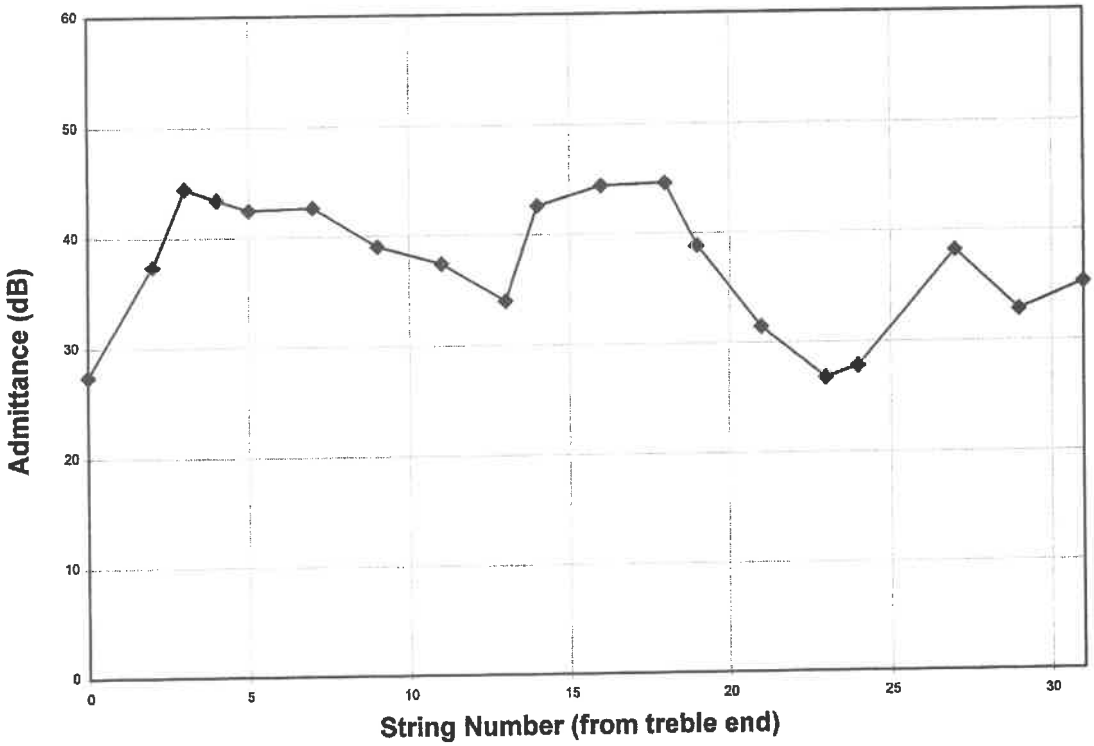

Figure 5.9 Relative Admittance v String Number from Treble End for Resonant Mode near 610 Hz (on cover bar)

5.7 Admittance Measurements off the Cover Bar.

The number of resonances per unit frequency range detected on the cover bar declines sharply between 600 Hz and 950 Hz, except at the bass end of the board. Above this range admittance measurements across the soundboard begin to show a marked increase as the driving point is moved from the cover bar to a point midway between the cover bar and the side rim of the board. This is observed at several positions along the length of the board. It was suspected that resonances of the S(2,n) classification might go undetected in measurements on the cover bar due to the central axis constituting a nodal line in this modal series. Input admittance measurements were, therefore, made at twenty driving points along the length of the board but on a line off the cover bar midway between the cover bar and the side rim of the soundboard. Closer inspection was carried out on admittance versus frequency plots at driving points along a line perpendicular to the cover bar and stretching across the board at a number of positions between the bass and the treble ends of the board.

As reported earlier in this chapter, the only additional resonant frequency detected by phasemeter and having measurable Q-factor uncovered by the measurements off the cover bar was near 760 Hz. Many admittance peaks, which could not be confirmed as resonances were detected in the frequency range between 600 Hz and 950 Hz. These had already been detected on the cover bar and are included in table 5.1.

Plots of 20×log(acceleration amplitude) versus frequency on the cover bar and off the cover bar at three string points are shown in figures 5.10, 5.11 and 5.12. (These are essentially equivalent to input admittance plots for this purpose as shown in section 3.10) Caution is required in interpreting input admittance measurements along a line across the soundboard. A steep rise in admittance off the cover bar does not necessarily signify a resonance of S(2,n) classification.

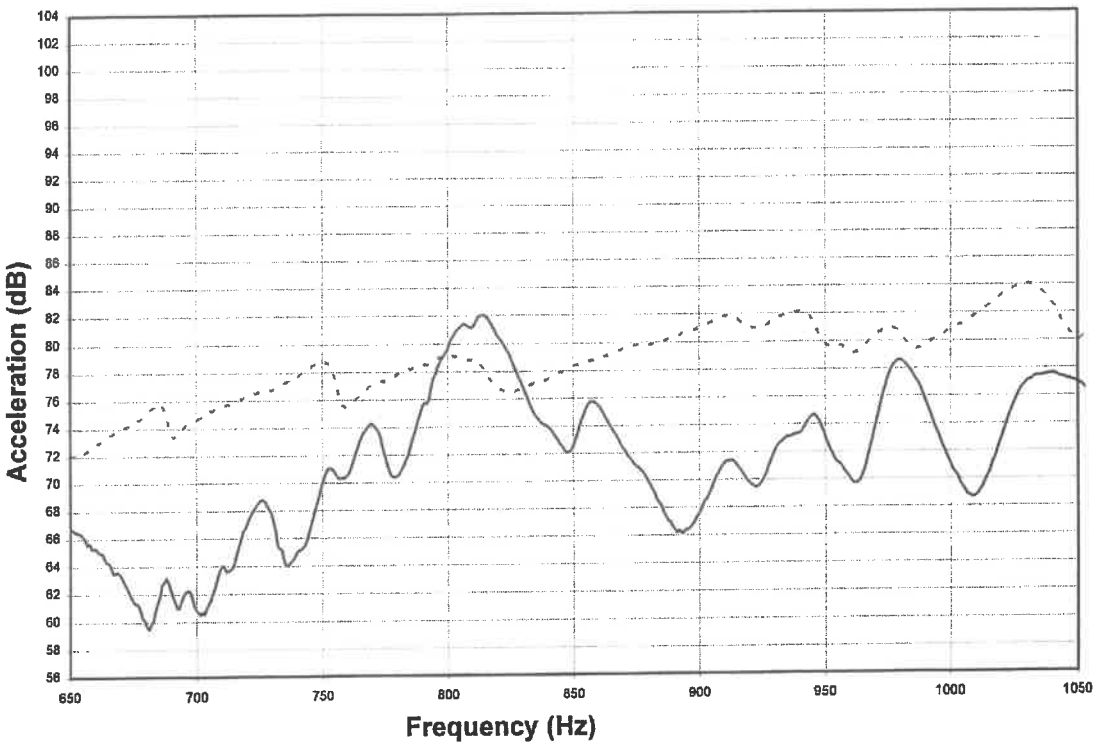

Figure 5.10 Acceleration v Frequency at String Point C2 on Completed Harp. (lighter trace at driving point off cover bar)

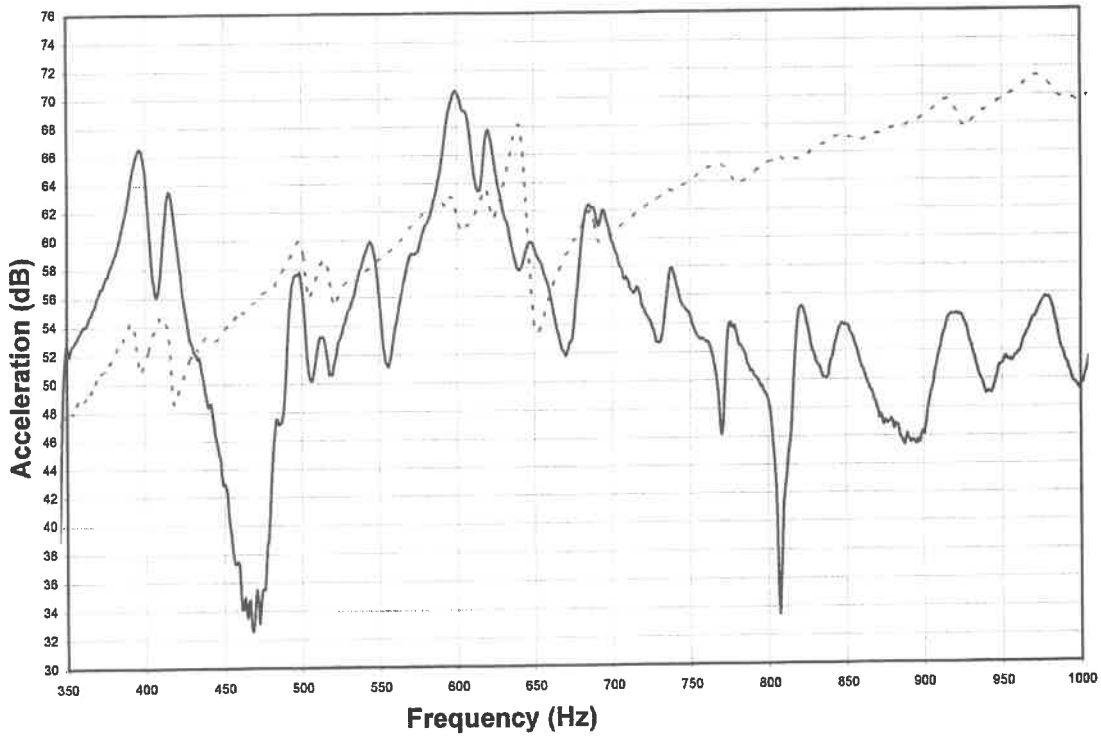

Figure 5.11 Acceleration v Frequency at String Point G3 on Completed Harp. (lighter trace at driving point off cover bar)

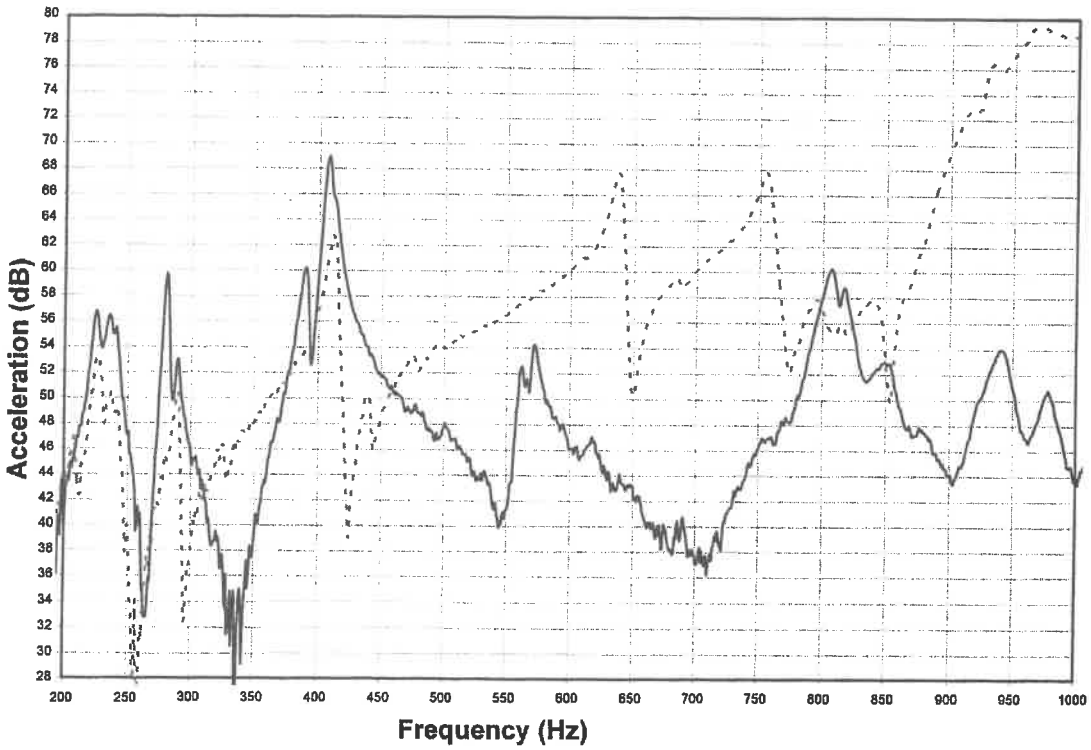

Figure 5.12 Acceleration v Frequency at String Point G4 on Completed Harp. (lighter trace at driving point off cover bar)

An inspection of the Chladni powder patterns presented in chapter 4, shows that nodal lines across the board are rarely straight lines perpendicular to the cover bar and this is markedly the case towards the bass end of the board in the S(1,n) series of modes. In addition, the large difference in board thickness between positions on the cover bar and off the cover bar could be expected to lead to different impedance matches between the driving system and the driven system. This could explain large increases in the driving point admittance of S(1,n) modes as the driving point is moved off the cover bar. Across the board measurements are not therefore decisive in differentiating between S(1,n) and S(2,n) modes. However in the S(2,n) series, a rise in admittance as the driving point is moved off the cover bar would be expected at all driving positions along the length of the board. Thus, a decline in admittance on moving off the cover bar even at one position along the length of the board, tends to rule out S(2,n) modal classification.

Using input admittance measurements only, a combination of plots of peak admittance along the length of the board and measurements across the board is necessary to differentiate between S(1,n) and S(2,n) modes with any degree of confidence. As can be seen from figure 5.11, there is either no significant change or a decline in admittance as the driving point is moved off the cover bar at string point G3 for all peaks at 690 Hz and below. It is considered likely that there is no strongly supported S(2,n) mode in separate existence below this frequency on the board. At driving points C2 (figure 5.10) and G4 (figure 5.12), the admittance of the mode at 810 Hz declines as the driving point is moved off the cover bar. It is therefore probable that this mode belongs to the S(1,n) series. The consistent rise in admittance at various positions along the length of the board as the driving point is moved off the cover bar at frequencies above 1 kHz indicates that the separate existence of strongly supported resonances of the S(1,n) series above this frequency is unlikely.

A plot of input admittance versus string number along the length of the board on the cover bar for the resonant frequency near 687 Hz is shown in figure 5.13(a). A similar plot off the cover bar is shown in figure 5.13(b). The plot on the cover bar indicates S(m,5) modal classification.

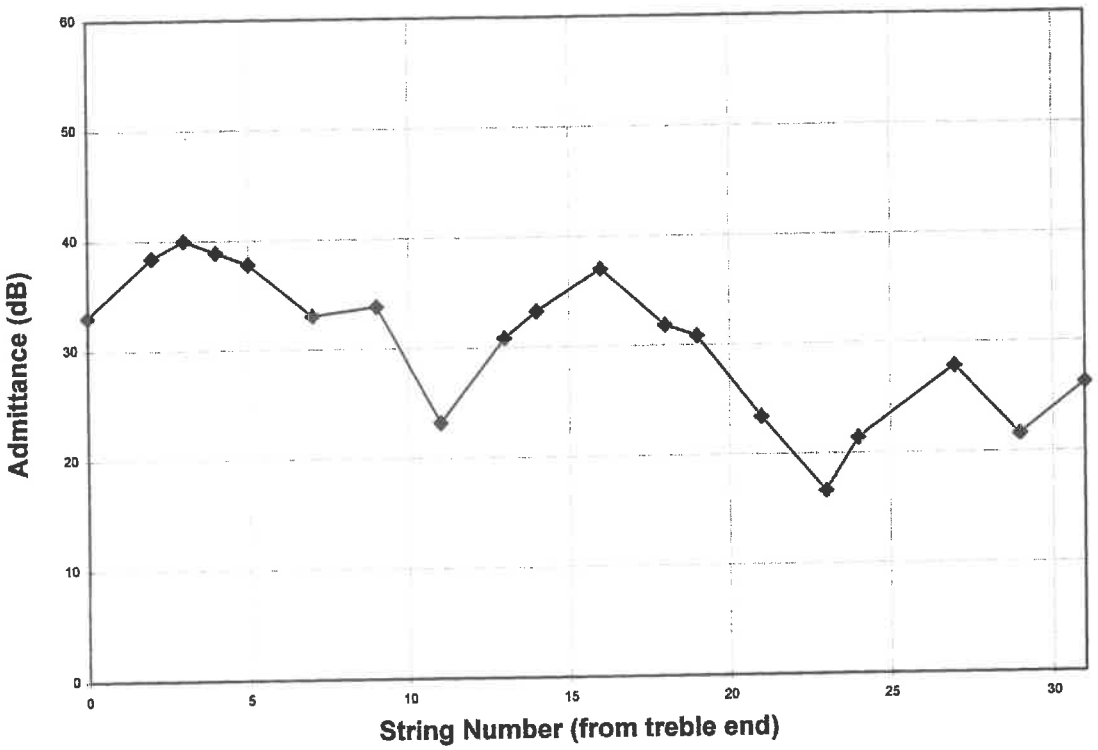

Figure 5.13(a) Relative Admittance v String Number from Treble End for Resonant Mode near 687 Hz (on cover bar)

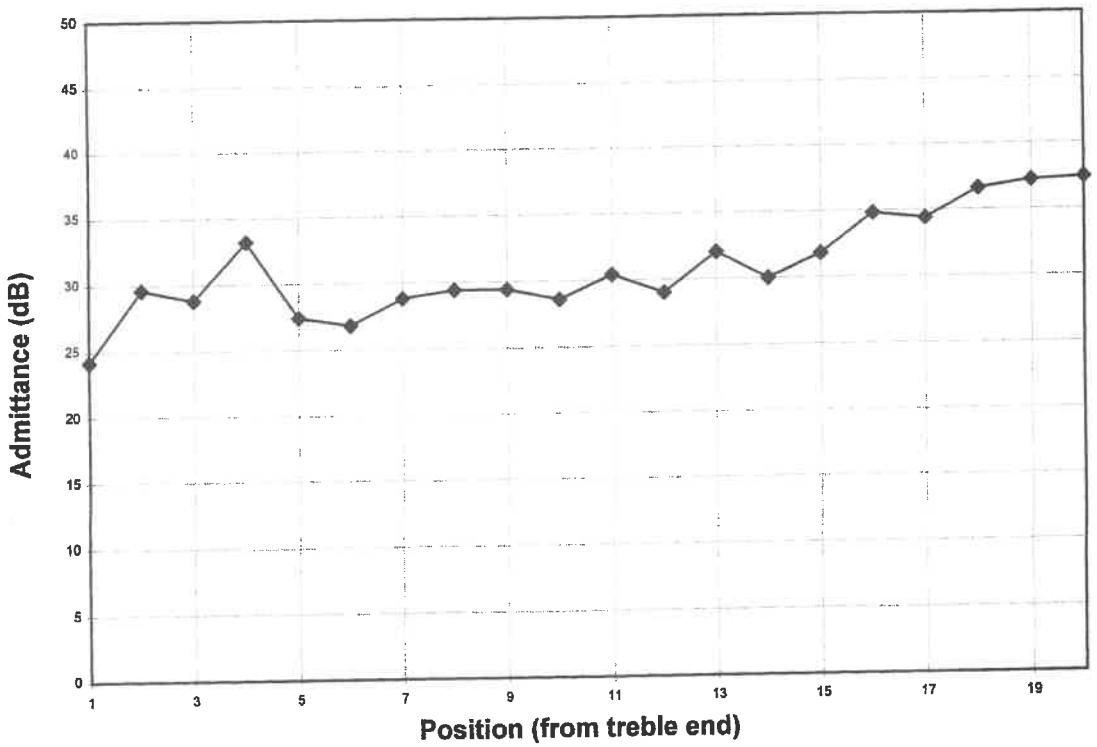

Figure 5.13(b) Relative Admittance v String Number from Treble End for Resonant Mode near 687 Hz (off cover bar)

Measurements off the bar indicate the likelihood of an S(1,n) modal classification. However, the large admittance increases at driving points off the bar near the bass end calls the S(1,n) designation into question. The fact that this mode has one more anti-nodal region along the length of the board than the mode at 610 Hz just below it on the frequency scale and that the mode just above it at 760 Hz has a smaller number of anti-nodal regions along the length of the board leads to the conclusion that the mode is probably of classification S(1,5).

A plot of input admittance along the length of the soundboard on the cover bar for the resonant mode near 760 Hz is shown in figure 5.14(a). A similar plot off the cover bar is shown in figure 5.14(b). The corresponding plots for the mode near 821 Hz are shown in figures 5.15(a) and 5.15(b). Similar plots for the mode near 933 Hz are shown in figures 5.16(a) & (b). In all these plots the peak-to-trough differences at certain regions of the board are very small, while within the same plot, a peak-to-trough difference of considerable size may exist in another region of the board. The necessity for the same resonant frequency to be accommodated at all parts of a board whose thickness and width change by a factor of approximately three from treble to bass end is likely to be a factor in this situation. Peak-to-trough differences are generally reduced in off-the-bar measurements even in modes that would appear to be of S(2,n) classification. In S(2,n) modes, points on nodal lines running across the board which are also on the cover bar are nodal from an across-the-board perspective as well as from a lengthwise perspective. Thus, while the input admittance at a point off the cover bar may be as much as 20 to 30 dB higher than on the cover bar, the admittance drop as the driving point is moved along the length of the board onto the next nodal line may be quite small. On the other hand, measurements on the cover bar may fail to detect small admittance changes along the length of the board in the S(2,n) modes, because the cover bar is a nodal line down the centre of the board. In addition to those peaks confirmed as resonances by phasemeter and Q-factor measurement which are plotted here, there are also other peaks in close proximity on the frequency scale. These may constitute splits in the resonant modes due to coupling.

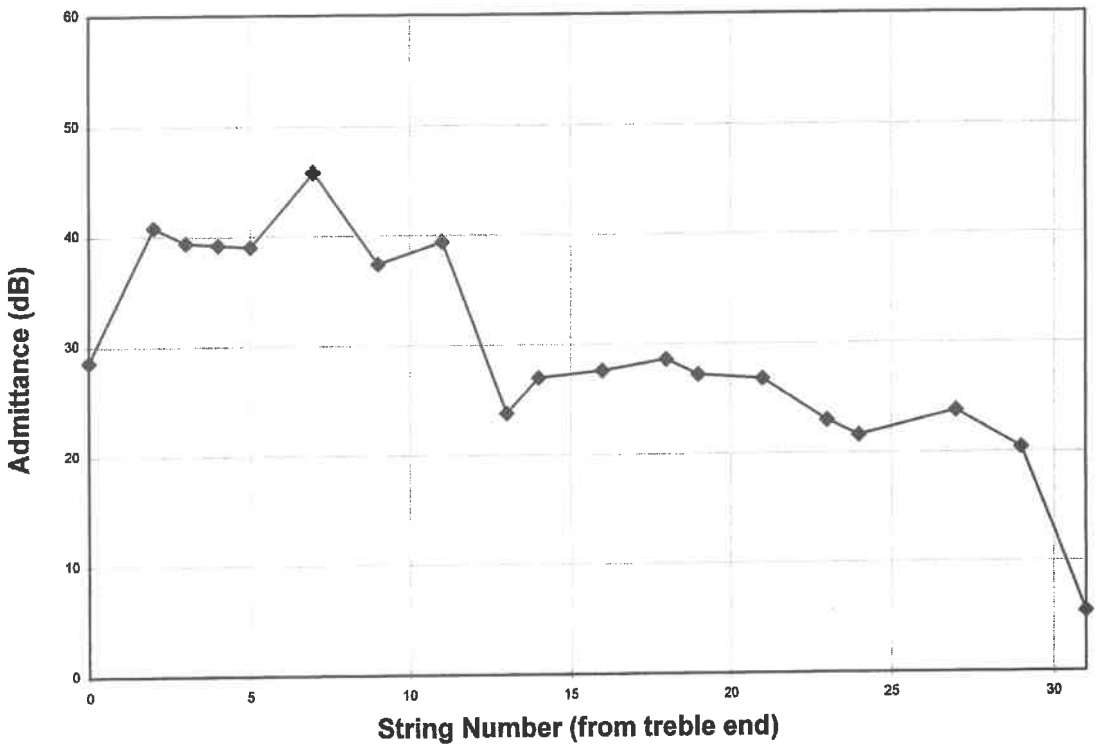

Figure 5.14(a) Relative Admittance v Position from Treble End for Resonant Mode near 760 Hz (on cover bar)

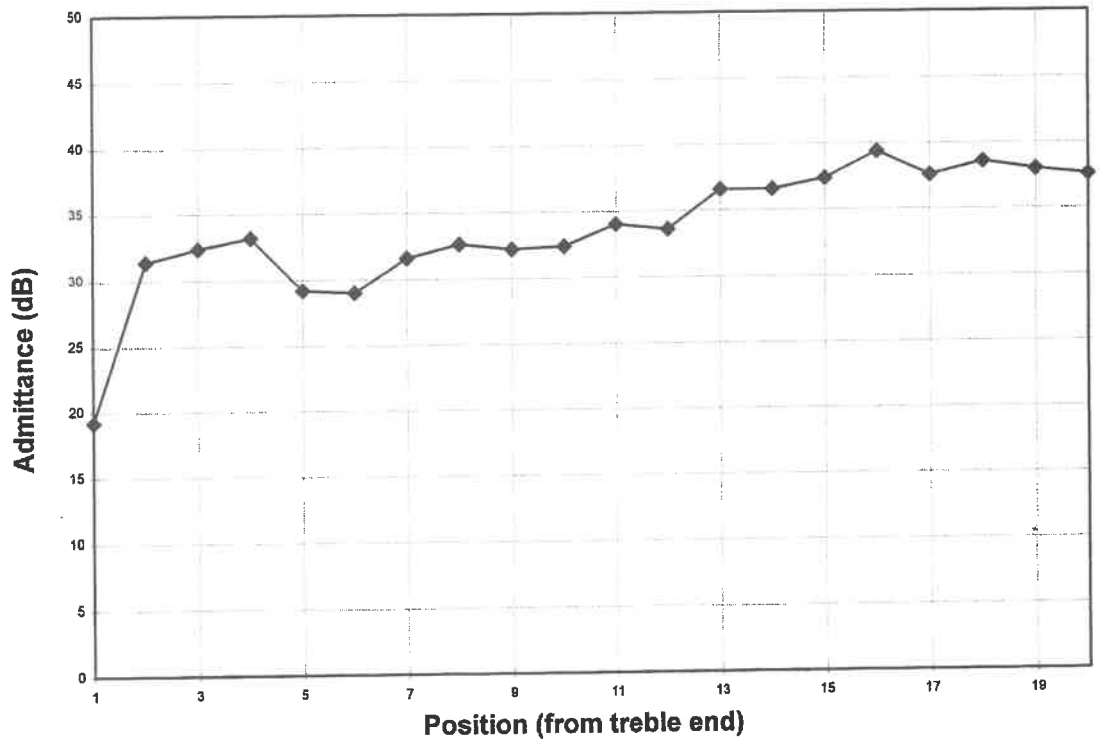

Figure 5.14(b) Relative Admittance v Position from Treble End for Resonant Mode near 760 Hz (off cover bar)

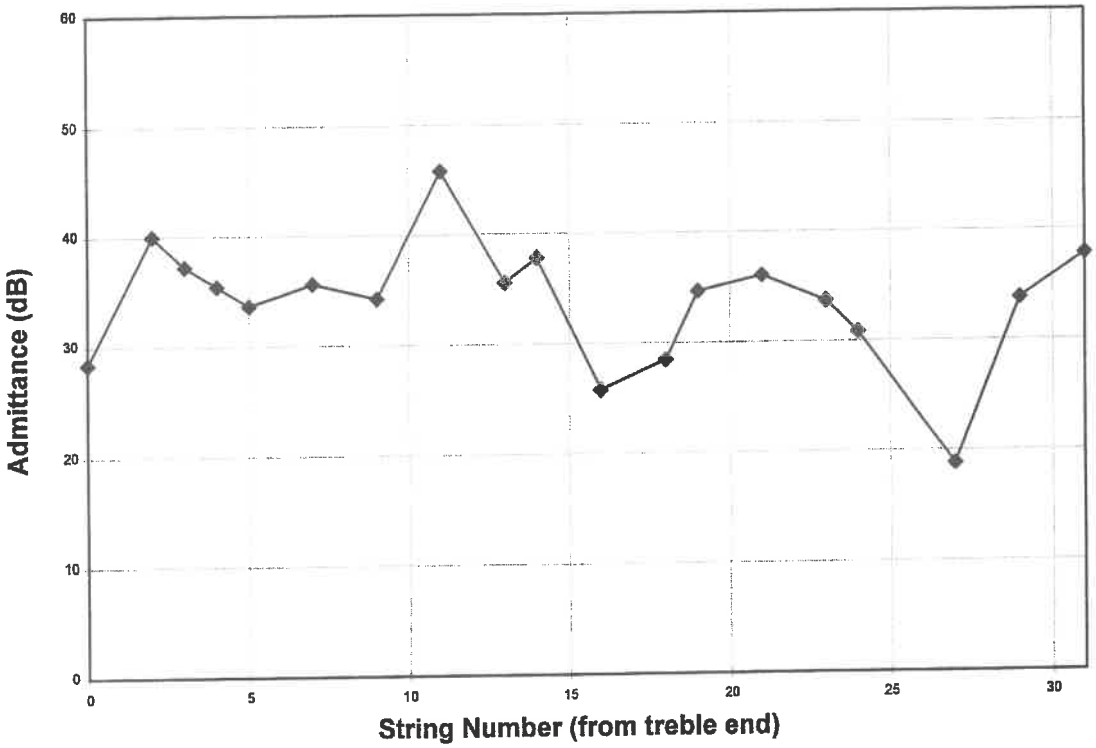

Figure 5.15(a) Relative Admittance v String Number from Treble End for Resonant Mode near 821 Hz (on cover bar)

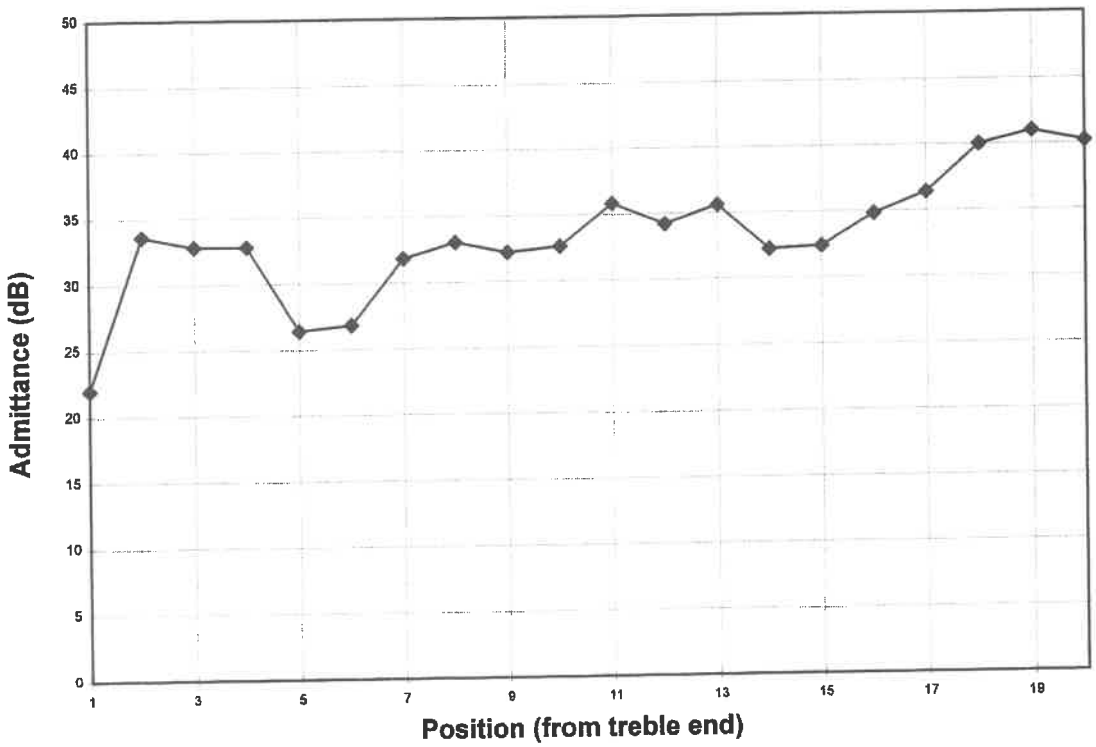

Figure 5.15(b) Relative Admittance v String Number from Treble End for Resonant Mode near 821 Hz (off cover bar)

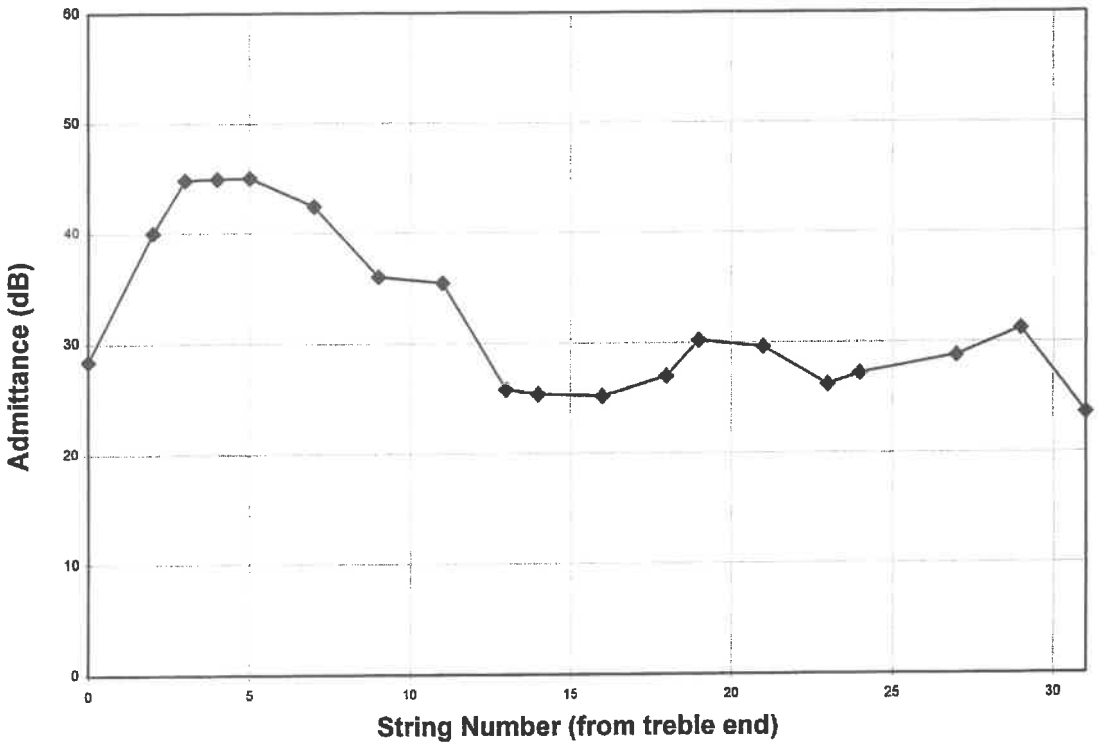

Figure 5.16(a) Relative Admittance v Position from Treble End for Resonant Mode near 933 Hz (on cover bar)

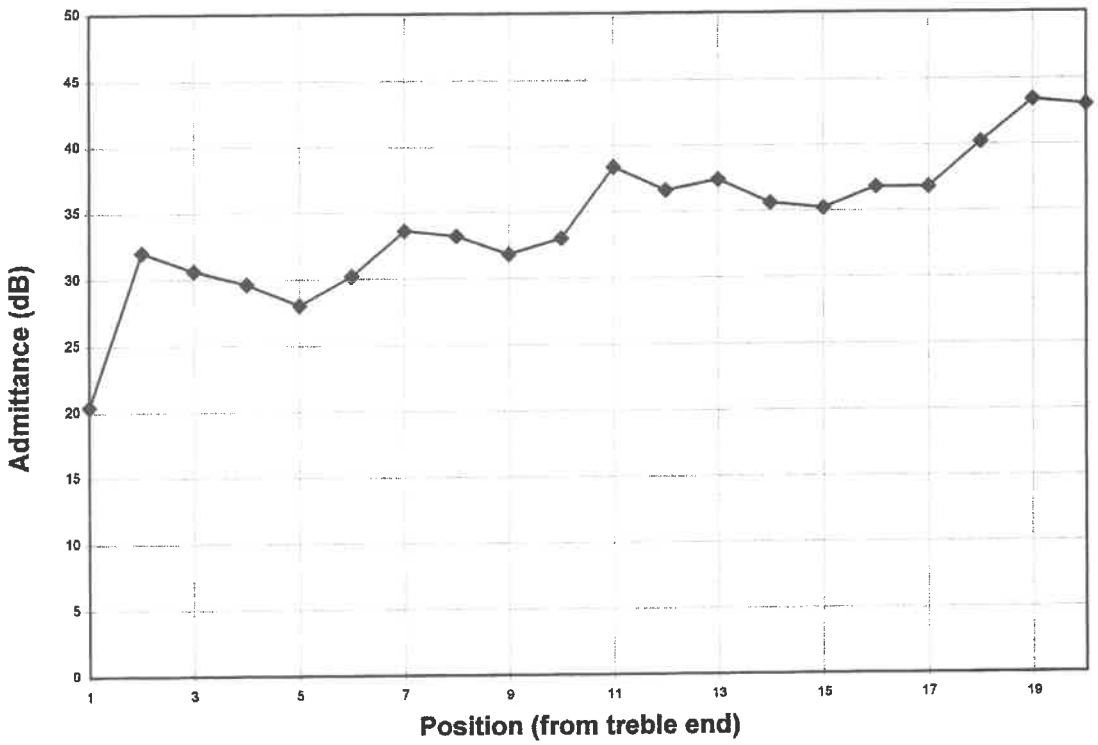

Figure 5.16(b) Relative Admittance v Position from Treble End for Resonant Mode near 933 Hz (off cover bar)

Accordingly, the task of deciding the exact modal classification of resonances in this frequency region cannot be undertaken with confidence with the data available. The use of additional driving points, both on and off the cover bar, did not provide further information that would be of assistance.

The mode at 760 Hz is almost certainly of the S(2,n) classification but the number of anti-nodal regions along the length of the board is uncertain. However, it is at least three. The mode at 821 Hz is most probably of S(1,n) classification but again the number of anti-nodal regions along the length of the board is uncertain. Because of its position in the hierarchy of modes it is probably the S(1,6) mode. The mode at 933 Hz is most probably of the S(2,n) classification with at least four anti-nodal regions along the length of the board.

5.8 Effect of String Removal on Resonant Frequencies.

Input admittance measurements were carried out on the cover bar after all the strings had been removed in order to investigate the effect of stringing on resonant frequencies. At a driving point near string hole G3 the frequency of the S(1,1) mode near 250 Hz in the strung harp fell to 211 Hz. The resonance near 291 Hz was detected at 267 Hz. The resonance near 319 Hz was detected at 276 Hz. The resonance near 394 Hz was detected at 392 Hz and the resonance near 416 Hz was unchanged. Similar changes were detected near string hole G4. The addition of tuned strings increases the frequency of the S(1,1) mode by approximately 18%, but has very little effect on that of the S(1,2) mode. This is broadly in accord with measurements of modal mass, reported above and confirms that for this instrument the S(1,1) mode is of relatively low effective mass and stiffness. The S(1,2) mode has a much greater effective stiffness and a greater effective mass. The frequency of the mode near 291 Hz is increased by 10% and that near 319 Hz by 16% by the addition of tuned strings. The mode near 291 Hz has, therefore, a considerably higher effective stiffness than that at 319 Hz.

Determinations were made of the tensions in the C strings of the harp. A measured length of each was weighed and the vibrating length of each was measured. The tensions computed for strings C1, C2, C3, C4 and C5 were, respectively ,53 N, 79 N, 96 N,151 N and 208 N.

5.9 The Mode near 291 Hz.

An experiment was carried out to investigate the nature of the resonance near 291 Hz. A plot of its admittance along the length of the board (figure 5.17), indicates that it does not belong to the S(1,n) or to the S(2,n) series of board modes, given its position on the frequency scale. As it was suspected to be the Helmholtz resonance of the air cavity, the holes in the back plate and the large opening in the soundbox at the base of the harp were covered over with cardboard and the resonant frequency was then re-measured by the input admittance method. There was no significant change in the resonant frequency of the mode. As hole area, chamber volume and lip length are the key determinants of the resonant frequency of a Helmholtz resonator, it was concluded that the resonance was not of the Helmholtz kind. In earlier experiments to measure the input admittance of the soundboard in the completed, strung harp, transfer admittance information had been collected by placing the large accelerometer at various positions on the back plate of the soundbox. An inspection of these data showed that the resonance at 291 Hz was strongly supported at most testing positions there. Experience in the earlier experiment on the isolated held barred board which was reported in chapter 4, led to an expectation that a holding frame if only immobilised at its ends could provide resonances of significant admittance in the same frequency range as early soundboard modes. The soundbox in the completed harp is only immobilised at its ends by the neck of the harp at the treble end and by the foot of the pillar at the bass end. Accordingly, pressure was exerted with the palm of the hand at a point on the back plate corresponding to a high admittance level for the mode near 291 Hz. Care was taken not to interfere directly with the soundboard in any way. Acceleration at string point F4 on the harp soundboard was then re-measured in the usual way.

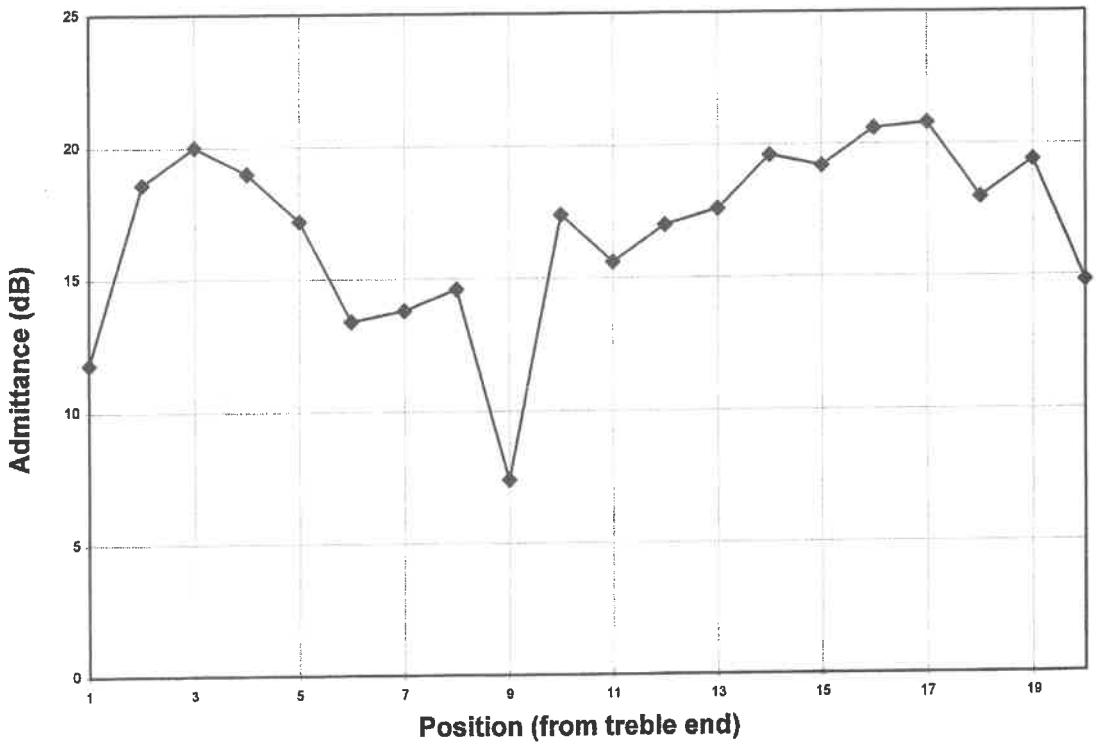

Figure 5.17 Admittance v Position on Soundboard from Treble End for Resonant Mode near 291 Hz.

The peak acceleration and therefore peak admittance, at 291 Hz was reduced by more than 4 dB while soundboard modes were largely unaffected. The acceleration versus frequency plots at string point F4 on the sound board with and without pressure on the soundbox 5.18 and 5.19.

Further work is required to establish with confidence the origin of this resonance. Driving point admittance measurements on the back plate of the soundbox should provide helpful information. There are indications based on the above experiment that it may be a bending mode of the soundbox as a whole. The high effective mass and high effective stiffness of the mode may be in accordance with these indications.

5.10 The Mode near 319 Hz.

The experiment described above was repeated at a driving point near string hole C2 on the soundboard where the resonance near 319 Hz has a large admittance level. Pressure was exerted on the soundbox at various positions on the back plate, but the peak admittance was unaffected. A driving point acceleration versus frequency plot was made using a driving point on top of the curve above the anchor point of the C3 string. The resulting acceleration versus frequency plot is displayed in figure 5.20. A peak of high Q-factor with peak-to-trough height of approximately 12 dB occurs near 316 Hz. A smaller peak rises approximately 4 dB above the noise level near 125 Hz. It was suspected that this resonance near 319 Hz was due to an in-plane vibration of the triangular structure of the harp. Accordingly, the curve was held with the hand while a driving point acceleration sweep was carried out at a driving point near string hole C2 on the soundboard. The acceleration sweeps with and without the holding of the curve are displayed in figures 5.21 and 5.22. At this driving point the resonance near 291 Hz has two little peaks. The acceleration and therefore the admittance level, of the resonance near 319 Hz is reduced by approximately 6 dB by holding the curve with the hand, while that near 291 Hz is largely unaffected.

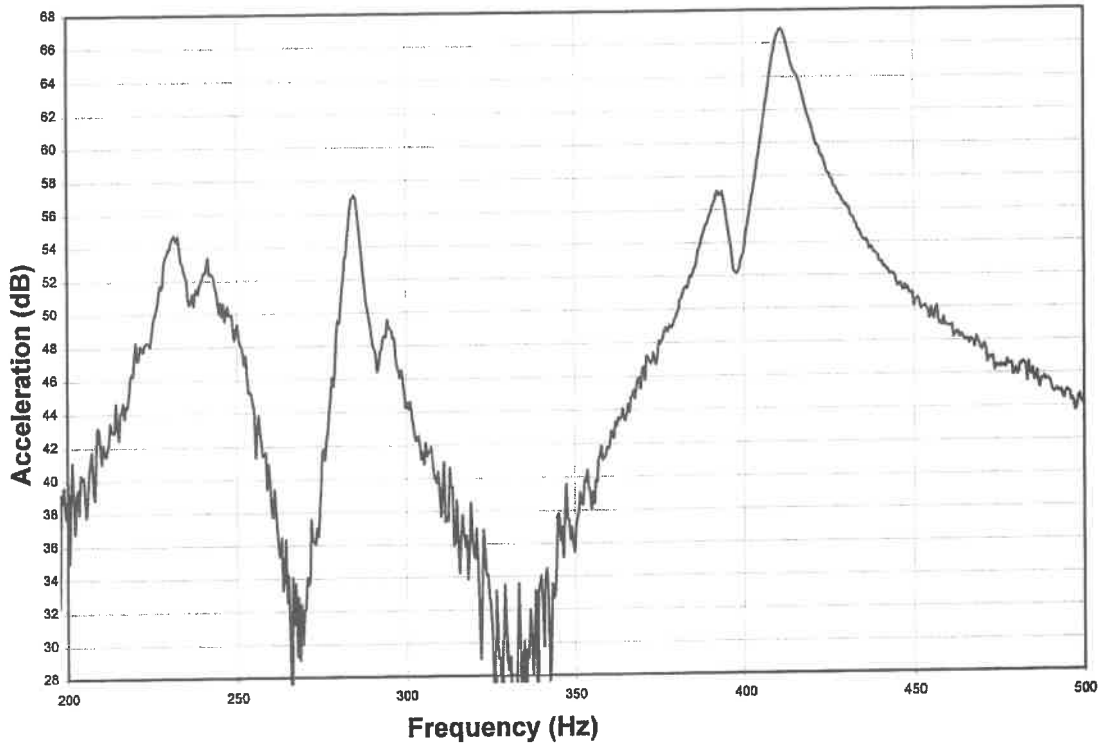

Figure 5.18 Acceleration v Frequency at String Point F4 on Harp Soundboard.

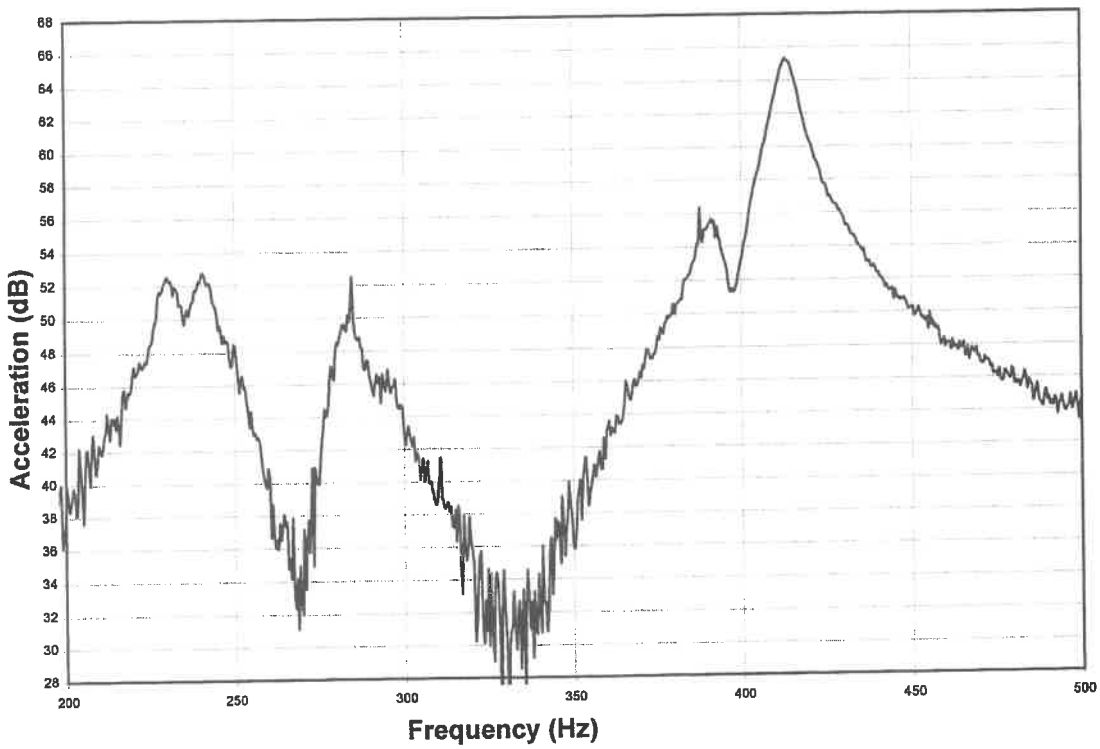

Figure 5.19 Acceleration v Frequency at String Point F4 on Harp Soundboard (hand on back plate of soundbox).

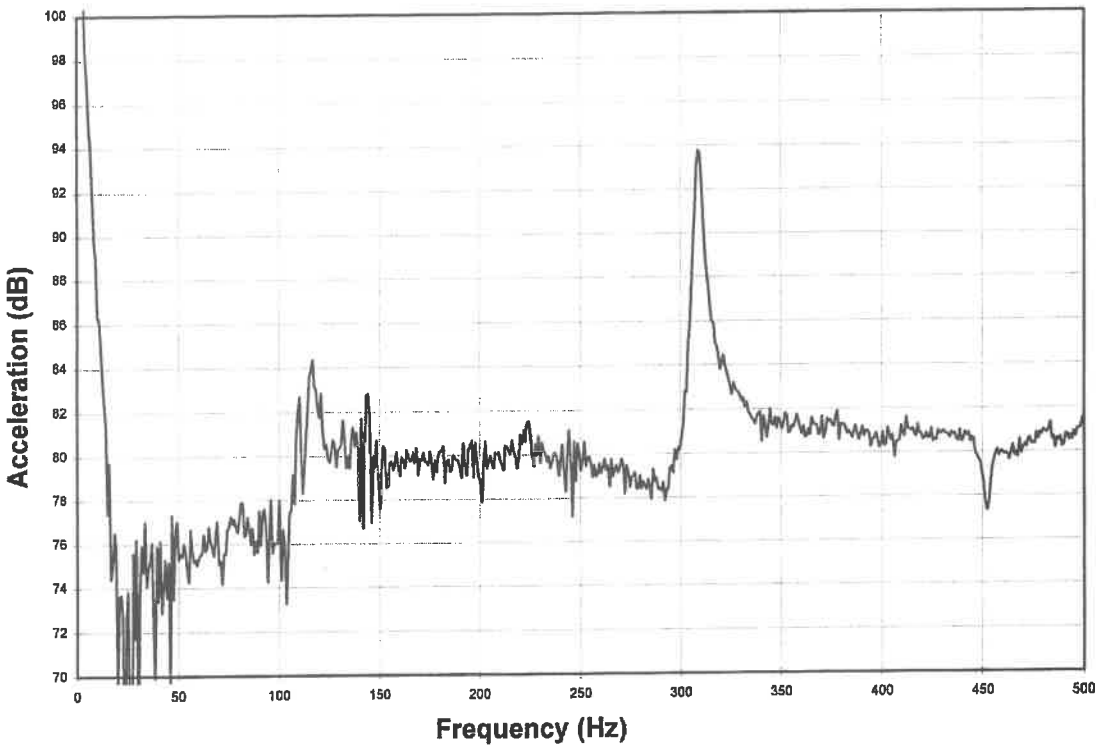

Figure 5.20 Acceleration v Frequency at Driving Point on top of String Arm at C3.

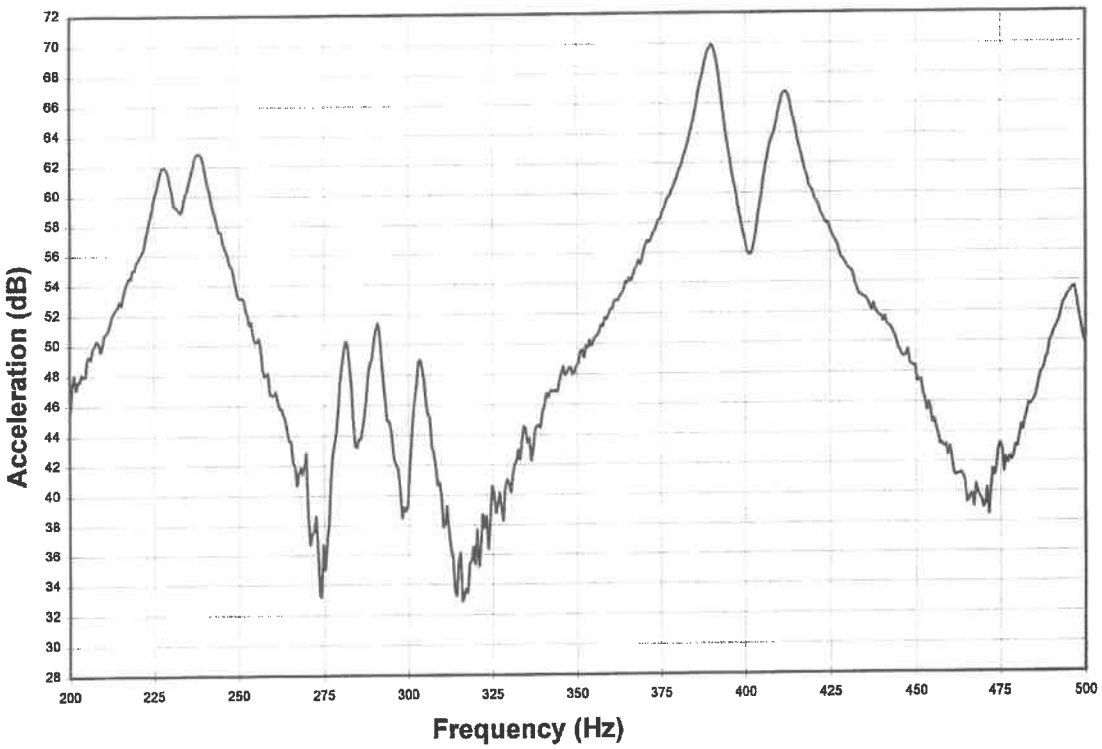

Figure 5.21 Acceleration v Frequency at String Point C2 on Harp Soundboard.

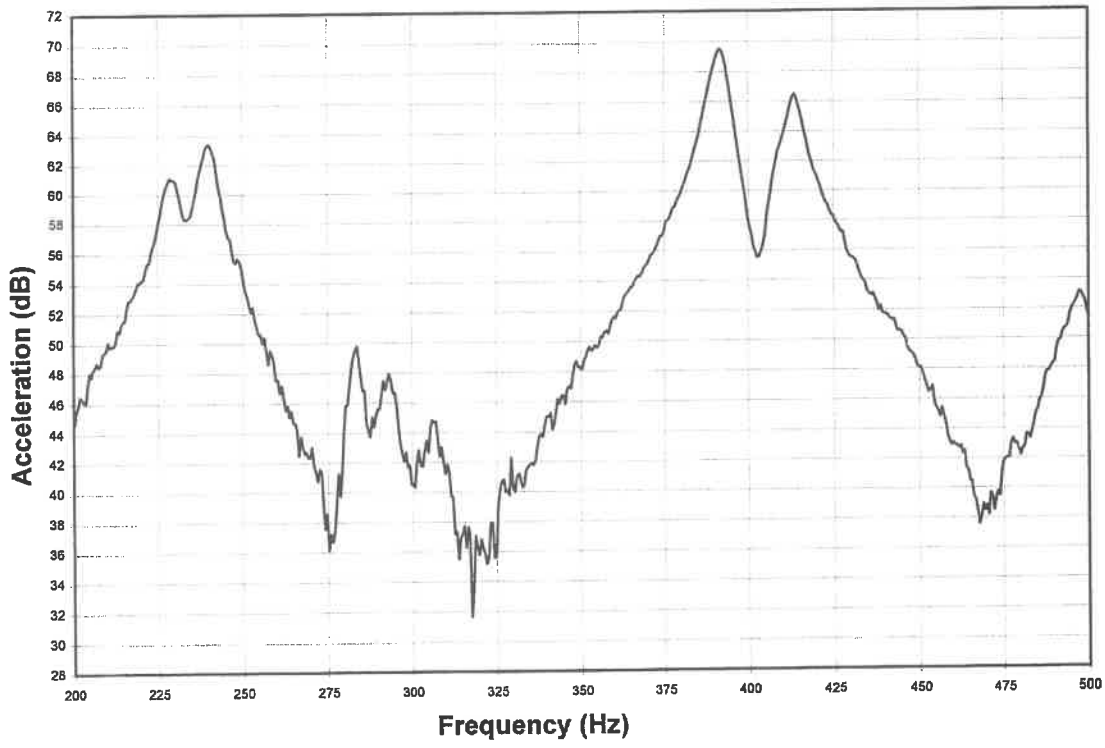

Figure 5.22 Acceleration v Frequency at String Point C2 on Harp Soundboard. (hand on string arm)

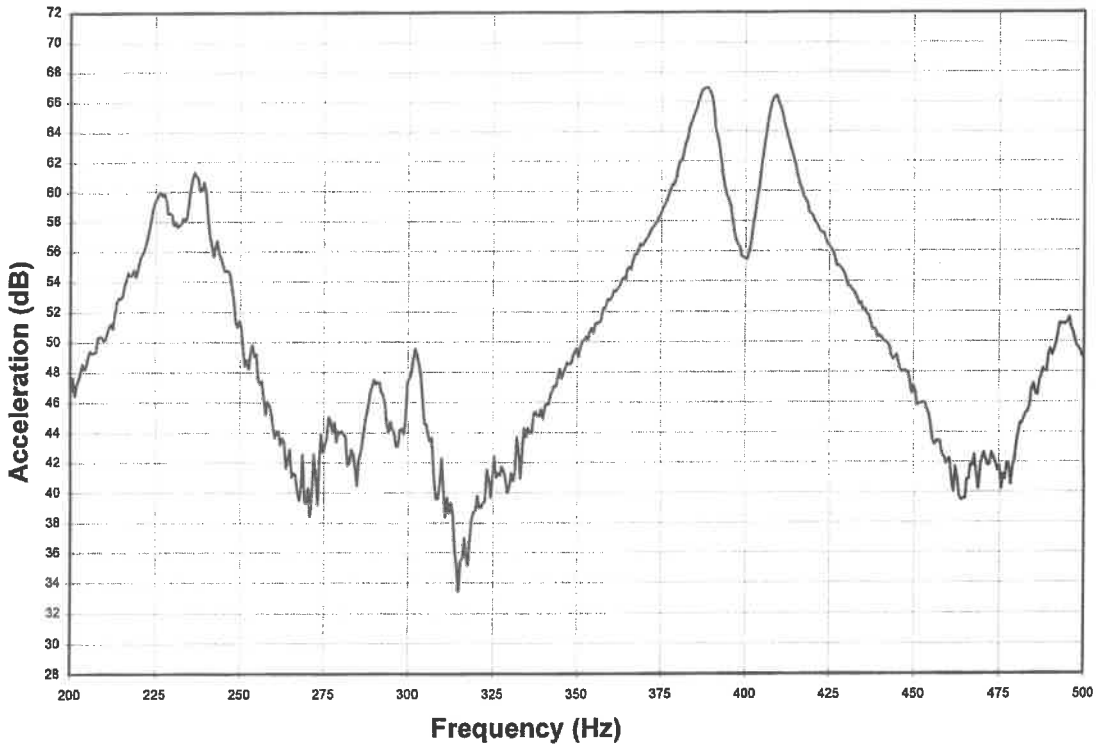

Figure 5.23 Acceleration v Frequency at String Point C2 on Harp Soundboard. (hand on back plate of soundbox)

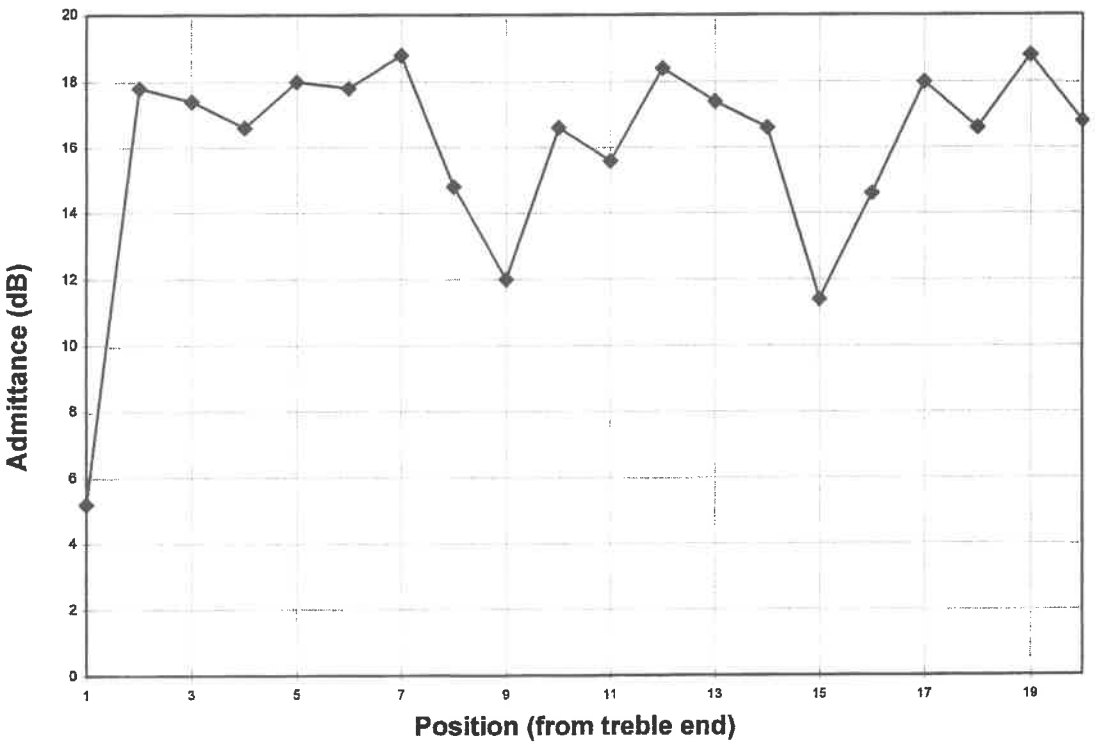

Figure 5.24 Admittance v Position on Soundboard from Treble End for Resonant Mode near 319 Hz.

The effect on the acceleration plot at C2 of holding the back of the box is shown in figure 5.23. In this case, the admittance level of the resonance near 291 Hz is again reduced by approximately 4 dB, while the admittance level of the resonance near 319 Hz is largely unaffected. A plot of admittance versus position along the length of the soundboard for the mode near 319 Hz is shown in figure 5.24.

5.11 Peaks below 250 Hz,

In Section 5.3 of this chapter reference was made to several low-frequency peaks whose height increases with frequency, which are observed on the admittance plot at G3 shown in figure 5.1. The origin of these peaks has not been established. However, observation of the plots of admittance versus position on the soundboard for the modes near 219 Hz and 391 Hz indicates that neither of these modes are the first in a series. It is expected that resonant bending vibrations of the soundbox as a whole are supported at lower frequencies than 291 Hz. Similarly there is a possibility that resonant vibrations of the triangular structure exist at lower frequencies than 319 Hz. These are possible explanations for the existence of the low frequency peaks below 250 Hz.

5.12 The Ó Meachair Spruce and Maple Harp

A small number of input admittance tests were made on a harp kindly provided by Ní Dhúill[4] for a short period between performances. This instrument was also an Ó Meachair Irish Folk Harp, but in this case the soundboard was of spruce and the body was of maple. Until recently, these were the species of wood universally used by Irish Folk Harp-makers. This harp was described in chapter 2.

Input admittance sweeps were carried out on this harp in an identical fashion to those carried out on the cedar and mahogany harp. Two driving points were used, one 1.0 cm above string point G3 and the other the same distance above string point C2. Figure 5.25 shows an input admittance plot for string point G3 over the frequency range 0 - 1000 Hz.

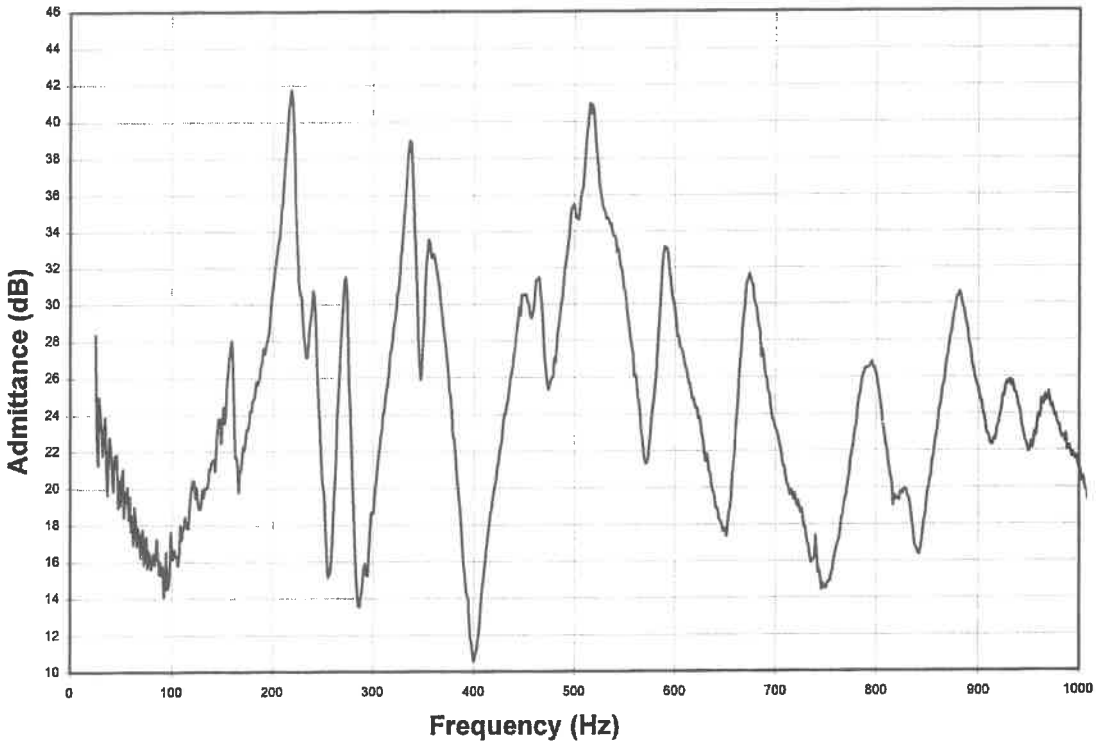

Figure 5.25 Admittance v Frequency Plot at String Point G3 on the Ó Meachair Spruce and Maple Harp

All the peak admittance frequencies detected up to 1000 Hz at both G3 and C2 on the spruce harp are set out in table 5.6. Bearing in mind that only two testing points were used and that, inevitably, some peaks will therefore have been missed, the number of resonances in each frequency band is probably about the same as on the cedar and mahogany harp. Q-factors were found to be somewhat lower than on the cedar and mahogany harp.

The similarity between the overall admittance profiles on both harps is striking. It is clear that the fundamental resonant mode of the soundboard occurs at 220 Hz in the spruce harp, compared to about 250 Hz in the cedar harp. The peak is split in each case. There is a very sharp peak near 270 Hz on the spruce harp. Comparison with the admittance plot on the cedar harp leads to the conclusion that this is probably either due to arching of the soundbox or to in-plane vibrations of the triangular structure.

The resonance with peaks at 334 Hz and 351 Hz, whose height relationship was reversed at the two testing points, is very similar in shape and height to that which occurs near 420 Hz on the cedar harp and is therefore almost certainly the second resonant mode of the board. Both harps have the third board mode occurring with a resonance peak between 500 Hz and 600 Hz. While on the spruce harp this resonance occurs with an admittance virtually equal to that of the fundamental soundboard resonance, on the cedar harp the admittance peak is a full 14 dB down on the first soundboard mode.

It is clear that the string frequencies being the same on both harps, the same note played on each will have important differences in quality because of the different frequency positions of the resonance peaks and the different relative admittances of these peaks. If plucked with the same force, some strings will be strongly heard, while others will be weakly heard. However, the player will attempt to compensate for this by plucking with varying force. But, because the strings are plucked in the plane of the triangular structure, there is a limit to the compensation that can be made without exciting adjacent strings. The strings in the treble area are so near to their breaking stresses that additional plucking force often causes these strings to break.

C2 f (Hz)	G3 f (Hz)
163	163
210	
221	220
241	242
251	
270	273
334	335
351	353
428	445
463	460
487	
510	510
532	
570	
582	582
607	
676	664
786	782
877	865
904	915

Table 5.6 Resonant Frequencies Detected at String Points C2 and G3 on the Ó Meachair Spruce and Maple Harp.

In addition to differences in tonal quality between the same note played on the two harps due to their different steady state responses, there will also be differences in the precise frequency components contained in the onset transient of the note as well as differences in the relative amplitude of the modal frequencies. This also contributes to a difference in the quality of the same note sounded on the two instruments.

However, the most striking feature of the admittance plots of the two Irish Folk Harps over the first 1000 Hz is the similarity of the admittance versus frequency plots, the large peak density which occurs and the very large (up to 30 dB) peak-to-trough variations associated with the early soundboard modes. All the early soundboard modes have multiple peaks in both harps. The similarity between musical notes played on both instruments is therefore expected to be the dominant feature.

5.13 Conclusions

The admittance versus frequency plot of the O`Meachair Cedar and Mahogany Irish Folk Harp has been established over the range 0-1000 Hz.

The modal classification of the first four soundboard modes has been established

Indications have been found that a transition from soundboard modes of S(1,n) classification to modes of S(2,n) classification takes place at or above a frequency of 700 Hz.

Preliminary investigations have been carried out into the origin of the resonant modes at 291 Hz and 319 Hz on the soundboard, which are a basis for further work.

Tests at two string points have been carried out on the O`Meachair Spruce and Maple Irish Folk Harp. The admittances plots of the two harps have been compared. Similarities and dissimilarities have been established.

A feature of the two harps and, indeed, of the isolated held, barred soundboard, is the splitting of all the early soundboard modes. Mechanical coupling with other parts of the structure of the harp has been ruled out as the cause of this mode splitting as has air coupling. It would appear that the origin of the splitting of modes lies in the structure of the soundboard itself or in the manner in which it is held. Different holding conditions of the central bars and of the remainder of the soundboard may provide an explanation. Further work is required so that this feature may be understood.

Firth, in his investigation of the Clarsach[3] found a whole body mode at 210 Hz and the first four modes in the S(1,n) series at 308 Hz, 428 Hz, 620 Hz, and 830 Hz. He does not identify a mode of the S(2,n) series in the 0 - 1 kHz frequency range investigated. Though the positions on the frequency scale of the modes identified on the Clarsach differ from those on the two O'Meachair harps, there is clearly a degree of similarity in the response of all three instruments.

It is hoped that the work done in this project may be of some assistance in making feasible the scientifically based construction of Irish folk harps in co-operation with existing harpmakers. It is proposed that further work be done to investigate the resonant vibrations of the harp soundboard at each stage in its progression from untapered edge-jointed pieces of wood to its final state when affixed to the soundbox in the completed harp. It is believed that the results of such investigations would be of considerable assistance in the development of a scientifically based manufacturing process.

Further efforts should be made to devise a reproducible method of immobilising and clamping isolated soundboards so that their vibrational characteristics can be readily compared.

Experiments should also be carried out on the air-borne sound produced by the harp with the object of establishing a correlation between the vibrations of the instrument body and sound energy output over the 0 - 1 kHz frequency range.

Much further work is required to relate the frequencies at which resonances occur, the strength of the response at each frequency and the Q-factor of each resonance to the mechanical parameters of the instrument body.

References

[1]Richardson, B.E., Investigation of Mode Coupling in the Guitar. Proc. Inst. Acous., Spring Conference, pp 81 - 88 (1984).

[2]Bell, A.J., An Acoustical Investigation of the Concert Harp. PhD thesis, University of St. Andrews, pp 68 - 93 (1987).

[3]Firth, I., On the Acoustics of the Harp. Acus., 37, pp 148 - 154 (1977).

[4]Ní Dhúill, Áine, Irish Folk and Concert Harpist. (1993)

APPENDIX

Accelerometer specifications and calibration data.

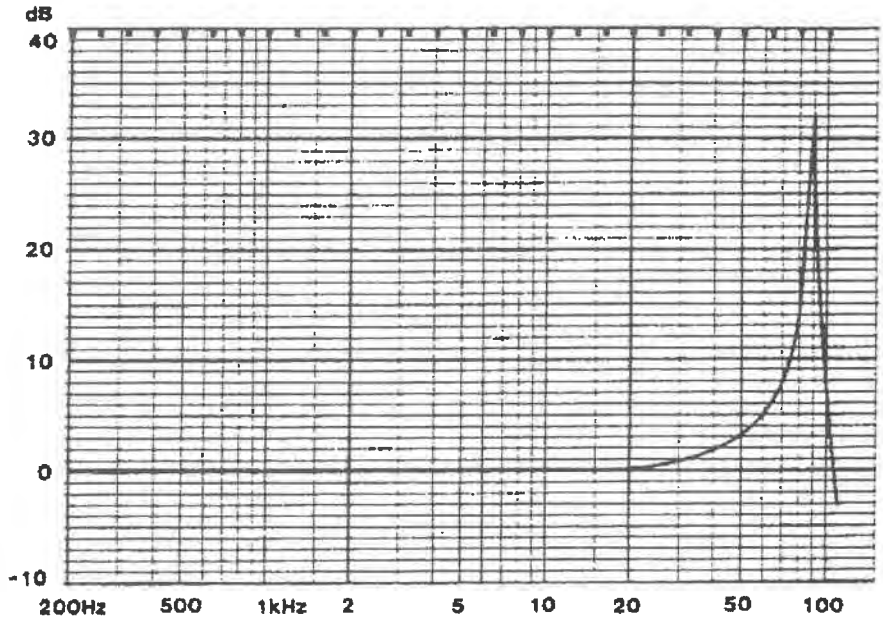

Figure 1 Typical Frequency Response Curve of B & K Accelerometer Type 4374 (Supplied by Manufacturer)

Calibration Chart for Accelerometer Type 4374

Serial No. 1587741

Brüel & Kjær

Reference Sensitivity at 159,2 Hz (ω = 1000 s^{-1}), 100 ms^{-2} and 22 °C

Charge Sensitivity* 0,102 pC/ms^{-2} or 1,00 pC/g

Voltage Sensitivity* (excl. AO 0038)

0,177 mV/ms^{-2} or 1,73 mV/g

Voltage Sensitivity* (incl. AO 0038)

0,147 mV/ms^{-2} or 1,44 mV/g

(Voltage Preamp. input Capacitance: 3,5 pF)

Capacitance (incl. integral cable) 578 pF

Typical Capacitance of cable AO 0038 ..... 110 pF

Maximum Transverse Sensitivity (at 30 Hz, 100 ms^{-2}) 3,0 %

Typical Undamped Natural Frequency ..... 118 kHz

Typical Mounted Resonance Frequency ..... 85 kHz

See reverse side of chart for frequency response curve

Typical Transverse Resonance Frequency, using Exciter Table 4290 with accelerometer mounted on a beryllium cube by cyanoacrylate adhesive: ..... 21 kHz

Polarity is positive on the center of the connector for an acceleration directed from the mounting surface into the body of the accelerometer

Resistance minimum 20 000 MΩ at room temperature

Date 91-02-01 Signature O.H.

1 g = 9,807 ms^{-2} or 10 ms^{-2} = 1,02 g

* This calibration is traceable to the National Bureau of Standards Washington D.C.

BC 0109–15

Figure 2 Specification of B & K Accelerometer Type 4374 (Supplied by Manufacturer)